JHEP

Published for SISSA by Springer

Received: May 28, 2011
Accepted: August 8, 2011
Published: August 23, 2011

New constraints (and motivations) for abelian gauge bosons in the MeV-TeV mass range

M. Williams,[a] **C.P. Burgess,**[a,b] **Anshuman Maharana**[c] **and F. Quevedo**[c,d]

[a] *Department of Physics & Astronomy, McMaster University*
1280 Main Street West, Hamilton ON, Canada
[b] *Perimeter Institute for Theoretical Physics*
31 Caroline Street North, Waterloo ON, Canada
[c] *DAMTP/CMS, University of Cambridge,*
Cambridge CB3 0WA, U.K.
[d] *Abdus Salam ICTP,*
Strada Costiera 11, Trieste 34014, Italy

E-mail: willimr2@mcmaster.ca, cburgess@perimeterinstitute.ca, am794@cam.ac.uk, f.quevedo@damtp.cam.ac.uk

Abstract: We survey the phenomenological constraints on abelian gauge bosons having masses in the MeV to multi-GeV mass range (using precision electroweak measurements, neutrino-electron and neutrino-nucleon scattering, electron and muon anomalous magnetic moments, upsilon decay, beam dump experiments, atomic parity violation, low-energy neutron scattering and primordial nucleosynthesis). We compute their implications for the three parameters that in general describe the low-energy properties of such bosons: their mass and their two possible types of dimensionless couplings (direct couplings to ordinary fermions and kinetic mixing with Standard Model hypercharge). We argue that gauge bosons with very small couplings to ordinary fermions in this mass range are natural in string compactifications and are likely to be generic in theories for which the gravity scale is systematically smaller than the Planck mass — such as in extra-dimensional models — because of the necessity to suppress proton decay. Furthermore, because its couplings are weak, in the low-energy theory relevant to experiments at and below TeV scales the charge gauged by the new boson can appear to be broken, both by classical effects and by anomalies. In particular, if the new gauge charge appears to be anomalous, anomaly cancellation does *not* also require the introduction of new light fermions in the low-energy theory. Furthermore, the charge can appear to be conserved in the low-energy theory, despite the corresponding gauge boson having a mass. Our results reduce to those of other authors in the special cases where there is no kinetic mixing or there is no direct coupling to ordinary fermions, such as for recently proposed dark-matter scenarios.

Keywords: Strings and branes phenomenology, Phenomenology of Large extra dimensions

ArXiv ePrint: hep-ph/1103.4556

doi:10.1007/JHEP08(2011)106

JHEP08(2011)106

Contents

JHEP08(2011)106

JHEP08(2011)106

1 Introduction and summary of results

New particles need not have very large masses in order to have evaded discovery; they can also be quite light provided they couple weakly enough to the other particles we *do* see. This unremarkable observation has been reinforced by recent dark matter models, many of which introduce new particles at GeV or lower scales in order to provide dark-matter interpretations for various astrophysical anomalies [1–13]. This model-building exercise has emphasized how comparatively small experimental efforts might close off a wide range of at-present allowed couplings and masses for putative new light particles [14–16].

Light spin-one bosons. Spin-one gauge bosons are particularly natural kinds of particles to seek at low energies, since (unlike most scalars) these can have light masses in a technically natural way. Furthermore, their couplings are reasonably restrictive, allowing only two kinds of dimensionless interactions with ordinary Standard Model particles: direct gauge couplings to ordinary matter and kinetic mixing [17] with Standard Model gauge bosons. Most extant surveys of constraints on particles of this type assume the existence of one or the other of these couplings, with older studies studying only direct gauge-fermion interactions [18–20] and later studies (particularly for dark-matter motivated models) [21–34] usually allowing only kinetic mixing.

In this paper we have both motivational and phenomenological goals. On the phenomenological side, we analyze the constraints on new (abelian) gauge bosons, including both direct gauge-fermion couplings and gauge-boson kinetic mixing. In this way we include all of their dimensionless couplings, which (if all other things are equal) should dominate their behaviour at low energies. We can follow the interplay of these couplings with one another, and how this changes the bounds that can be inferred concerning the allowed parameter space. In particular we find in some cases (such as beam dump experiments) that bounds derived under the assumption of the absence of the other coupling can sometimes weaken, rather than strengthen, once the most general couplings are present.

Our motivational goal in this paper is twofold. First, we argue that the existence of gauge bosons directly coupled to ordinary fermions is very likely to be a generic and

robust property of any phenomenologically successful theory for which the gravity scale is much smaller than the GUT scale [35–46]. Next, we argue that these gauge bosons often very naturally have extremely weak gauge interactions within reasonable UV extensions of the low-energy theory, such as extra-dimensional models [47, 48] and low-energy string vacua [49]. Besides motivating the otherwise potentially repulsive feature of having very small couplings, the smallness of these couplings (together with the low value for the fundamental gravity scale) also naturally tends to make the corresponding gauge bosons unusually light.

The remainder of this paper is organized as follows. The rest of this section, section 1, briefly summarizes the basic motivational arguments and phenomenological results. Section 2 then provides a more detailed theoretical background that motivates the sizes and kinds of couplings we consider, which may be skipped for those interested only in the bounds themselves. In section 3 we briefly summarize the basic properties of the new gauge boson, with details given in an appendix. By diagonalizing all kinetic terms and masses we identify the physical combination of couplings that are bounded in the subsequent sections. The next three sections, section 4, section 5 and section 6, then explore the bounds on these couplings that are most restrictive for successively lighter bosons, starting at the weak scale and working down to MeV scales.

1.1 Motivational summary

Why consider light gauge bosons that couple directly to ordinary fermions? And why should their couplings be so small? We here briefly summarize the more lengthy motivations given below, in section 2.

Low-scale gravity and proton decay. Weakly coupled gauge bosons are likely to be generic features of any (phenomenologically viable) UV physics for which the fundamental gravity scale is systematically small relative to the GUT scale, $M_{\rm GUT} \sim 10^{15}\,$GeV. Such bosons arise because of the difficulty of reconciling a low gravity scale with the observed stability of the proton. After all, higher-dimension baryon- and lepton-violating interactions that generically cause proton decay are not adequately suppressed if they arise accompanied by a gravity scale that is much smaller than $M_{\rm GUT}$. Similarly, global symmetries cannot themselves stop proton decay if the present lore about the absence of global symmetries in quantum gravity [50] should prove to be true (as happens in string theory, in particular [51, 52]).

This leaves low-energy gauge symmetries as the remaining generic mechanism for suppressing proton decay. Indeed, extra gauge bosons are often found in string vacua, and when the string scale is much smaller than the GUT scale, $M_s \ll M_{\rm GUT}$, these bosons typically play a crucial role in protecting protons from decaying. Furthermore, very weak gauge couplings appear naturally in such string compactifications, once modulus stabilization is included. In these systems the gauge couplings can be small because they are often inversely proportional to the volume of some higher-dimensional cycle, whose volume gets stabilized at very large values [53, 54]. Similar things can also occur in non-stringy extra-dimensional models [55, 56].

JHEP08(2011)106

Unbroken gauge symmetry without unbroken gauge symmetry. We believe there is a generic low-energy lesson to be drawn from how proton decay is avoided in phenomenological string constructions. This is because in these models, even though proton decay is forbidden by conservation of a gauged charge, the gauge boson that gauges this symmetry is not massless [49]. This combines the virtues of an unbroken symmetry (no proton decay), with the virtues of a broken symmetry (no new forces mediated by a massless gauge boson).[1] Usually this happy situation arises in the string examples because the gauge symmetry in question is anomalous, if judged solely by the light fermion content, with anomaly freedom restored through Green-Schwarz anomaly cancellation. But in four dimensions Green-Schwarz anomaly cancellation relies on the existence of a Goldstone boson, whose presence also ensures that the gauge boson acquires a nonzero mass.

For these constructions the effective lagrangian obtained just below the string scale from matching to the stringy UV completion is invariant under the symmetry apart from an anomaly-cancelling term that breaks the symmetry in just the way required to cancel the fermion loop anomalies. Section 2 argues that this property remains true (to all orders in perturbation theory) as one integrates out modes down to low energies. Leading symmetry breaking contributions arise non-perturbatively, exponentially suppressed by the relevant gauge couplings. Consequently they remain negligibly small provided only that the gauge groups involved in the anomalies are weakly coupled. Although supersymmetry also plays a role in the explicit string examples usually examined, our point here is that this is not required for the basic mechanism that allows massive gauge bosons to coexist with conservation of the corresponding gauge charge.

1.2 Phenomenological summary

We next summarize, for convenience of reference, the combined bounds obtained from the constraints examined throughout the following sections.

Mass vs coupling. Figure 1 presents a series of exclusion plots in the $\alpha_X - M_X$ plane, where $\alpha_X = g_X^2/4\pi$ is the gauge-fermion coupling and M_X is the gauge boson mass. Each panel shows these bounds for different fixed values of the kinetic mixing parameter, $\sin\eta$ (for details on the definition of variables, see section 3). The figure shows the collective exclusion area of all of the different bounds considered in this paper. For concreteness they are calculated for a vector-like charge assignment, $X_{fL} = X_{fR}$, with the choice $X = B - L$ denoted by a lighter shading and the choice $X = B$ denoted with a heavier shading. Comparison of the cases $X = B$ and $X = B - L$ shows how much the bounds strengthen once direct couplings to leptons are allowed.

For $\eta = 0$, the dominant bounds are from neutrino scattering, upsilon decay, anomalous magnetic moments, beam-dump experiments, neutron-nucleus scattering and nucleosynthesis. Once kinetic mixing is introduced, many of these bounds improve, with the exception of the beam-dump bounds. Once $\sin\eta \gtrsim 0.06$, kinetic mixing becomes sufficiently strong that the W-mass bound prevails over any other bounds in the $M_X \lesssim M_Z$ region.

[1] Superconductors are similar in this regard: the photon acquires a mass without implying gross violations of charge conservation.

JHEP08(2011)106

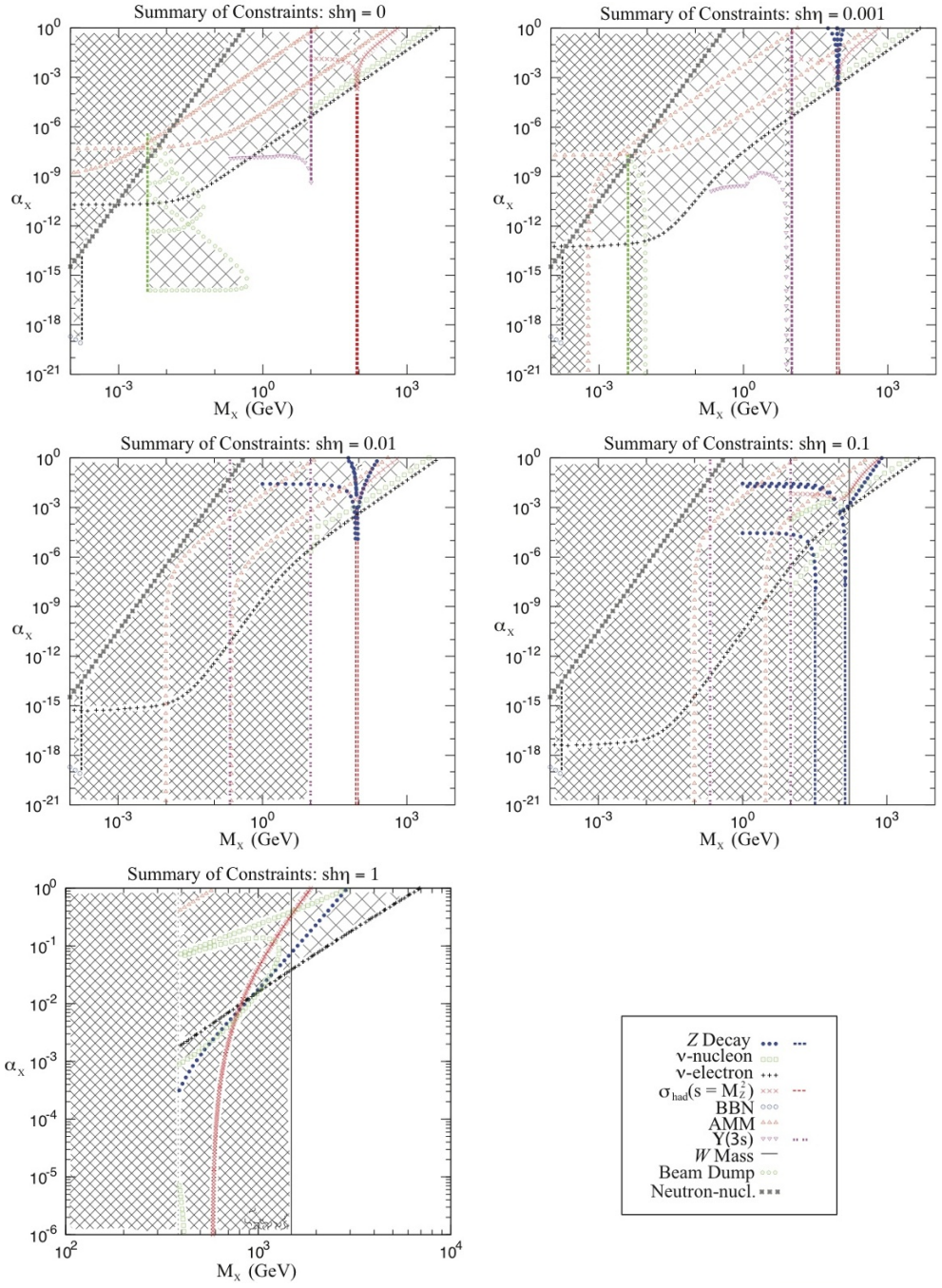

Figure 1. Summary of the constraints presented herein. Each plot shows the bound on the new gauge coupling, α_X, as a function of M_X for various values of the kinetic-mixing parameter, $\sin\eta$, assuming a vector coupling $X_{f_L} = X_{f_R} := X$, with $X = B - L$ ($X = B$) drawn as sparse (dense) cross-hatching.

For $\sin\eta = 1$, we discard the region where the oblique T parameter is large (for details, see section 4), and focus on the region where $M_X > 385\,\text{GeV}$. In this region, it is the neutrino-electron scattering bound and the W-mass bound that dominate.

JHEP08(2011)106

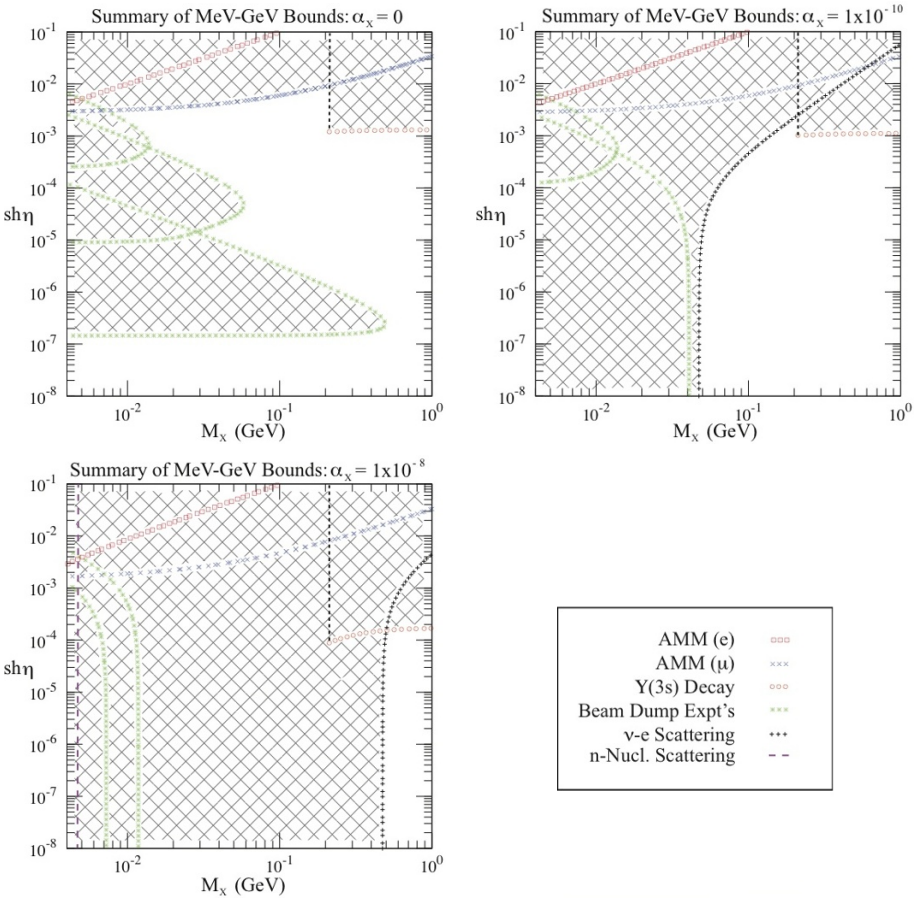

Figure 2. Summary of the constraints on kinetic mixing relevant in the MeV-GeV mass range. Each plot shows the bound on the kinetic mixing parameter $\sin\eta$ as a function of M_X, for $\alpha_X = 0$, 1×10^{-10} and 1×10^{-8}. The plot assumes a coupling $X_{\ell_L} = X_{\ell_R} = -1$, such as would be true if $X = B - L$. Hatched regions are excluded.

Mass vs mixing angle. It is useful to show these same bounds as exclusion plots in the mixing-angle/boson-mass plane, for fixed choices of the gauge-fermion coupling, α_X. This allows contact to be made with similar bounds obtained in the context of dark matter-inspired U(1) models [14–16, 29–33], which correspond to the $\alpha_X \to 0$ limit of the bounds we find here. This version of the plots is shown in figure 2, restricted to the MeV-GeV mass range (in order to facilitate the comparison with earlier work).

For small, but non-zero, gauge coupling ($\alpha_X \sim 10^{-10}$) the bounds from beam dump experiments weaken significantly. However, another strong bound from neutrino-electron scattering also begins to take effect. This bound dominates for larger α_X, and once $\alpha_X \gtrsim 10^{-7}$ the entire MeV−GeV mass range is excluded.

Since the bounds in figure 2 all rely on coupling to leptons, in the case where $X = B$ the constraints arise through the kinetic mixing and are independent of α_X. The resulting plot for $X = B$ is therefore the same as is shown in the figure for $\alpha_X = 0$. However, as the gauge coupling is increased the neutron-nucleus scattering bound — discussed in section 6.4 — eventually becomes important, first being visible as an exclusion in the $\sin\eta$ — M_X plane in the panel for $\alpha_X \simeq 10^{-8}$ in figure 2.

JHEP08(2011)106

2 Theoretical motivation

This section elaborates the motivations for weakly coupled, very light gauge bosons alluded to above. This is done both by summarizing the consistency conditions they must satisfy within the low-energy effective theory relevant to experiments, and by describing how such bosons actually arise from several representative UV completions in string theory and extra-dimensional models.

2.1 Low-energy gauge symmetries, consistency and anomaly cancellation

Very general arguments [57–63] indicate that the interplay between unitarity and Lorentz invariance require massless gauge bosons only to couple to conserved charges that generate exact symmetries of the matter action. Consequently we normally expect the direct couplings of very light gauge bosons to be similarly restricted. This section reviews these arguments, emphasizing how they can break down [64–68] if the energy scale, Λ, of any UV completion is sufficiently small compared with the gauge boson mass, M, and coupling, g: $\Lambda \lesssim 4\pi M/g$. For the present purposes it suffices to restrict our attention to abelian gauge bosons (see however [67, 68] for some discussion of the nonabelian case).

The upshot of the arguments summarized here is that massive spin-one bosons can couple in an essentially arbitrary way if their mass, M, lies within a factor $g/4\pi$ of the scale of UV completion. But once M becomes smaller than $g\Lambda/4\pi$, then the corresponding boson must gauge an honest-to-God, linearly realized exact symmetry. In particular this symmetry must be anomaly free. However any anomalies that Standard Model fermions give a putative new gauge charge needn't be cancelled by adding new, exotic low-energy fermions; they can instead be cancelled by the Goldstone boson whose presence is in any case required if the gauge boson has a mass. But this latter sort of cancellation also requires the UV completion scale to satisfy $\Lambda \lesssim 4\pi M/g$.

Notice that for any given M the condition $\Lambda \lesssim 4\pi M/g$ need not require Λ to lie below the TeV scale if the coupling g is small enough. For instance, if $M \simeq 1\,\mathrm{MeV}$ then Λ lies above the TeV scale provided $g \lesssim 10^{-5}$ (an upper limit often required in any case by the strong phenomenological bounds we find below). And, as subsequent sections argue, such small couplings can actually arise in a natural way from reasonable UV completions.

2.1.1 Massless spin-one bosons

What goes wrong if a spin-one particle is not coupled to matter by gauging an exact symmetry of the matter action? If the spin-one particle is massless, then the problem is that one must give up either Lorentz invariance or unitarity (provided the particle has non-derivative, Coulomb-like couplings that survive in the far infrared). Lorentz invariance and unitarity fight one another because the basic field, $A_\mu(x)$, cannot transform as a Lorentz 4-vector if A_μ creates and destroys massless spin-one particles [57–63]. Instead it transforms as a 4-vector *up to a gauge transformation*, $A_\mu \to A_\mu + \partial_\mu \omega$, and so interactions must be kept gauge invariant in order to be Lorentz invariant [69].

JHEP08(2011)106

2.2 Massive spin-one bosons

For massive spin-one particles the argument proceeds differently, as is now described. The difference arises because a 4-vector field, A_μ, can represent a *massive* spin-one particle [57–59].

To examine the relevance of symmetries, it is worth first considering coupling massive spin-one particles to other matter fields, ψ, in some arbitrary non-gauge-invariant way, with lagrangian density $\mathcal{L}(A_\mu, \psi)$. The first observation to make is that any such a lagrangian can be made gauge invariant for free, by introducing a Stückelberg field, ϕ, according to the replacements $A_\mu \to \mathcal{A}_\mu := A_\mu - \partial_\mu \phi$ and $\psi \to \Psi := \exp[-i\phi\, Q]\psi$, where Q is a hermitian matrix acting on the fields ψ. With this replacement the lagrangian $\mathcal{L}(\mathcal{A}_\mu, \Psi)$ is automatically invariant under the symmetry $A_\mu \to A_\mu + \partial_\mu \omega$, $\phi \to \phi + \omega$ and $\psi \to \exp[i\omega\, Q]\psi$, since both $\mathcal{A}_\mu$ and Ψ are themselves invariant under these replacements. The original non-symmetric formulation corresponds to the specific gauge $\phi = 0$. For gauge symmetry, absence of gauge invariance is evidently equivalent to nonlinearly realized gauge invariance (similar arguments can also be made in the nonabelian case [67, 68]).

But this gauge invariance is obtained at the expense of introducing a new scale. Since ϕ is dimensionless, its kinetic term involves a scale, v,

$$\mathcal{L}_{\rm kin} = -\frac{1}{4g^2} F_{\mu\nu}F^{\mu\nu} - \frac{v^2}{2}\left(\partial_\mu \phi - A_\mu\right)\left(\partial^\mu \phi - A^\mu\right). \tag{2.1}$$

In $\phi = 0$ gauge the scale v is seen to be related to the gauge boson mass by the relation $M = gv$. In a general gauge the scale v controls the size of couplings between the canonically normalized field, $\varphi = \phi\, v$, and other particles. For instance the coupling

$$\mathcal{L}_{\rm coupling} = -i(\overline{\psi}\gamma^\mu Q\psi)\left(A_\mu - \frac{\partial_\mu \varphi}{v}\right), \tag{2.2}$$

shows that the $(\overline{\psi}\gamma^\mu Q\psi)\partial_\mu\varphi$ coupling is dimension-five, being suppressed by the scale $v = M/g$.

Lagrangians with nonrenormalizable couplings like this must be interpreted as effective field theories, whose predictive power relies on performing a low-energy expansion in powers of E/Λ, for some UV scale Λ. The interpretation of the scale v then generically depends on the how high Λ is relative to $4\pi M/g = 4\pi v$. We consider each case in turn.

Light spin-one bosons: $M \ll g\Lambda/4\pi$. If the gauge boson is very light compared with the UV scale, then its low-energy interactions should be describable by some renormalizable theory. But renormalizability is only consistent with a dimension-five interaction[2] like the $(\overline{\psi}\gamma^\mu Q\psi)\partial_\mu\varphi$ coupling of eq. (2.2) if this coupling is a *redundant* interaction, such as it would be if it could be removed by a field redefinition. A sufficient condition for an interaction of the form $J^\mu\partial_\mu\varphi$ to be redundant in this way is if the field equations for ψ were to imply the quantity $J^\mu(\psi)$ satisfies $\partial_\mu J^\mu = 0$ [70, 71]. This shows that if the gauge boson is to be arbitrarily light relative to Λ, its low-energy, renormalizable couplings must

[2]The careful reader will recognize that this argument assumes negligible anomalous dimensions, and so needs re-examination for strongly coupled theories.

JHEP08(2011)106

be to a (dimension-three) conserved current. This is the usual prescription for obtaining these couplings by gauging a linearly realized matter symmetry, for which J^μ is the usual Noether current.

More generic massive spin-one bosons: $M \gtrsim g\Lambda/4\pi$. If, on the other hand, the dimension-five coupling $(\overline{\psi}\gamma^\mu Q\psi)\partial_\mu\varphi$ is not redundant, then there must be an upper bound on the UV scale: $\Lambda \lesssim 4\pi v = 4\pi M/g$. Sometimes this may be seen from the energy-dependence predicted for the cross section of reactions in the low energy theory: if $\sigma(E) \propto 1/(4\pi v)^2$ then this would be larger than the unitarity bound $\sigma \lesssim 1/E^2$ for energies $E \gtrsim \Lambda \simeq 4\pi v$, indicating the failure at these energies of the low-energy approximation. If so, the full UV completion must intervene at or below these energies to keep the theory unitary.

The upshot is that spin-one particles can couple fairly arbitrarily to matter provided they are massive, and provided the energy scale, Λ, of any UV completion satisfies $\Lambda \lesssim 4\pi M/g$, where M is the gauge boson mass and g is its coupling strength. (Everyday examples of spin-one particles of this type include the ρ meson or spin-one nuclei.) It is only spin-one particles with $M < g\Lambda/4\pi$ that must gauge linearly realized symmetries.

2.3 Anomaly cancellation

Any new gauge symmetry — henceforth denoted $\mathrm{U}(1)_X$ — must be an exact symmetry (though possibly spontaneously broken), and in particular must be anomaly free. This is true regardless of whether the symmetry is the linearly realized symmetry of a light gauge boson, or the nonlinearly realized symmetry of a massive gauge boson.

Of particular interest in this paper are models where the new symmetry acts on ordinary fermions, because a robust motivation for thinking about light gauge bosons is the avoidance of proton decay in models with a low gravity scale (more about which below). In this case these ordinary fermions usually contribute gauge anomalies for the new symmetry, and an important issue is how these anomalies are ultimately cancelled. The two main anomaly-cancellation scenarios then divide according to whether or not anomalies cancel among the SM fields themselves, or require the addition of new particles.

2.3.1 Anomaly cancellation using only SM fields

The simplest situation is where the new gauge symmetry is simply a linear combination of one or more of the SM's four classical global symmetries — baryon number B, electron number L_e, muon number L_μ and tau number L_τ. In this situation there are only two independent combinations of these symmetries that are anomaly free[3] [72], corresponding to arbitrary linear combinations of the anomaly-free symmetries $L_e - L_\mu$ and $L_\mu - L_\tau$:

$$X = a(L_e - L_\mu) + b(L_\mu - L_\tau)\,. \tag{2.3}$$

Of course, evidence for neutrino oscillations [73–75] make it unlikely that these symmetries are unbroken in whatever replaces the Standard Model in our ultimate understanding of Nature.

[3]Notice that $B - L$ carries a Standard Model anomaly in the absence of sterile right-handed neutrinos (see below).

JHEP08(2011)106

2.3.2 Anomaly cancellation using the Green-Schwarz mechanism

If more general combinations of B, L_e, L_μ and L_τ are to be gauged, it is necessary to introduce new particles that can cancel their Standard Model anomalies. For a new $\mathrm{U}(1)_X$ symmetry the minimal way to do this is to add only the Goldstone boson, which must in any case be present if the corresponding gauge boson has a mass (as it typically must to avoid mediating a macroscopic, long-range new force, whose presence is strongly disfavoured by observations [76–79]). For a $\mathrm{U}(1)_X$ symmetry this can always be done using the 4D version [80] of the Green-Schwarz mechanism [81]. Besides its intrinsic interest, this is a way of cancelling anomalies that actually arises from plausible UV physics, such as low energy string models.

In principle, there are four types of new anomalies that can arise in 4D once the SM is supplemented by a new gauge symmetry, $\mathrm{U}(1)_X$. These are proportional to $\mathrm{Tr}[XXX]$, $\mathrm{Tr}[XXY]$, $\mathrm{Tr}[XYY]$ and $\mathrm{Tr}[XG^aG^a]$, where the trace is over all left-handed fermions and X denotes the new symmetry generator, Y is Standard Model hypercharge, and G^a represents the generators of the Standard Model nonabelian gauge groups, $\mathrm{SU}(2)_L \times \mathrm{SU}(3)_c$, as well as the generators of Lorentz transformations. In four dimensions CPT invariance implies the absence of pure gravitational anomalies, and anomaly cancellation within the Standard Model ensures the absence of anomalies of the form $\mathrm{Tr}[YYY]$ and $\mathrm{Tr}[G^aG^bG^c]$.

It is always possible to redefine the new symmetry generator, $V := X + \zeta\, Y$, to remove one of the two mixed anomalies. For instance, $\mathrm{Tr}[VVY] = \mathrm{Tr}[XXY] + 2\,\zeta\,\mathrm{Tr}[XYY]$ can be made to vanish by choosing ζ appropriately (provided $\mathrm{Tr}[XYY]$ does not vanish). It suffices then to consider only the case of nonzero anomalies of the form $\mathrm{Tr}[VVV]$ and $\mathrm{Tr}[VG^aG^a]$, where G^a now includes also the generator Y. The anomaly then can be written in the G^a- and Lorentz-invariant form[4]

$$\begin{aligned}\delta\Gamma &= -\int \mathrm{d}^4x\;\omega\Big\{c_X F_V \wedge F_V + c_a \mathrm{Tr}[F_a \wedge F_a] - c_L \mathrm{Tr}[R \wedge R]\Big\} \\ &= -\int \mathrm{d}^4x\;\omega\Big\{c_X\Big(F_X + \zeta\, F_Y\Big) \wedge (F_X + \zeta\, F_Y) + c_a \mathrm{Tr}[G^a \wedge G^a] - c_L \mathrm{Tr}[R \wedge R]\Big\}\,,\end{aligned} \tag{2.4}$$

where Γ is the 'quantum action' (generator of 1PI correlations), the symmetry parameter is normalized by $\delta X_\mu = \partial_\mu \omega$ and the coefficients, c_X, c_a and c_L, are calculable. Here $F_V = \mathrm{d}V = F_X + \zeta\, F_Y$ is the gauge-boson field strength for the generator $X + \zeta\, Y$, while F_a is the same for the Standard Model gauge bosons and R is the gravitational curvature 2-form.

Given the coefficients c_X, c_a and c_L, here is how 4D Green-Schwarz anomaly cancellation works [80]. Consider the gauge kinetic lagrangian, including the Stückelberg field ϕ,

$$\begin{aligned}\mathcal{L} = \mathcal{L}_{\mathrm{inv}} &- \frac{1}{4g^2} F^X_{\mu\nu} F_X^{\mu\nu} - \frac{1}{4g_a^2} \mathrm{Tr}[G^a_{\mu\nu} G_a^{\mu\nu}] - \frac{v^2}{2} (\partial^\mu \phi - X^\mu)(\partial_\mu \phi - X_\mu) \\ &+ \phi\Big\{c_X\Big(F_X + \zeta\, F_Y\Big) \wedge (F_X + \zeta\, F_Y) + c_a \mathrm{Tr}[G^a \wedge G^a] - c_L \mathrm{Tr}[R \wedge R]\Big\}\,.\end{aligned} \tag{2.5}$$

[4] A similar formulation can be made using the anomaly in its 'consistent' form, rather than the 'covariant' form used in the text.

JHEP08(2011)106

Here $\mathcal{L}_{\rm inv}$ denotes those parts of the lagrangian that are invariant under all of the gauge symmetries that are not written explicitly. The second line is not invariant under gauge transformations because ϕ is not; its variation precisely cancels the fermion anomaly, eq. (2.4).

An important observation is that the anomaly cancelling term is dimension-five, and so is not renormalizable. For instance, in terms of the canonically normalized field, $\varphi = \phi v$, the first anomaly cancelling term is $\mathcal{L}_{\rm anom} = (\varphi/f) F_X \wedge F_X + \cdots$, where $f = v/c_X$. As before, this implies the existence of a UV-completion scale, Λ, above which the low-energy effective description breaks down [66]. For weakly coupled theories typically $\Lambda \lesssim 4\pi v \simeq 4\pi M/g \simeq 4\pi c_X f$ marks the scale where the fields arise that are required to extend the Goldstone boson to a linear representation of the symmetry.

Perhaps the most interesting feature of cancelling anomalies with the Green-Schwarz mechanism in this way is that the lagrangian remains invariant under the U(1) symmetry, apart from the anomaly-cancelling term. This is interesting because it means that the corresponding charge still appears to be conserved in the low-energy theory, *despite the gauge field being massive*. This opens up interesting phenomenological possibilities for the gauging of symmetries like $\mathrm{U}(1)_B$ and $\mathrm{U}(1)_{B-L}$, which appear to be conserved in Nature but which are also ruled out as sources of the new long-range force that a massless gauge boson would imply.

One might worry that arbitrary symmetry-breaking interactions might be generated by embedding the anomaly cancelling interactions (or the fermion triangle anomaly graph) into a quantum fluctuation. For instance if $X = B$, so the new gauge boson couples to baryon number, then why can't some complicated loop generate a $\Delta B = \pm 1$ interaction, $\mathcal{O}_{\pm 1}$, that can mediate proton decay? After all, this can be $\mathrm{U}(1)_B$ invariant if it arises multiplied by a factor $e^{\mp i\phi}$, which carries baryon number $\Delta B = \mp 1$.

The difficulty with generating this kind of interaction is that it must involve ϕ undifferentiated. But if we restrict $\mathcal{L}_{\rm anom}$ to constant ϕ configurations, it becomes a total derivative. For constant ϕ, the dependence of observables on ϕ is similar to the dependence of observables on the vacuum angle, θ. Consequently it arises at best only non-perturbatively, proportional at weak coupling to a power of $\sim \exp[-8\pi^2/g^2]$, where g is the anomalous gauge coupling. As a result the only potentially dangerous contribution of this type comes from the mixed X-QCD-QCD anomaly, which can generate nontrivial ϕ-dependence once we integrate down to scales $\lesssim \Lambda_{QCD}$. This is not dangerous in particular for the classical symmetries, B, L_e, L_μ and L_τ, since these do not have mixed QCD anomalies [72].

2.3.3 Anomaly cancellation using new fermions

More complicated possibilities for new gauge bosons emerge if new, light exotic fermions are allowed that also carry the new X charge (and so can also take part in the anomaly cancellation). We briefly describe some features involving such new exotic particles, although they do not play any role in our later phenomenological studies.

The simplest example along these lines is $X = B - L$, which is anomaly-free provided only that the SM spectrum is supplemented by three right-handed neutrinos (one for each generation). Furthermore, conservation of L is consistent with all evidence for

JHEP08(2011)106

neutrino oscillations, although it would be ruled out should neutrinoless double-beta decay ever be witnessed.

A practical way in which such new fermions can arise at TeV scales is if the UV theory at these scales is supersymmetric. In this case the plethora of new superpartners can change anomaly cancellation in one of two ways (or both). They can either directly contribute to the anomalies themselves, and possibly help anomalies cancel without recourse to the Green-Schwarz mechanism. Alternatively, they can modify the details of how the Green-Schwarz mechanism operates if the UV scale, v, associated with it is larger than the supersymmetry breaking scale, $M_{\rm susy}$.

In particular, supersymmetry typically relates the kinetic term for the Stückelberg field, (2.5), with a Fayet-Iliopoulos term in the scalar potential [83],

$$S_{\rm FI} = -\frac{1}{g^2}\int d^4x \left(\tau - \sum_i q_i \phi_i^\dagger \phi_i\right)^2 , \tag{2.6}$$

where τ is a dynamical field whose vev acts as the low-energy Fayet-Iliopoulos parameter; the q_i are the charges of the fields ϕ_i under the U(1) in question. In string examples the field τ corresponds to a modulus of the compactification, which controls the size of a cycle in the internal geometry on which some branes wrap. We note that the vanishing of the D-term is consistent with vanishing vevs of the charged fields if $\tau = 0$, i.e. the symmetry survives as an *exact* global symmetry when the cycle size vanishes (the singular locus). Small values of the vev are obtained if the cycle size is small.

2.4 Motivations from UV physics

The above summary outlines some of the theoretical constraints on coupling ordinary fermions to very light gauge bosons. This section shows how very small couplings can naturally appear in well-motivated ultraviolet physics, such as extra-dimensional models or string vacua. In particular, they often arise due to considerations of proton stability in constructions for which the gravity scale is small compared with the Planck scale, as we now explain.

2.4.1 Proton decay in low-scale gravity models

One of the surprises of the late 20th century was the discovery that the scale, M_g, of quantum gravity could be much smaller than the Planck scale, $M_p = (8\pi G)^{-1/2} \simeq 10^{18}\,\text{GeV}$ [35–42]. From the point of view of particle physics this possibility is remarkable for several reasons. Most obvious is the potential it allows for experimental detection if it should happen that M_g is in the vicinity of the TeV scale [43–46].

But there is a potentially more wide-reaching consequence that $M_g \ll M_p$ has for the low-energy sector: the suppression by powers of M_g/M_p it allows for otherwise UV-sensitive radiative corrections [84]. This suppression arises because the contribution of short-wavelength degrees of freedom can saturate at M_g, allowing their effects to be suppressed by powers of the gravitational coupling.

JHEP08(2011)106

The most precise examples of this are provided by string theory, in the regime where the string scale is low, $M_g := M_s \ll M_p$ [35–42]. String theory makes the suppression of UV-sensitive contributions precise by providing an explicit stringy ultraviolet completion within which the effects of the full UV sector can be explored. Large-volume (LV) models [53, 54] are particularly useful laboratories for these purposes, since these systematically exploit the expansion of inverse powers of the extra-dimensional volume (in string units), $\mathcal{V} := (\text{Vol})/\ell_s^6 \gg 1$, and it is ultimately these kinds of powers that enforce the suppressions of interest since $M_s/M_p \propto \mathcal{V}^{-1/2}$.

Proton decay — that is, its experimental absence — turns out to impose a very general constraint on any fundamental theory of this type, with $M_g \ll M_p$. It does so because having M_g very small removes two of the standard ways of keeping the proton stable in specific models. On one hand quantum gravity, and string theory in particular [51, 52], seems to preclude the existence of global symmetries, and this forbids ensuring proton stability by simply using a conserved global charge (such as baryon number).

If M_g is too small then it is also unlikely that such a symmetry simply emerges by accident for the lowest-dimension interactions in the low-energy effective theory. The problem in this case is that we know that generic higher-dimensional interactions,

$$\mathcal{L}_{\text{eff}} = \sum_i \frac{c_i \mathcal{O}_i}{M_g^{d_i-4}}\,, \tag{2.7}$$

eventually do arise in the low-energy effective theory, such as the standard baryon-number violating 4-quark operators arising at dimension $d_i = 6$ [85, 86] in the low-energy limit of grand-unified theories (GUTs) [87–91]. But a dimension-six interaction of the form $\mathcal{O}/M^2$ generically contributes a proton-decay rate of order $\Gamma \simeq m_p^5/M^4$, where m_p is the proton mass, which is too large to agree with observations once M falls below $M_{\text{GUT}} \simeq 10^{16}\,\text{GeV}$.

The way theories with $M_g \ll M_p$ usually evade proton decay is through the appearance of a *gauged* U(1), whose conservation forbids the decay. Of course, to be useful the gauged U(1) that appears must couple to the proton or its decay products in order to forbid its decay. But because this means ordinary particles couple to the new gauge boson, it potentially introduces other phenomenological issues. If the gauge symmetry is conserved, why isn't the gauge boson massless? If the gauge boson is light, why isn't the new boson seen in low-energy observations? If the gauge boson is heavy, the corresponding symmetry must be badly broken and so how can it help with proton decay? Interestingly, extant models can naturally address both of these issues, and often the low-energy mechanism that is used is Green-Schwarz anomaly cancellation with gauge boson mass generated through the Stückelberg mechanism described above. Sometimes this mechanism is also combined with supersymmetry to suppress the dangerous decays.

The existence of these gauge bosons, their properties, and the way they evade the above issues, may be among the few generic low-energy consequences of viable theories with a low gravity scale: $M_g \ll M_{\text{GUT}}$.

Sample symmetries. The simplest proposals for new low-energy gauge groups that forbid proton decay are either baryon or lepton number, $X = B$ or $X = L$. If the anomalies

JHEP08(2011)106

for these symmetries due to Standard Model fermions are cancelled through the Green-Schwarz mechanism, then no new light particles are required besides the massive gauge boson itself.

More complicated examples are possible if the low-energy theory at TeV scales is supersymmetric. In this case symmetries like $B - L$, that in themselves cannot forbid proton decay, can help suppress proton decay if taken together with supersymmetry [49]. (For instance, the parity $R = (-)^{F+3(B-L)}$ that is usually used to suppress proton decay in the MSSM is a combination of fermion number and $B - L$.)

More general combinations of B and L can also suppress proton decay in supersymmetric theories. Ref. [49] provides a list of the kinds of symmetries of this type that can be relevant to proton decay, as well as the conditions they must satisfy in order to have their anomalies be cancelled through the Green-Schwarz mechanism. The general form for the low-energy charge may be written

$$X = mT_R + nA + pL\,, \tag{2.8}$$

where T_R is right-handed isospin; A is an axionic PQ symmetry; and L is lepton number, with the charge assignments given in the table. The coefficients m, n and p are subject to (but not over-constrained by) several anomaly cancellation conditions [49]. In particular B and L violating interactions can be forbidden up to and including dimension six for some choices of these symmetries in the supersymmetric limit, as can the μ-terms of the superpotential — $W \simeq \mu_L L\overline{H}$ and $W \simeq \mu H\overline{H}$ — if $n \neq 0$.

	Q	U	D	L	E	H	$\overline{H}$
T_R	0	1	-1	0	-1	1	-1
A	0	0	1	1	0	-1	0
L	0	0	0	1	-1	0	0
X	0	m	$n-m$	$n+p$	$-m-p$	$m-n$	$-m$

2.4.2 Very light and weakly coupled gauge bosons from extra-dimensional models

For the phenomenological discussions of later sections we consider gauge bosons in the MeV to TeV mass range, whose direct couplings to Standard Model fermions are much smaller than those arising within the Standard Model itself. This section and the next one describe several way that very light and weakly coupled bosons can arise from reasonable UV physics.

Extra-dimensional supergravity provides a simple way to obtain very light gauge bosons that are very weakly coupled. A concrete example is six-dimensional chiral gauged supergravity [92–94], for which the bosonic part of the gravity multiplet contains the metric, g_{MN}, a Kalb-Ramond 2-form potential, B_{MN}, and a scalar, ϕ. Because it is chiral this supergravity potentially has anomalies, whose cancellation imposes demands on the matter content. In six dimensions Green-Schwarz anomaly cancellation is not automatic, because cancellation of the pure gravitational anomalies requires the existence of a specific number

JHEP08(2011)106

of gauge multiplets [95, 96]. Given these multiplets, mixed gauge-gravity anomalies can be cancelled through the Green-Schwarz mechanism using the couplings of the field B_{MN}.

The resulting supergravity admits simple solutions for which the extra dimensions are a sphere [97], whose moduli can be stabilized by a combination of background fluxes in the extra dimensions [47, 48], and branes coupling to the 6D dilaton [55, 56, 98, 99]. An important feature of this stabilization is that the value of the dilaton field becomes related by the field equations to the size of the extra dimensions:

$$e^{\phi} = \frac{1}{(M_6 r)^2}\,, \tag{2.9}$$

where M_6 denotes the 6D Planck scale. This ensures these models are a rich source of U(1) gauge bosons, some of whom can have massless modes that survive to low energies below the Kaluza-Klein scale. Some of these gauge modes also naturally acquire masses through the Stückelberg mechanism [47, 48] (with the Stückelberg field arising as a component of the Kalb-Ramond field, B_{MN}).

Besides having light gauge bosons, these models also naturally furnish them with very small coupling constants. This is because the loop-counting parameter for all bulk interactions turns out to be the value of the 6D dilaton, ϕ, with $g^2 \simeq e^{\phi}$. But modulus stabilization, eq. (2.9), ensures that this coupling can be extremely small because it scales inversely with the size of the extra dimensions (measured in 6D Planck units).

2.4.3 Very light and weakly coupled gauge bosons from low-energy string vacua

A related mechanism also often arises in low-scale string models. In early heterotic models the role of the Goldstone boson is played by a member of the dilaton super-multiplet: $a \simeq \mathrm{Im}\, S$ [83], while in later Type I and Type II models it is twisted closed string multiplets that instead play this role [49, 100]. Although the universal couplings of the dilaton restrict the kinds of symmetries that can arise in heterotic constructions of this type, the same is not true for Type I and II models.

There is a simple reason why additional U(1) gauge groups often arise. The basic building blocks for constructing models of particle physics in type IIB and IIA string theory are D-branes. Generically, the gauge group associated with a stack of N D-branes is U(N), but the Standard Model gauge group involves special unitary groups, SU(3)×SU(2)×U(1). Typical GUT models also involve special unitary groups, like SU(5), SU(3)×SU(2)×SU(2)×U(1) (Left-Right symmetric models) or SU(4) × SU(2) × SU(2) (Pati-Salam models). It is the additional U(1)s that distinguish the Standard Model SU(N) factors from the U(N) factors arising from the D-branes, that give new low-energy gauge symmetries.

Furthermore, anomaly cancellation in string theory typically demands the presence of additional D-brane stacks, in addition to those providing the Standard Model gauge group factors. These stacks also lead to extra U(1)s under which Standard Model particles are charged. Extra U(1)s also appear naturally in F-theory models (for a recent discussion see [101]). In many concrete examples these additional gauge fields correspond to $\mathrm{U}(1)_B$ or $\mathrm{U}(1)_{B-L}$, hence can be relevant for the stability of the proton [49, 102, 103] (see also [104] for a recent discussion).

JHEP08(2011)106

Masses and couplings. For string vacua the masses and couplings of any gauged U(1)s can be computed, as we now briefly describe.

Consider first the U(1)s associated with the same stack of D-branes as gives rise to the Standard Model gauge group. As discussed earlier, such gauge bosons often acquire masses from the Stückelberg mechanism. The size of the mass generated in this way is the string scale when the U(1) is anomalous [104, 105], but it is the smaller Kaluza-Klein scale for non-anomalous U(1)s.

For models with the compactification volume not too much larger than the string scale, these U(1) gauge bosons are very heavy. On the other hand, for large-volume models the string scale can be quite low, leading to additional U(1)s potentially as light as the TeV scale. The latter can have interesting low energy phenomenology (see for instance [102, 103, 106–110]). In these models the strength of the gauge coupling for the additional U(1)s is roughly the same as for the Standard Model gauge couplings (evaluated at the string scale), because both have the same origin: the world-volume theory of the stack. Hence they cannot be extremely small.

The masses and couplings of the extra U(1) gauge bosons vary more widely when they arise from D-brane stacks whose SU(N) factors are not part of the Standard Model gauge group. For instance, the case of additional U(1)s associated with D7 branes wrapping bulk four cycles of the compactification is discussed in detail in [52]. The value of the gauge coupling in this case is inversely proportional to the volume (in string units) of the cycle, Σ, that the D7 brane wraps,

$$g^2 \approx \frac{4\pi}{\mathcal{V}_\Sigma}\,. \tag{2.10}$$

In the context of the large volume scenario (LVS) of modulus stabilization [53, 54], the size of the bulk cycle associated with the overall volume of compactification can easily be approximately $\mathcal{V}_\Sigma \gtrsim 10^9$ in string units, set by the requirement that one generate TeV-scale soft terms. Thus one can obtain gauge couplings as low as $g \lesssim 2\times 10^{-4}$ [52, 111] (couplings larger than this can be obtained if the D7 brane wraps a cycle different from the one associated with the overall volume). With couplings this small, the gauge boson mass can be $M_X \simeq gv \lesssim 100\,\mathrm{MeV}$ even if v is a TeV.

3 Gauge boson properties

With the above motivation, our goal in the remainder of the paper is to work out various constraints on the parameters of a massive (yet comparatively light) gauge boson, the X boson, that couples to a new U(1)$_X$ symmetry. Since the lowest dimension interactions dominate in principle at low energies, we include in our analysis all of the dimensionless couplings that such a boson could have with Standard Model particles: i.e. both direct fermion-gauge couplings and gauge kinetic mixing. We see how these are constrained by present data as a function of the gauge boson mass.

More specifically, we consider an effective lagrangian density below the supersymmetry breaking scale of the form

$$\mathcal{L} = \mathcal{L}_{\rm SM} + \mathcal{L}_X + \mathcal{L}_{\rm mix} \tag{3.1}$$

JHEP08(2011)106

where $\mathcal{L}_{\rm SM}$ is the usual Standard Model lagrangian; $\mathcal{L}_X$ describes the X boson, including its couplings to the SM fermions; and $\mathcal{L}_{\rm mix}$ is the kinetic-mixing interaction between the X boson and that of the SM gauge factor $\mathrm{U}(1)_Y$ [17]. Explicitly

$$\mathcal{L}_X = -\frac{1}{4} X_{\mu\nu} X^{\mu\nu} - \frac{m_X^2}{2} X_\mu X^\mu + i J_X^\mu X_\mu \,, \tag{3.2}$$

where $X_{\mu\nu} := \partial_\mu X_\nu - \partial_\nu X_\mu$ is the curl of the appropriate gauge potential, X_μ, and J_X^μ is the current for the $\mathrm{U}(1)_X$ gauge symmetry involving the SM fermions. Similarly, $\mathcal{L}_{\rm mix}$ has the form,

$$\mathcal{L}_{\rm mix} = \chi\, B_{\mu\nu} X^{\mu\nu} \tag{3.3}$$

where B_μ is the SM gauge boson for the gauge factor $\mathrm{U}(1)_Y$.

The analysis we provide complements and extends earlier studies of extra gauge boson phenomenology. In the lower part of the mass range we may compare with [18], who some time ago considered the special cases $X = B - L$ and $\chi = 0$. Contact is also possible in this mass range with more recent Dark Matter models [14–16, 29, 30] in the absence of direct matter couplings, $g_X J^\mu = 0$. At masses much lower than those considered here other constraints on kinetic mixing have also been studied, from the cosmic microwave background [34], and from the absence of new long-range forces [76–79] or milli-charged particles [17, 21–27].

There is also a broad literature on the phenomenology of gauge bosons at the upper end of the mass range, largely done in the context of a Z' field and often motivated by GUTs [87–89, 112–127]. Until recently, most did not include the kinetic mixing term. Constraints including kinetic mixing arising from precision electroweak experiments are considered in [128–130]; more recent bounds are found in [28, 131–133]. Many of these analyses overlap parts of our parameter space. For instance Z' searches, such as [134], give bounds on the mass of the Z' that apply in the regime that the couplings to fermions are identical to that of the Z. Others [19, 20, 135] derive bounds for a Z' coupled only to baryon number.

One difference between the models examined here and those usually considered for Z' phenomenology at the weak scale, such as those of ref. [136–138], is the absence in $\mathcal{L}$ of mixing between the X and the Z bosons in the mass matrix (i.e. a term of the form $\mathcal{L}_{\rm mix} = \delta m^2 Z_\mu X^\mu$). We do not consider this type of mixing because we imagine the models of interest here to break the X symmetry with a SM singlet. Notice that because the SM Higgs is uncharged under the X symmetry, the strong bounds as found, for example, in [139] don't apply.

3.1 The mixed lagrangian

In this section we diagonalize the gauge boson kinetic mixing terms (and SM mass terms) and identify the physical combination of parameters relevant for phenomenology within the accuracy to which we work. Our goal in so doing is to follow ref. [140–142] and identify once and for all how the gauge boson mixing contributes to fermion couplings and to oblique parameters [143–146] modified by the gauge-boson mixing. This allows an efficient identification of how observables depend on the mixing parameters.

JHEP08(2011)106

We begin by writing the lagrangian of interest more explicitly, after spontaneous symmetry breaking. Because it is the Z and photon that potentially mix with the X boson, we also focus on these sectors of the SM lagrangian. In order to distinguish the fields before and after mixing, where appropriate we denote the still-mixed fields with carets, e.g. $\hat{X}_\mu$, reserving variables like X_μ for the final, diagonalized fields.

With this notation, the lagrangian of interest is

$$\mathcal{L} = \mathcal{L}_{\text{gauge}} + \mathcal{L}_f + \mathcal{L}_{\text{int}} \,, \tag{3.4}$$

where

$$\mathcal{L}_{\text{gauge}} = \mathcal{L}_{\text{kin}} + \mathcal{L}_{\text{mass}} \tag{3.5}$$

with

$$\mathcal{L}_{\text{kin}} = -\frac{1}{4}\hat{W}^3_{\mu\nu}\hat{W}_3^{\mu\nu} - \frac{1}{4}\hat{B}_{\mu\nu}\hat{B}^{\mu\nu} - \frac{1}{4}\hat{X}_{\mu\nu}\hat{X}^{\mu\nu} + \frac{\chi}{2}\hat{B}_{\mu\nu}\hat{X}^{\mu\nu} \tag{3.6}$$

$$\mathcal{L}_{\text{mass}} = -\frac{1}{2}\left(m_3\hat{W}^3_\mu - m_0\hat{B}_\mu\right)\left(m_3\hat{W}_3^\mu - m_0\hat{B}^\mu\right) - \frac{m_X^2}{2}\,\hat{X}_\mu\hat{X}^\mu \,, \tag{3.7}$$

and

$$\mathcal{L}_f = -\sum_f \overline{f}\left(\partial\!\!\!/ + m_f\right) f \tag{3.8}$$

$$\begin{aligned}\mathcal{L}_{\text{int}} = i\sum_f \Big\{ & g_2\left(\overline{f}\gamma^\mu T_{3f}\gamma_L f\right)\hat{W}^3_\mu + g_1\left[\overline{f}\gamma^\mu\left(Y_{fL}\gamma_L + Y_{fR}\gamma_R\right) f\right]\hat{B}_\mu \\ & + g_X\left[\overline{f}\gamma^\mu\left(X_{fL}\gamma_L + X_{fR}\gamma_R\right) f\right]\hat{X}_\mu\Big\} \,.\end{aligned} \tag{3.9}$$

Here T_{3f}, Y_{fL} and Y_{fR} denote the usual SM charge assignments, while X_{fL} and X_{fR} are the fermion charges under the new $\mathrm{U}(1)_X$ symmetry. The SM masses, m_3 and m_0, are defined as usual [72] in terms of the standard model gauge couplings, g_1 and g_2, and the Higgs VEV, v: $m_3 = \frac{1}{2}\,g_2 v$ and $m_0 = \frac{1}{2}\,g_1 v$. γ_L and γ_R are the usual left- and right-handed Dirac projectors.

Defining the gauge-field-valued vector $\hat{\mathbf{V}}$ to be

$$\hat{\mathbf{V}} = \begin{bmatrix}\hat{W}^3 \\ \hat{B} \\ \hat{X}\end{bmatrix} \,, \tag{3.10}$$

the above lagrangian can be written in matrix form

$$\mathcal{L}_{\text{gauge}} + \mathcal{L}_{\text{int}} = -\frac{1}{4}\hat{\mathbf{V}}^T_{\mu\nu}\hat{K}\hat{\mathbf{V}}^{\mu\nu} - \frac{1}{2}\hat{\mathbf{V}}^T_\mu\hat{M}\hat{\mathbf{V}}^\mu + i\hat{\mathbf{J}}^T_\mu\hat{\mathbf{V}}^\mu \tag{3.11}$$

where

$$\hat{K} := \begin{bmatrix}1 & 0 & 0 \\ 0 & 1 & -\chi \\ 0 & -\chi & 1\end{bmatrix} \quad \text{and} \quad \hat{M} := \begin{bmatrix}m_3^2 & -m_3 m_0 & 0 \\ -m_3 m_0 & m_0^2 & 0 \\ 0 & 0 & m_X^2\end{bmatrix} \,, \tag{3.12}$$

JHEP08(2011)106

and

$$\hat{\mathbf{J}}_\mu := \begin{bmatrix} J^3_\mu \\ J^Y_\mu \\ \hat{J}^X_\mu \end{bmatrix} = \sum_f \begin{bmatrix} g_2 \left[\overline{f}\gamma_\mu T_{3f}\gamma_L f\right] \\ g_1 \left[\overline{f}\gamma_\mu \left(Y_{f_L}\gamma_L + Y_{f_R}\gamma_R\right) f\right] \\ g_X \left[\overline{f}\gamma_\mu \left(X_{f_L}\gamma_L + X_{f_R}\gamma_R\right) f\right] \end{bmatrix} . \tag{3.13}$$

The off-diagonal elements of $\hat{M}$ ensure it has a zero eigenvalue, and the condition that the matrix $\hat{K}$ be positive definite requires $\chi^2 < 1$.

3.2 Physical couplings

In order to put this lagrangian into a more useful form we must diagonalize the kinetic and mass terms, and then eliminate the SM electroweak parameters in terms of physically measured input quantities like the Z mass, M_Z, the fine-structure constant, $\alpha = e^2/4\pi$, and Fermi's constant, G_F, as measured in muon decay.

The diagonalization is performed explicitly in the appendix, leading to the diagonalized form

$$\mathcal{L} = -\frac{1}{4}\,\mathbf{V}^T_{\mu\nu}\mathbf{V}^{\mu\nu} - \frac{M_Z^2}{2}\,Z_\mu Z^\mu - \frac{M_X^2}{2}\,X_\mu X^\mu + i\mathbf{J}^T_\mu \mathbf{V}^\mu \,, \tag{3.14}$$

where the physical masses are

$$M_X^2 = \frac{m_Z^2}{2}\left(1 + \hat{s}_W^2 \mathrm{sh}^2\eta + r_X^2 \mathrm{ch}^2\eta + \vartheta_X\sqrt{\left(1 + \hat{s}_W^2\mathrm{sh}^2\eta + r_X^2\mathrm{ch}^2\eta\right)^2 - 4r_X^2\mathrm{ch}^2\eta}\right) \tag{3.15}$$

and

$$M_Z^2 = \frac{m_Z^2}{2}\left(1 + \hat{s}_W^2 \mathrm{sh}^2\eta + r_X^2 \mathrm{ch}^2\eta - \vartheta_X\sqrt{\left(1 + \hat{s}_W^2\mathrm{sh}^2\eta + r_X^2\mathrm{ch}^2\eta\right)^2 - 4r_X^2\mathrm{ch}^2\eta}\right) . \tag{3.16}$$

In these expressions $m_Z^2 := \frac{1}{4}\left(g_1^2 + g_2^2\right)v^2$,

$$\hat{c}_W := \cos\hat{\theta}_W := \frac{g_2}{\sqrt{g_1^2 + g_2^2}} \quad \text{and} \quad \hat{s}_W := \sin\hat{\theta}_W := \frac{g_1}{\sqrt{g_1^2 + g_2^2}} \,, \tag{3.17}$$

while

$$\mathrm{sh}\,\eta := \sinh\eta := \frac{\chi}{\sqrt{1-\chi^2}} \quad \text{and} \quad \mathrm{ch}\,\eta := \cosh\eta := \frac{1}{\sqrt{1-\chi^2}} \,. \tag{3.18}$$

Finally, the quantities r_X and ϑ_X are defined by

$$r_X := \frac{m_X}{m_Z} \quad \text{and} \quad \vartheta_X := \begin{cases} +1 & \text{if} \quad r_X > 1 \\ -1 & \text{if} \quad r_X < 1 \end{cases} , \tag{3.19}$$

which ensures $M_Z \to m_Z$ and $M_X \to m_X$ as $\eta \to 0$.

The currents in the physical basis are similarly read off as

$$\mathbf{J}_\mu := \begin{bmatrix} J^Z_\mu \\ J^A_\mu \\ J^X_\mu \end{bmatrix} = \begin{bmatrix} \check{J}^Z_\mu c_\xi + \left(-\check{J}^Z_\mu \hat{s}_W \mathrm{sh}\,\eta + \check{J}^A_\mu \hat{c}_W \mathrm{sh}\,\eta + \check{J}^X_\mu \mathrm{ch}\,\eta\right) s_\xi \\ \check{J}^A_\mu \\ -\check{J}^Z_\mu s_\xi + \left(-\check{J}^Z_\mu \hat{s}_W \mathrm{sh}\,\eta + \check{J}^A_\mu \hat{c}_W \mathrm{sh}\,\eta + \check{J}^X_\mu \mathrm{ch}\,\eta\right) c_\xi \end{bmatrix} , \tag{3.20}$$

JHEP08(2011)106

where

$$\begin{bmatrix} \check{J}^Z_\mu \\ \check{J}^A_\mu \\ \check{J}^X_\mu \end{bmatrix} := \begin{bmatrix} \hat{J}^3_\mu\, \hat{c}_W - \hat{J}^Y_\mu\, \hat{s}_W \\ \hat{J}^3_\mu\, \hat{s}_W + \hat{J}^Y_\mu\, \hat{c}_W \\ \hat{J}^X_\mu \end{bmatrix} = \sum_f \begin{bmatrix} i\hat{e}_Z \overline{f}\gamma_\mu \left[T_{3f}\gamma_L - Q_f \hat{s}^2_W\right] f \\ ie\, \overline{f}\gamma_\mu Q_f f \\ ig_X \overline{f}\gamma_\mu \left[X_{fL}\gamma_L + X_{fR}\gamma_R\right] f \end{bmatrix} ,$$

and $e := g_2\hat{s}_W = g_1\hat{c}_W$, $\hat{e}_Z := e/(\hat{s}_W\hat{c}_W)$ and $Q_f = T_{3f} + Y_{fL} = Y_{fR}$. Finally, $c_\xi := \cos\xi$ and $s_\xi := \sin\xi$ with the angle ξ given by

$$\tan 2\xi = \frac{-2\hat{s}_W \mathrm{sh}\eta}{1 - \hat{s}^2_W \mathrm{sh}^2\eta - r^2_X \mathrm{ch}^2\eta} \,. \tag{3.21}$$

Writing the resulting lagrangian as

$$\mathcal{L} = \mathcal{L}_{\rm SM} + \delta\mathcal{L}_{\rm SM} + \mathcal{L}_X \,, \tag{3.22}$$

shows that the X boson has two kinds of physical implications: (i) direct new couplings between the X boson and SM particles; (ii) modifications (due to mixing) of the couplings among the SM particles themselves.

3.2.1 Modification of SM couplings

The modification to the SM self-couplings caused by $Z - X$ mixing are given by

$$\delta\mathcal{L}_{\rm SM} = -\frac{z}{2}\, m^2_Z Z_\mu Z^\mu + i\hat{e}_Z \sum_f \left[\overline{f}\gamma^\mu \left(\delta g_{fL}\gamma_L + \delta g_{fR}\gamma_R\right) f\right] Z_\mu \,, \tag{3.23}$$

with [142] $z := (M^2_Z - m^2_Z)/m^2_Z$ and

$$\delta g_{fL(R)} = (c_\xi - 1)\, \hat{g}_{fL(R)} + s_\xi \left(\mathrm{sh}\,\eta\, \hat{s}_W (Q_f \hat{c}^2_W - \hat{g}_{fL(R)}) + \mathrm{ch}\,\eta\, \frac{g_X}{\hat{e}_Z} X_{fL(R)} \right) . \tag{3.24}$$

The last step before comparing these expressions with observations is to eliminate the parameters $\hat{s}_W$ and m_Z (the second of which enters the interactions through r_X) from the lagrangian in favour of a physically defined weak mixing angle, s_W, and the physical mass, M_Z. This process reveals the physical combination of new-physics parameters that is relevant to observables, and thereby provides a derivation [142] of the X-boson contributions to the oblique electroweak parameters [143–146].

To this end define the physical weak mixing angle, s_W, so that the Fermi constant, G_F, measured in muon decay is given by the SM formula,

$$\frac{G_F}{\sqrt{2}} := \frac{e^2}{8 s^2_W c^2_W M^2_Z} \,. \tag{3.25}$$

But this can be compared with the tree-level calculation of the Fermi constant obtained from W-exchange using the above lagrangian, giving (see appendix)

$$\hat{s}^2_W = s^2_W \left[1 + \frac{z\, c^2_W}{c^2_W - s^2_W}\right] , \tag{3.26}$$

to linear order in z (which we assume is small — as is justified shortly by the phenomenological bounds).

JHEP08(2011)106

Eliminating $\hat{s}_W$ in favour of s_W in the fermionic weak interactions introduces a further shift in these couplings, leading to our final form for the neutral-current lagrangian:

$$\mathcal{L}_{\rm NC} = ie_Z \sum_f \overline{f}\gamma^\mu \left[\left(g_{fL}^{\rm SM} + \Delta g_{fL} \right) \gamma_L + \left(g_{fR}^{\rm SM} + \Delta g_{fR} \right) \gamma_R \right] f\, Z_\mu \,, \tag{3.27}$$

where $e_Z := e/s_W c_W$ and

$$\begin{aligned} \Delta g_{fL(R)} &= -\frac{z}{2} g_{fL(R)}^{\rm SM} - z \left(\frac{s_W^2 c_W^2}{c_W^2 - s_W^2} \right) Q_f + \delta g_{fL(R)} \\ &= \frac{\alpha T}{2}\, g_{fL(R)}^{\rm SM} + \alpha T \left(\frac{s_W^2 c_W^2}{c_W^2 - s_W^2} \right) Q_f + \delta g_{fL(R)} \,. \end{aligned} \tag{3.28}$$

The SM couplings are (as usual) $g_{fL}^{\rm SM} := T_{3f} - Q_f s_W^2$ and $g_{fR}^{\rm SM} := -Q_f s_W^2$, while the oblique parameters [143–146] S, T and U are given by

$$\alpha S = \alpha U = 0 \,, \tag{3.29}$$

and

$$\alpha T = -z \,. \tag{3.30}$$

3.2.2 Direct X-boson couplings

The terms explicitly involving the X boson similarly are

$$\mathcal{L}_X = -\frac{1}{4} X_{\mu\nu} X^{\mu\nu} - \frac{M_X^2}{2} X_\mu X^\mu + i \sum_f \overline{f} \gamma_\mu \left(k_{fL} \gamma_L + k_{fR} \gamma_R \right) f X^\mu \,,$$

with

$$k_{fL(R)} = c_\xi \,\mathrm{ch}\,\eta\, g_X X_{fL(R)} + c_\xi \,\mathrm{sh}\,\eta\, \frac{e}{c_W} (Q_f c_W^2 - g_{fL(R)}^{\rm SM}) - s_\xi\, e_Z g_{fL(R)}^{\rm SM} \,. \tag{3.31}$$

We are now in a position to compute how observables depend on the underlying parameters, and so bound their size. When doing so we follow [142] and work to linear order in the deviations, $\Delta g_{fL(R)}$, of the SM couplings, since we know these are observationally constrained to be small.

4 High-energy constraints

This section considers the constraints on the X boson coming from its influence on various precision electroweak observables measured at high-energy colliders. There are two main types of observables to consider: those that test the changes that X-boson mixing induces in SM couplings; and those sensitive to the direct couplings of the X boson to SM fermions. We consider each type in turn.

We begin with two well-measured observables that are sensitive only to changes to the SM self-couplings: the W boson mass, M_W, and the Z-boson branching fraction into leptons, $\Gamma(Z \to \ell^+\ell^-)$. Later subsections then consider reactions to which direct X exchange can contribute, such as the cross section, $\sigma_{\rm res}(e^+e^- \to h)$, for electron-positron annihilation into hadrons evaluated at the Z resonance.

JHEP08(2011)106

Consistency limits on accessible parameter space Since the SM is in such good agreement with experiment [147], it is useful to linearize corrections to the SM parameters as we have done in the previous section. To be consistent, we limit ourselves to considering the subset of parameter space which is consistent with this linearization procedure. In practice, we require that the following two conditions of z be satisfied:

1. z must be real (see the discussion in the appendix), which amounts to demanding that it is obtained by a physically allowed choice for the initial parameters m_X and χ. This implies that
$$\Delta_X^2 - R_X^2 s_W^2 \mathrm{sh}^2\eta \geq 0\,, \tag{4.1}$$
where Δ_X is defined in eq. (A.28). This simplifies to
$$|\Delta_X - \kappa| \geq \sqrt{\kappa(\kappa+1)} \tag{4.2}$$
where
$$\kappa := s_W^2 \mathrm{sh}^2\eta\,. \tag{4.3}$$

2. z must be small: $z \ll 1$. To quantify this statement, we assume that z (or, equivalently, αT) will be at most within 2σ from its global fit value [142]:
$$|z| \leq 0.014\,. \tag{4.4}$$
This bound has been considered in [148] in the context of hidden sector dark matter models.

In figure 3, we show the regions in the $M_X - \mathrm{sh}\,\eta$ parameter space that are excluded by each of these bounds. From this, we see that the first condition is dominant when $\mathrm{sh}\,\eta < 3\times 10^{-2}$, whereas for greater values of $\mathrm{sh}\,\eta$, it is the second condition that is dominant.

4.1 Effects due to modified W, Z couplings

We start with several examples of constraints that probe the induced changes to the SM self-couplings.

4.1.1 The W mass

Mixing with the X boson modifies the SM prediction for the W mass due to its contribution to the electroweak oblique parameter T, as follows [142–146]:

$$\begin{aligned} M_W^2 &= m_W^2 = m_Z^2\left(1-\hat{s}_W^2\right) && (4.5)\\ &= \left[M_Z^2\left(1+\alpha T\right)\right]\left[1-s_W^2\left(1-\frac{c_W^2\,\alpha T}{c_W^2-s_W^2}\right)\right] && (4.6)\\ &\simeq (M_W^2)_{\mathrm{SM}}\left[1+\alpha T\left(1+\frac{s_W^2}{c_W^2-s_W^2}\right)\right]\,, && (4.7)\end{aligned}$$

where $(M_W^2)_{\mathrm{SM}}$ is the full SM prediction, including radiative corrections: $(M_W^2)_{\mathrm{SM}} = M_Z^2(1-s_W^2)+$ loops. Because both the SM radiative corrections and the oblique corrections are known to be small, we can neglect their product in the above expression.

JHEP08(2011)106

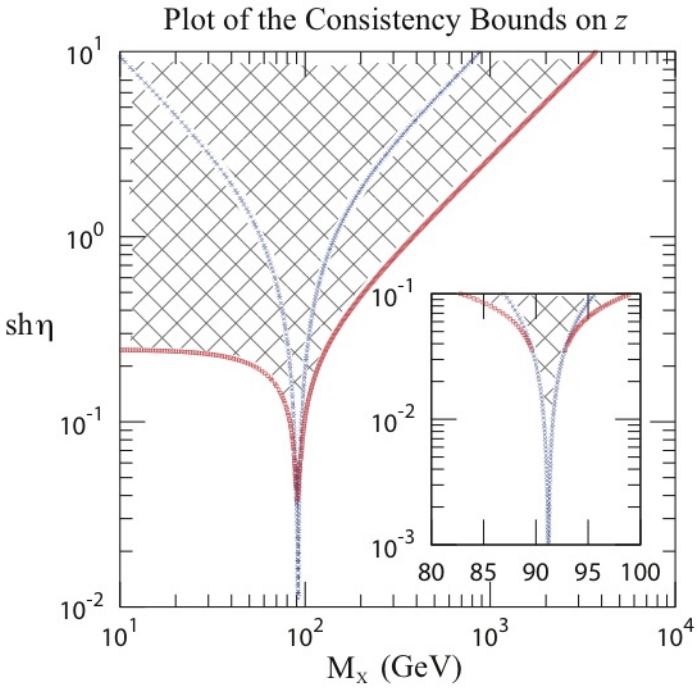

Figure 3. Plot of the bounds on z as a function of M_X and $\mathrm{sh}\,\eta$. The blue crosses limit the region in which z is real, and the red squares limit the region in which $z \ll 1$. The hatched regions are excluded.

At this point one might ask why bother examine the W mass correction separately, since the W mass is one of the observables included in the global fits to oblique parameters, and we have already assumed that z must be small enough to ensure that the oblique parameter T lies within its 2-σ range obtained from global electroweak fits (as in figure E.2 of [147]). The reason we re-examine the W mass is that it leads to a slightly stronger constraint, because the mixing between the Z and X bosons does not contribute to the S parameter, and this prior information leads to a slightly stronger limit on T (as is shown in figure 4).

Using the result, eq. (3.30), $\alpha T = -z$ together with eq. (A.27) for z as a function of η and M_X gives the desired expression for ΔM_W as a function of η and M_X. In the limit when the Z and X masses are very close to one another — i.e. when Δ_X is such that the equality in eq. (4.2) holds — the expression for z becomes

$$z = \frac{\kappa - \Delta_X}{1 + \Delta_X} = -\vartheta_X s_W |\eta| + s_W^2 \eta^2 + \mathcal{O}(\eta^3) \qquad \text{(near-degenerate } Z \text{ and } X \text{ masses)}\,, \quad (4.8)$$

and so

$$|\Delta M_W| \simeq M_Z c_W \left[\frac{c_W^2}{c_W^2 - s_W^2}\left(\frac{s_W|\eta|}{2}\right)\right] \simeq 2.75 \text{ GeV}\left(\frac{\eta}{0.1}\right)\,. \quad (4.9)$$

JHEP08(2011)106

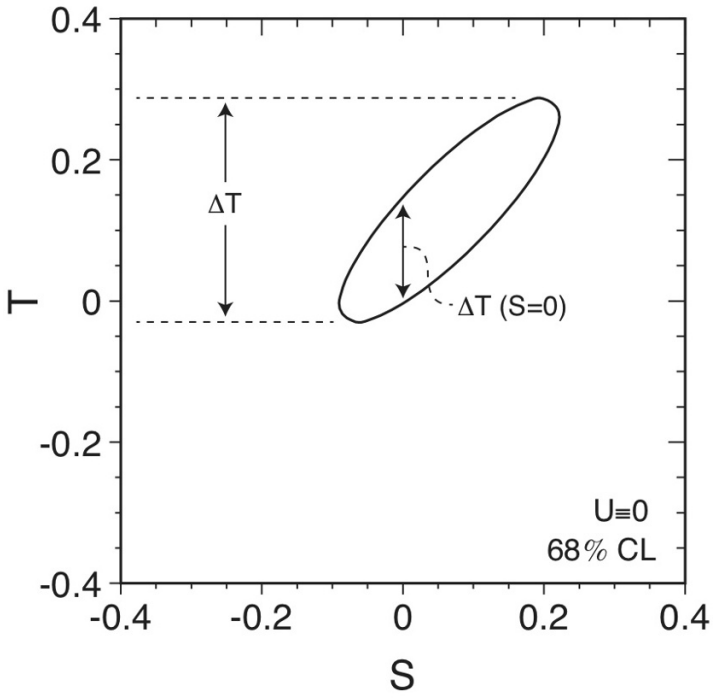

Figure 4. Plot of the EWWG bound on the S and T oblique parameters, showing how T is more tightly constrained given prior knowledge that $S = 0$.

Moving away from degeneracy, we find the expression for z can be simplified as follows:

$$z = \frac{\kappa - \Delta_X \left(1 - \sqrt{1 - \frac{\kappa R_X^2}{\Delta_X^2}}\right)}{1 + \Delta_X \left(1 - \sqrt{1 - \frac{\kappa R_X^2}{\Delta_X^2}}\right)} = \kappa - \frac{\kappa R_X^2}{2\Delta_X} + \mathcal{O}(\kappa^2) = \frac{s_W^2 \eta^2}{1 - R_X^2} + \mathcal{O}(\eta^4)\,, \tag{4.10}$$

where $R_X := M_X/M_Z$ (cf. eq. (A.22)). So when M_X and M_Z are very different,

$$\Delta M_W \simeq \frac{s_W^2 c_W^3}{2(c_W^2 - s_W^2)} \left(\frac{\eta^2 M_Z^3}{M_X^2 - M_Z^2}\right) \simeq 1.10 \times 10^5 \left(\frac{\eta^2}{M_X^2 - M_Z^2}\right) \text{ GeV}^3\,. \tag{4.11}$$

The large-M_X limit of eq. (4.11) agrees with the result given in [133], which finds

$$\Delta M_W \simeq (17 \text{ MeV}) \left(\frac{\eta}{0.1}\right)^2 \left(\frac{250 \text{ GeV}}{M_X}\right)^2\,. \tag{4.12}$$

The experimental agreement of the measured W mass with the SM prediction implies $\Delta M_W \leq 0.05\,\text{GeV}$ [149] (2σ uncertainty), and the constraint this imposes on $\sh\,\eta$ as a function of M_X is shown in figure 5. Several points about the comparison given in the figure are of note:

- The W-mass bound on η is model-independent inasmuch as it relies only on the kinetic mixing and does not depend at all on the fermion quantum numbers to which X couples;

JHEP08(2011)106

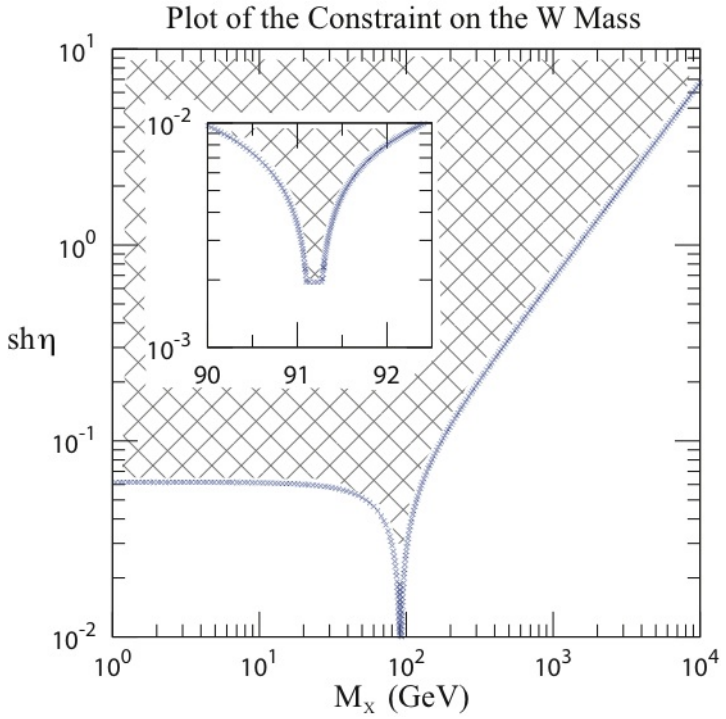

Figure 5. Constraint obtained from limiting the influence of kinetic mixing on the SM value of the W mass. The hatched regions are excluded.

- The strongest constraints on η occur for M_X nearest to the Z pole, where $|\eta_{\rm pole}| \leq 1.8 \times 10^{-3}$;
- When $M_X \ll M_Z$, the bound on η becomes approximately M_X-independent: $|\eta| \leq 6.2 \times 10^{-2}$. This behaviour is also visible in the analytic expression, eq. (4.11);
- When $M_X \gg M_Z$, the W mass bounds the ratio η/M_X: giving $M_X/\eta \gtrsim 1.5\,\text{TeV}$.

4.1.2 Z decay

The Z decay rate has been measured with great accuracy at LEP and SLC (for details regarding their analysis, see [147]). The experimental value [149] for the decay $Z \to \ell^+\ell^-$, where ℓ can be any of the charged leptons, is $\Gamma_{\ell^+\ell^-} = 83.984 \pm 0.086\,\text{MeV}$ ($1\,\sigma$), and agrees well with the SM result [149] $83.988 \pm 0.016\,\text{MeV}$. The modified Z-fermion couplings change the tree-level decay rate,

$$\Gamma_{\ell^+\ell^-} = \frac{M_Z e_Z^2}{24\pi}\left(g_{\ell L}^2 + g_{\ell R}^2\right)\,, \tag{4.13}$$

where the couplings $g_{\ell I} = g_{\ell I}^{\rm SM} + \Delta g_{\ell I}$ (with $I = L, R$) are defined by the interaction (3.27). The deviation from the SM prediction therefore is

$$\Delta\Gamma_{\ell^+\ell^-} := \Gamma_{\ell^+\ell^-} - \Gamma_{\ell^+\ell^-}^{\rm SM} \simeq \frac{M_Z e_Z^2}{24\pi} \sum_{I=L,R} \left[2 g_{\ell I}^{\rm SM} + \Delta g_{\ell I}\right] \Delta g_{\ell I}\,. \tag{4.14}$$

JHEP08(2011)106

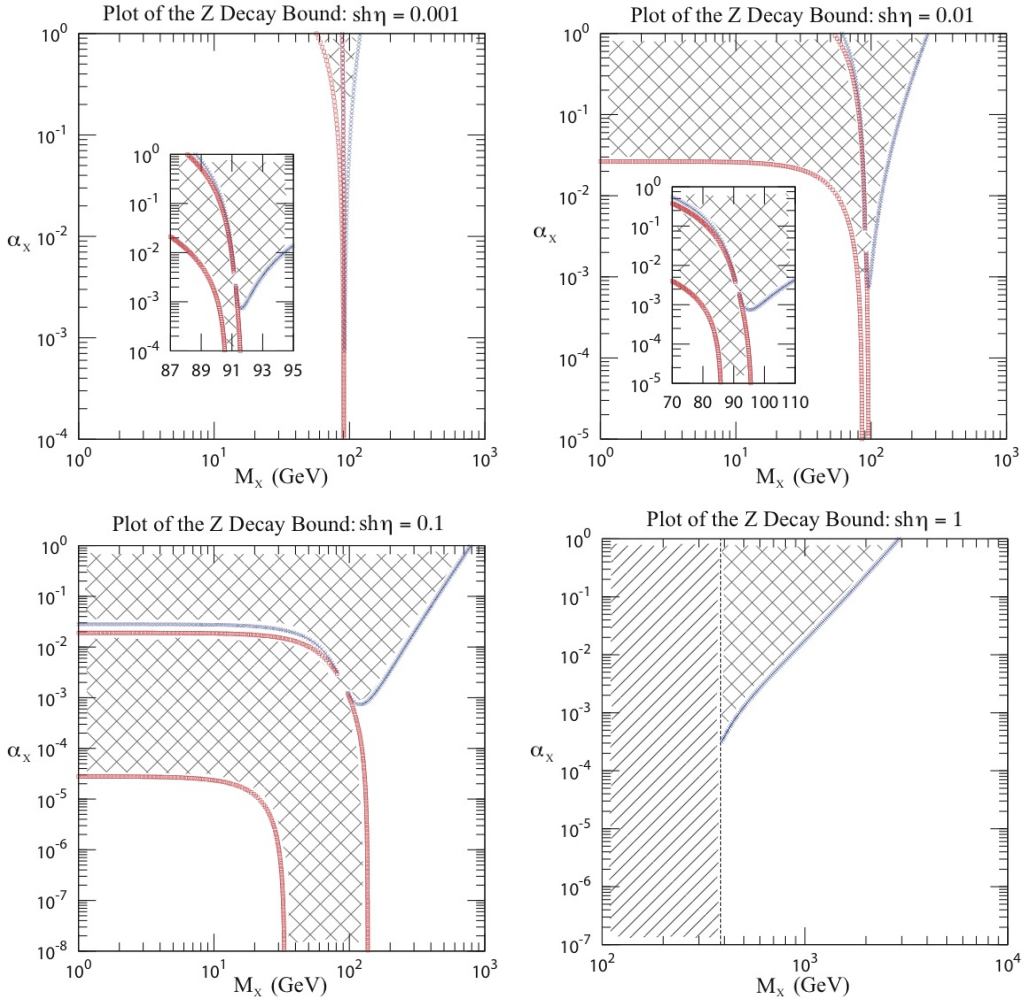

Figure 6. The constraint arising from $Z \to \ell^+\ell^-$ decay on the coupling $\alpha_X = g_X^2/4\pi$ as a function of M_X, for various values of $\mathrm{sh}\,\eta$. The parameters agreeing with the positive bound ($\Delta\Gamma = +\Delta\Gamma_{\mathrm{exp}}$) are marked with blue crosses, while those agreeing with the negative bound ($\Delta\Gamma = -\Delta\Gamma_{\mathrm{exp}}$) are marked with red squares. The plot assumes a coupling $X_{\ell_L} = X_{\ell_R} = -1$, such as would be true if $X = B - L$. Hatched regions are excluded.

Notice that this vanishes if $\Delta g_{\ell I} = 0$ or when $\Delta g_{\ell I} = -2g_{\ell I}^{\mathrm{SM}}$. It can therefore happen that $\Delta\Gamma_{\ell^+\ell^-}$ vanishes for two separate regions as one varies through parameter space.

To obtain bounds on η and M_X we use eq. (3.28) to eliminate $\Delta g_{f L(R)}$, giving

$$g_{\ell I} = \left(c_\xi - \frac{z}{2}\right)\left(-\frac{1}{2}\,\delta_{IL} + s_W^2\right) + \frac{z c_W^2 s_W^2}{c_W^2 - s_W^2} - s_\xi\left[\left(-\frac{1}{2}\,\delta_{IL} + 1\right) s_W \mathrm{sh}\,\eta - X_{\ell I}\frac{g_X}{e_Z}\mathrm{ch}\,\eta\right] \tag{4.15}$$

Here $-\frac{1}{2}\,\delta_{IL} + s_W^2$ is the SM contribution, $g_{\ell I}^{\mathrm{SM}}$, where δ_{IL} denotes a Kronecker delta function. Requiring $\Delta\Gamma_{\ell^+\ell^-}$ to be smaller than the experimental (2 σ) experimental error gives the desired bound on the parameters g_X, η and M_X. Figure 6 shows the excluded values in the $\alpha_X = g_X^2/4\pi$ vs M_X plane, with the leptonic X-boson charge assumed to be $X_{\ell_L} = X_{\ell_R} = -1$ (such as would apply if $X = B - L$). Each panel of the figure corresponds to a different

JHEP08(2011)106

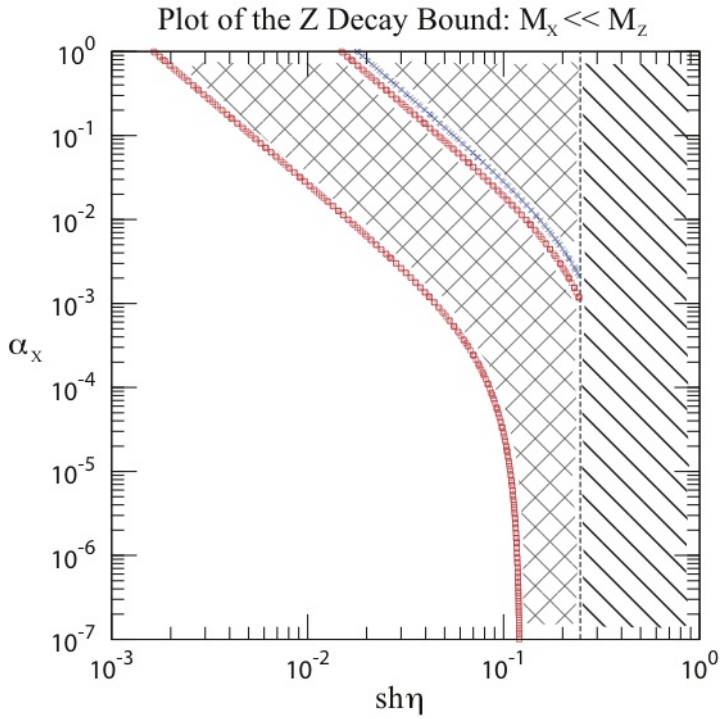

Figure 7. Plot of the constraint arising from considering Z decay into leptons in the limit where $M_X \ll M_Z$. The upper bound ($\Delta\Gamma = +\Delta\Gamma_{\rm exp}$) is marked with blue crosses; the lower bound ($\Delta\Gamma = -\Delta\Gamma_{\rm exp}$) is marked with red squares. Hatched regions are excluded.

choice for $\sh\,\eta$. For the panel in which $\sh\,\eta = 1$ bounds at lower mass scales than roughly 385 GeV are not plotted, since these would conflict with a $z = -\alpha T$ satisfying the global electroweak fit, as outlined in figure 3.

In order to understand the features present in the plots it is useful to consider the small-η limit of z and ξ. As discussed above for the W mass bound, the small-η limit when M_X and M_Z are very similar or very different must be considered separately. The expressions when M_X and M_Z are very different are

$$z \simeq \frac{s_W^2 \eta^2}{1 - R_X^2} \quad \text{and} \quad \xi \simeq \frac{s_W \eta}{R_X^2 - 1}\,. \tag{4.16}$$

As might be expected, all terms in $\Delta g_{\ell I}$ are suppressed by a factor of $1/R_X^2 \simeq M_Z^2/M_X^2$ and so go to zero when $M_X \gg M_Z$. In the opposite limit, $R_X \to 0$, $\Delta g_{\ell I} \simeq X_{\ell I}\eta s_W (g_X/e_Z) + \eta^2 s_W^2 c_W^4/(c_W^2 - s_W^2)$, which can pass through zero (if $X_{\ell I}\eta < 0$) when $|X_{\ell I}|(g_X/e_Z) \simeq \mathcal{O}(\eta)$.

Several features of these plots should be highlighted:

- The best bounds come for $M_X \simeq M_Z$, even for small couplings g_X, because in this limit the $Z-X$ mixing parameter ξ becomes maximal ($\tan 2\xi \to \infty$), leading to strong constraints.

- For a similar reason, once η is sufficiently large ($\sh\,\eta \simeq 0.1$ — see also figure 7) the regime of vanishingly small α_X remains excluded because $\Delta g_{\ell L(R)}$ is dominated by the oblique corrections to the weak mixing angle.

JHEP08(2011)106

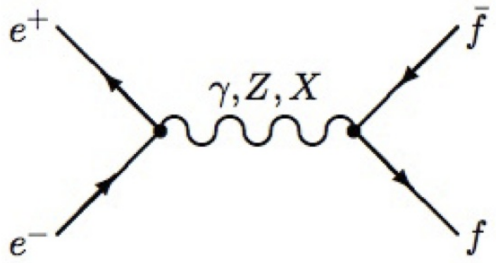

Figure 8. Relevant tree-level Feynman diagrams corresponding to electron-positron annihilation into fermion-antifermion pairs.

- For $M_X \gg M_Z$ the excluded area approaches a straight line, corresponding to a bound on the ratio g_X/M_X^2, as expected from the form of $\Delta g_{\ell L(R)}$.
- The graph is more intricate for $M_X \ll M_Z$, with slivers of allowed parameter space emerging for a narrow, η-dependent but M_X-independent, value of α_X. This happens (for sufficiently large η) because $\Delta\Gamma = 0$ is a multiple-valued condition on the parameters, as discussed above.

Figure 7 provides a view of the bounds taken on a different slice through the three-dimensional parameter space (η, α_X, M_X). This figure plots the constraints on α_X vs $\mathrm{sh}\,\eta$, in the regime where $M_X \ll M_Z$, showing how a wider range of α_X is allowed as $\mathrm{sh}\,\eta$ shrinks. Note that bounds are only shown for the region where $z \ll 1$.

4.2 Processes involving X-boson exchange

In this section we consider precision electroweak observables, like the resonant cross section for $e^+e^- \to$ hadrons, that receive direct contributions from X-boson exchange, in addition to the modifications to SM Z-boson couplings.

4.2.1 The annihilation cross section

We again proceed by computing the leading change to the tree-level cross section for $e^+e^- \to f\overline{f}$ at leading order in the new interactions. Interference terms between SM loops and X-boson contributions may be neglected under the assumption that their product is negligible [142]. The relevant Feynman diagrams are shown in figure 8, where the exchanged boson is either a photon, Z or X boson.

Neglecting fermion masses the relevant spin-averaged squared matrix element for this process is (see, e.g. [72] for a treatment of SM scatterings using similar conventions)

$$\frac{1}{4}\sum |\mathcal{M}|^2 = N_c\left[\left(|A_{LL}(s)|^2 + |A_{RR}(s)|^2\right)u^2 + \left(|A_{LR}(s)|^2 + |A_{RL}(s)|^2\right)t^2\right], \quad (4.17)$$

where s, t and u are the usual Mandelstam variables and

$$A_{IJ}(s) := \frac{e^2 Q_e Q_f}{s} + \frac{e_Z^2 g_{eI} g_{fJ}}{s - M_Z^2 + i\Gamma_Z M_Z} + \frac{k_{eI} k_{fJ}}{s - M_X^2 + i\Gamma_X M_X}. \quad (4.18)$$

The total unpolarized cross section that follows from this is

$$\sigma\left(e^+e^- \to f\overline{f}\right) = \frac{N_c s}{48\pi}\left(|A_{LL}|^2 + |A_{RR}|^2 + |A_{LR}|^2 + |A_{RL}|^2\right) . \tag{4.19}$$

The couplings g_{fI} and k_{fI} in these expressions are defined in terms of η, g_X and M_X by eqs. (3.28) and (3.31). The quantities Γ_Z and Γ_X are only important near resonance, and denote the full decay widths for the Z and X boson, respectively:

$$\Gamma_Z = \frac{e_Z^2 M_Z}{24\pi} \sum_{2m_f \le M_Z} \left[g_{fL}^2 + g_{fR}^2\right] N_c \tag{4.20}$$

$$\text{and} \quad \Gamma_X = \frac{M_X}{24\pi} \sum_{2m_f \le M_X} \left[k_{fL}^2 + k_{fR}^2\right] N_c\,, \tag{4.21}$$

where N_c is the colour degeneracy for fermion f.

4.2.2 The hadronic cross section at the Z pole

Summing the above over all quarks lighter than M_Z and evaluating at $\sqrt{s} = M_Z$ gives the leading correction to the resonant cross section into hadrons, $\sigma_{had}\left(s = M_Z^2\right)$, which is well-measured to be 41.541 ± 0.037 nb [149]. Requiring the deviation from the SM to be smaller than the 2σ error gives the desired constraints. Figure 9 shows a number of exclusion limits for the coupling α_X vs the X-boson mass (for $X_{fL} = X_{fR} = (B-L)_f$, and M_X in the range of $10 - 10^3$ GeV), with each panel corresponding to a different choice for η.

These plots reflect several features seen in the analytic expressions for the couplings:

- For $M_X \ll M_Z$ and when η is small enough, the mass dependence of the bound on α_X completely drops out, leaving $\alpha_X \lesssim 10^{-2}$ in this limit. For larger η small values of α_X can still be ruled out because the contributions of mixing are already too large. This mixing also ensures that the region near $M_X = M_Z$ tends to give the strongest bounds.

- The regime $M_X \gg M_Z$ similarly constrains only the combination $M_X^2/\alpha_X \gtrsim 800\,\text{GeV}$ (when η is small).

- For η not too small and M_X smaller than M_Z, figure 9 shows a window of unconstrained couplings, for the same kinds of reasons discussed above for $\Gamma_{\ell^+\ell^-}$.

Figure 10 shows a sample slice of the constraint region in the α_X vs $\sh\eta$ plane, in the limit $M_X \ll M_Z$. Once again, bounds are not plotted within regions of parameter space for which z is not $\ll 1$. This plot shows that the smallest η for which small α_X can be ruled out is $\sh\eta \gtrsim 0.06$. Once η is larger than this, mixing rules out the X boson even with arbitrarily small gauge couplings.

JHEP08(2011)106

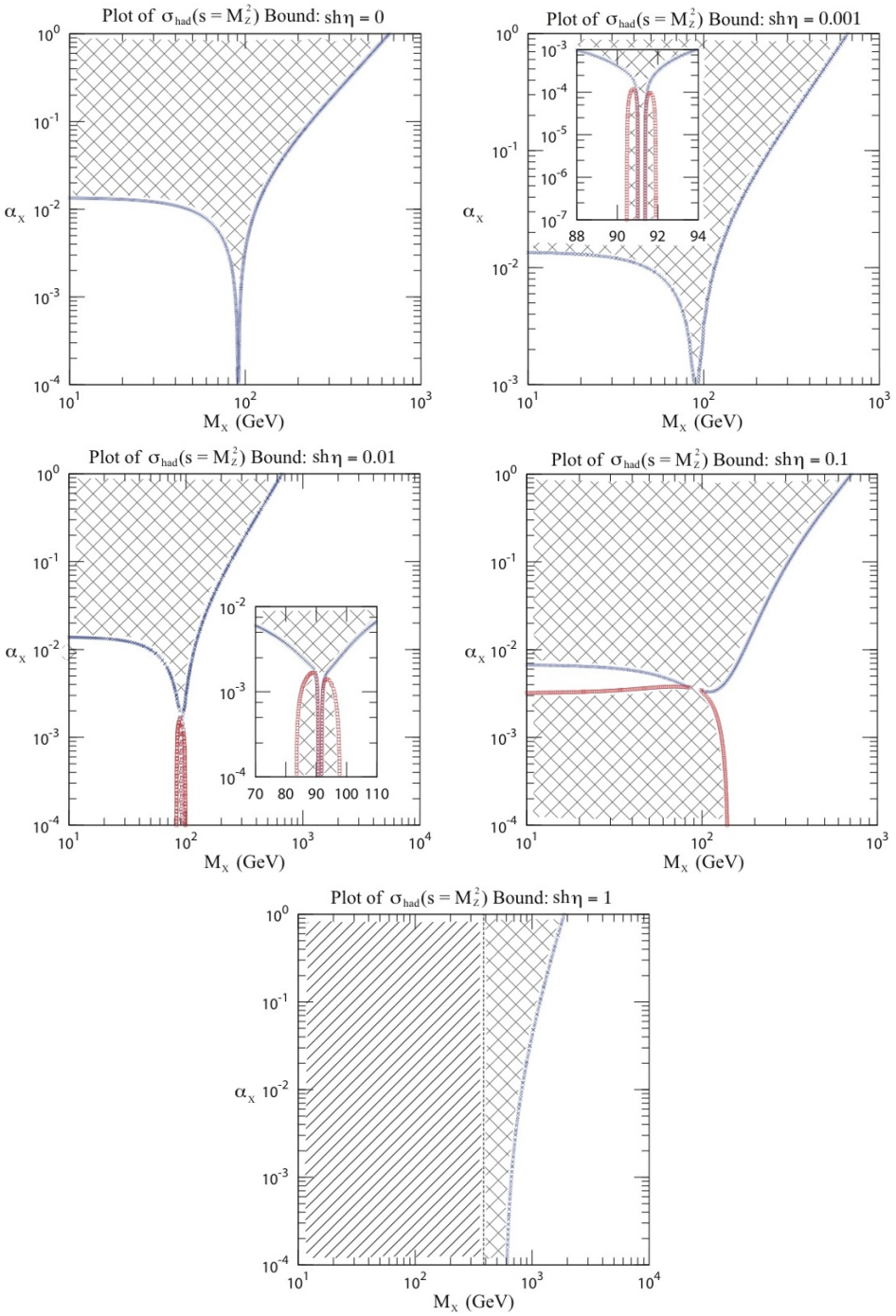

Figure 9. The constraint obtained from σ_{had} evaluated for $\sqrt{s} = M_Z$, as a bound in the $\alpha_X - M_X$ plane for various values of sh η. Blue crosses (red squares) indicate parameters where predictions differ by $2\,\sigma$ from experiment on the upper (lower) side. The hatched regions are excluded, while diagonal shading indicates a region excluded by global fits to oblique parameters.

JHEP08(2011)106

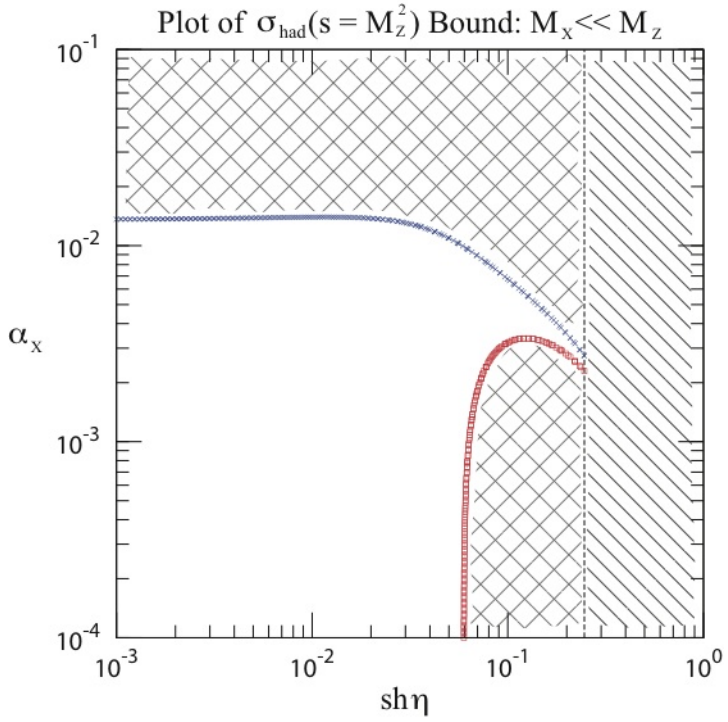

Figure 10. Plot of the constraint from $\sigma_{had}\left(s = M_Z^2\right)$ in the region where $M_X \ll M_Z$. The parameters agreeing with the positive bound are marked with blue crosses, while those agreeing with the negative bound are marked with red squares. The hatched regions are excluded.

5 Constraints at intermediate energies

Better constraints on lower-mass X bosons can be obtained from low-energy scattering of muon neutrinos with electrons and nuclei. The purpose of this section is to quantify these bounds by identifying how the cross section depends on the parameters g_X, η and M_X. We consider electron and nuclear scattering in turn.

5.1 Neutrino-electron scattering

The Feynman graphs relevant for $\nu_\mu e^- \to \nu_\mu e^-$ scattering are those of figure 8, with three changes: (i) the gauge bosons are exchanged in the t-channel rather than s-channel; (ii) there is no photon-exchange graph and (iii) omission of right-handed neutrino polarizations.

Crossing to t-channel can be obtained by performing the following substitution

$$s \to t,\ t \to u,\ u \to s \tag{5.1}$$

among the Mandelstam variables in the invariant amplitude $\frac{1}{2}\sum|\mathcal{M}|^2$. With these replacements, the differential cross section for the process $\nu_\mu e^- \to \nu_\mu e^-$ is

$$\frac{\mathrm{d}\sigma}{\mathrm{d}t}\left(\nu_\mu e^- \to \nu_\mu e^-\right) = -\frac{1}{8\pi s^2}\left[|A_{LL}(t)|^2 s^2 + |A_{RL}(t)|^2 (s+t)^2\right], \tag{5.2}$$

where

$$A_{IJ}(t) = e_Z^2 \frac{g_{eI} g_{\nu J}}{t - M_Z^2} + \frac{k_{eI} k_{\nu J}}{t - M_X^2}. \tag{5.3}$$

JHEP08(2011)106

In the rest frame of the initial electron $s \simeq 2\, m_e E_\nu$ and $t \simeq -2y\, m_e E_\nu$, where E_ν is the incoming neutrino energy and y is the fractional neutrino energy loss, $y := E_e^f / E_\nu$ where E_e^f is the energy of the outgoing electron. (In such experiments [150–152], E_ν, $E_e^f \sim 1\text{–}10\,\text{GeV}$ so ratios of the form m_e/E_ν and m_e/E_e^f can be neglected.) In terms of these new variables the differential cross section is

$$\frac{\mathrm{d}\sigma}{\mathrm{d}y}\left(\nu_\mu e^- \to \nu_\mu e^-\right) = \frac{m_e E_\nu}{4\pi}\left[\left|A_{LL}[t(yE_\nu)]\right|^2 + \left|A_{RL}[t(yE_\nu)]\right|^2 (1-y)^2\right] . \tag{5.4}$$

The cross section for anti-neutrino scattering is easily found from the above by interchanging $A_{LL} \leftrightarrow A_{RL}$.

5.1.1 Special case: Low-energy limit with $\eta = 0$

One case of practical interest is when the boson masses, M_Z and M_X, are much greater than the invariant energy exchange in the process of interest (i.e. $\sqrt{|t|} \ll M_X, M_Z$). When this holds the amplitudes, A_{IL}, can be simplified to

$$\begin{aligned} A_{IL} &\simeq -\frac{e_Z^2 g_{eI} g_{\nu L}}{M_Z^2} - \frac{k_{eI} k_{\nu L}}{M_X^2} \\ &= -\frac{e_Z^2 g_{\nu L}}{M_Z^2}\left[g_{eI} + \frac{M_Z^2}{M_X^2}\left(\frac{k_{\nu L} k_{eI}}{e_Z^2 g_{\nu L}}\right)\right] , \end{aligned} \tag{5.5}$$

allowing the effects of X-boson exchange be interpreted as an effective shift in the electron's electroweak couplings. For $E_\nu \simeq 1\,\text{GeV}$ and y order unity this approximation remains good down to $M_X \simeq 30\,\text{MeV}$.

The resulting cross section is particularly simple in the case of no kinetic mixing, for which we can substitute the SM values $g_{eI} = -\frac{1}{2}\delta_{IL} + s_W^2$ and $g_{\nu L} = \frac{1}{2}$ and the X-boson couplings $k_{eI} = g_X X_{eI}$ and $k_{\nu J} = g_X X_{\nu J}$, and obtain

$$A_{IL} \simeq -2\sqrt{2}\, G_F \left(-\frac{1}{2}\,\delta_{IL} + s_W^2 + \frac{g_X^2 X_{eI} X_{\nu L}}{2\sqrt{2}\, G_F M_X^2}\right) , \tag{5.6}$$

using the SM result $2\sqrt{2}\, G_F \simeq e_Z^2/2M_Z^2$. We see that the X-boson contribution can be regarded as an additional contribution to s_W^2 in this limit. This is convenient because it allows the simple use of constraints on s_W^2 to directly constrain the ratio g_X^2/M_X^2.

The bounds are usually taken from the following ratio [151, 152] of total cross sections,

$$R := \frac{\sigma(\nu_\mu e^- \to \nu_\mu e^-)}{\sigma(\overline{\nu}_\mu e^- \to \overline{\nu}_\mu e^-)} . \tag{5.7}$$

Given the differential cross section

$$\frac{\mathrm{d}\sigma}{\mathrm{d}y}\left(\nu_\mu e^- \to \nu_\mu e^-\right) = \frac{2G_F^2 m_e E_\nu}{\pi}\left[g_{eL}^2 + g_{eR}^2 (1-y)^2\right] , \tag{5.8}$$

the total cross section becomes

$$\sigma\left(\nu_\mu e^- \to \nu_\mu e^-\right) = \frac{2G_F^2 m_e E_\nu}{\pi}\left(g_{eL}^2 + \frac{g_{eR}^2}{3}\right) , \tag{5.9}$$

JHEP08(2011)106

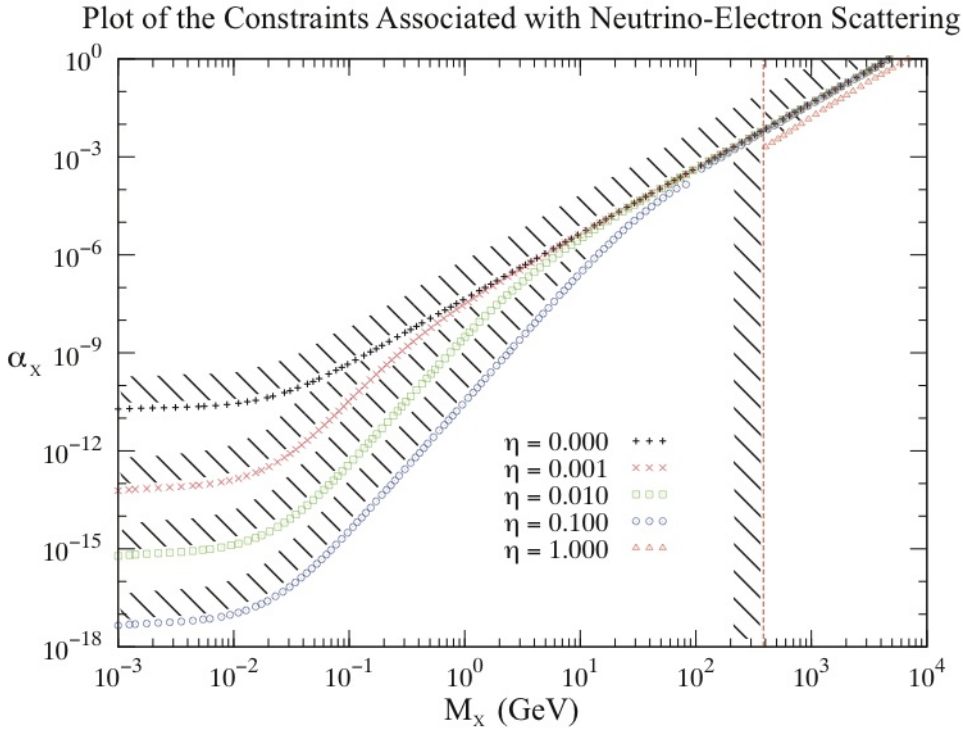

Figure 11. Bound obtained on $\alpha_X = g_X^2/4\pi$ by limiting the influence of the X boson on the $\nu - e^-$ cross section ratio R, obtained as a function of M_X for various values of $\sh\,\eta$. The vertical line indicates the region ruled out by electroweak oblique fits when $\eta = 1$.

and so

$$\sigma\left(\overline{\nu}_\mu e^- \to \overline{\nu}_\mu e^-\right) = \frac{2G_F^2 m_e E_\nu}{\pi}\left(\frac{g_{eL}^2}{3} + g_{eR}^2\right). \tag{5.10}$$

Specializing to SM couplings the result depends only on s_W:

$$R = \frac{3g_{eL}^2 + g_{eR}^2}{g_{eL}^2 + 3g_{eR}^2} = \frac{3 - 12s_W^2 + 16s_W^4}{1 - 4s_W^2 + 16s_W^4} = \frac{1 + \kappa + \kappa^2}{1 - \kappa + \kappa^2}, \tag{5.11}$$

where $\kappa \equiv 1 - 4s_W^2 \ll 1$.

Using the experimental limit [150] $\Delta s_W^2 = 0.0166$ (2σ error) with $G_F = 1.1664 \times 10^{-5}$ GeV^{-2} [149] to constrain $\Delta s_W^2 = g_X^2/2\sqrt{2}\,G_F M_X^2$ (assuming the choice $X_{eI}X_{\nu L} = 1$, as would be true for $X = B - L$ for example), gives [153]

$$\frac{M_X}{g_X} \gtrsim 4 \text{ TeV}. \tag{5.12}$$

5.1.2 General case: $\eta \neq 0$

More generally, the couplings k_{fI} also acquire contributions from $Z - X$ mixing even when $g_X = 0$, as the above calculations show. In this case the more general bounds on g_X, η and M_X can be extracted by demanding that these contribute within the experimental limit ΔR. Since the experimental limit is often quoted in terms of s_W^2 [150], we translate

JHEP08(2011)106

using $\Delta R = \left|\mathrm{d}R_{SM}/\mathrm{d}s_W^2\right| \Delta s_W^2$. In obtaining R, we integrate over y using $\sqrt{|t|} \ll M_Z^2$, but *without* assuming that $\sqrt{|t|} \ll M_X^2$. When evaluating R, we set E_ν to a nominal value of 1 GeV. Figure 11 shows the resulting bound in the $\alpha_X - M_X$ plane, for several choices for η assuming $X_{eI} X_{\nu L} = 1$.

The resulting curves inspire a few comments:

- For large M_X the bound is independent of η due to the M_X/M_Z suppression of the mixing in Δg and Δk. This allows the direct g_X^2/M_X^2 term to dominate. The bounds in this regime are relatively strong, and compete with those found in direct searches (e.g., by CDF [154] in the case of a SM-like Z').

- For smaller M_X, it is the terms in the couplings that are linear in η that influence the deviation from the $\eta = 0$ result. To see this, note that

$$\Delta g_{\nu L} = -\eta \frac{s_W}{e_Z} g_X X_{\nu L} + \mathcal{O}(\eta^2), \tag{5.13}$$

  and so there will be a term in $|A_{IL}|^2$ that is linear in η with the parametric dependence g_X/M_X^2. When $g_X \ll 0$, it is this term that is dominant compared to the g_X^2/M_X^2 term from X-boson exchange. However, when $g_X \sim \eta$, this new term is no longer dominant and the bound regresses back to its original slope from the $\eta = 0$ case at high masses.

- Once $1 \leq M_X \leq 10\,\mathrm{MeV}$ and $M_X \lesssim \sqrt{|t|}$, the bound loses its dependence on M_X and levels out to some fixed value. This is expected from the form of eq. (5.3).

- When $\mathrm{sh}\,\eta = 1$, much of the parameter space is excluded due to the requirement that $z \ll 1$. Therefore, only a small region with $M_X > 385\,\mathrm{GeV}$ is bounded by electron-neutrino scattering in this case.

5.2 Neutrino-nucleon scattering

For the bounds from neutrino-nucleon scattering it is worth first recalling how the standard analysis is performed. In terms of the neutral-current quark couplings, the quark-level cross sections for neutral-current muon-neutrino scattering are

$$\begin{aligned} \sigma\left(\nu_\mu u \to \nu_\mu u\right) &= \sigma_0 \left(g_{uL}^2 + \frac{g_{uR}^2}{3}\right), \qquad \sigma\left(\nu_\mu d \to \nu_\mu d\right) = \sigma_0 \left(g_{dL}^2 + \frac{g_{dR}^2}{3}\right) \\ \sigma\left(\overline{\nu}_\mu u \to \overline{\nu}_\mu u\right) &= \sigma_0 \left(\frac{g_{uL}^2}{3} + g_{uR}^2\right), \qquad \sigma\left(\overline{\nu}_\mu d \to \overline{\nu}_\mu d\right) = \sigma_0 \left(\frac{g_{dL}^2}{3} + g_{dR}^2\right) \end{aligned} \tag{5.14}$$

while those for charged currents are

$$\sigma\left(\nu_\mu d \to \mu^- u\right) = \sigma_0 \quad \text{and} \quad \sigma\left(\overline{\nu}_\mu u \to \mu^+ d\right) = \frac{\sigma_0}{3}, \tag{5.15}$$

where $\sigma_0 := 2 N_c G_F^2 m_e E_\nu/\pi$ and $N_c = 3$.

These show that the quark neutral-current and charged-current cross sections are all proportional to one another. The resulting cross section for neutrino-nucleon scattering in

JHEP08(2011)106

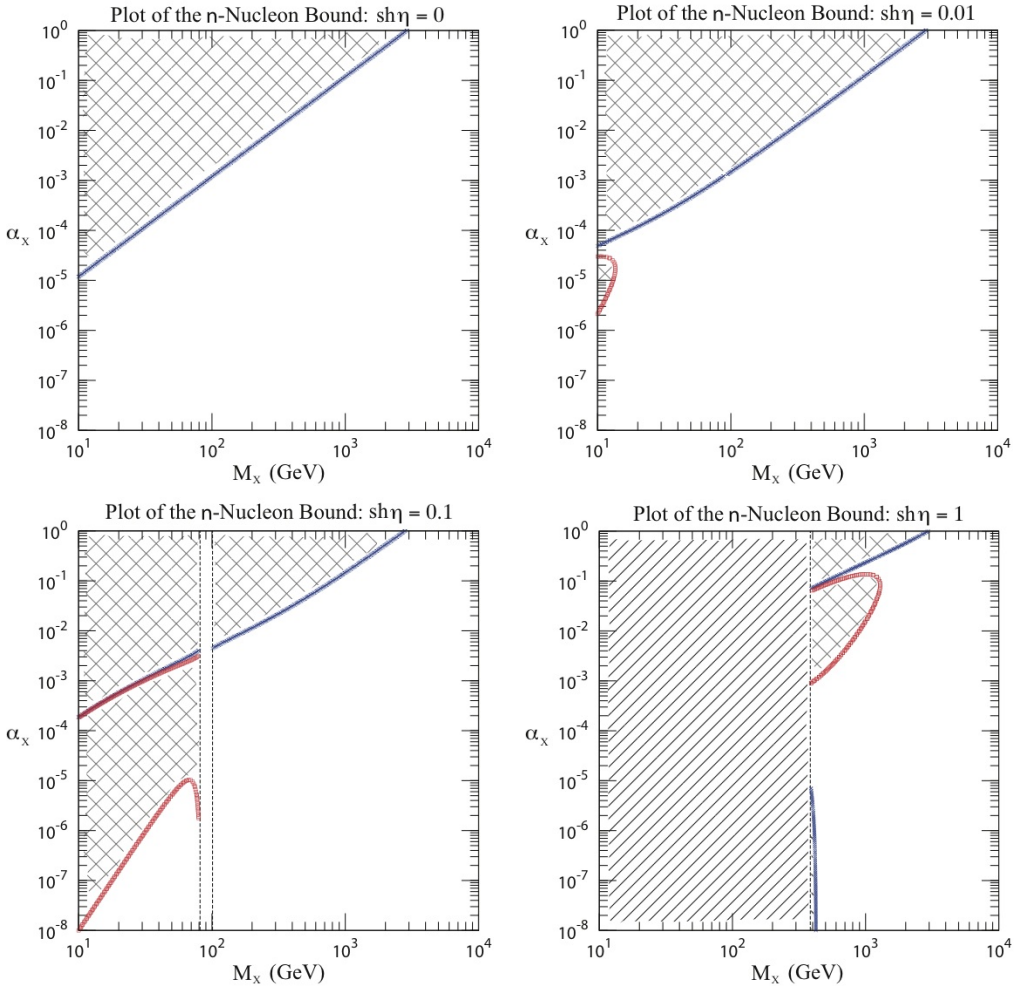

Figure 12. Plot of the constraint from R^- (neutrino-nucleon scattering) assuming $X = B - L$. Here, we plot the bound on α_X as a function of M_X for various values of η. Blue squares (red crosses) indicate parameters whose predictions lie $2\,\sigma$ above (below) the central experimental value. The vertical line indicates the region excluded by precision oblique fits.

the deep-inelastic limit is obtained by summing incoherently over the quark contributions, giving

$$\begin{aligned}\sigma\left(\nu_\mu N \to \nu_\mu X\right) &= \varepsilon_L^2\,\sigma\left(\nu_\mu N \to \mu^- X\right) + \varepsilon_R^2\,\sigma\left(\overline{\nu}_\mu N \to \mu^+ X\right)\\ \sigma\left(\overline{\nu}_\mu N \to \overline{\nu}_\mu X\right) &= \varepsilon_L^2\sigma\left(\overline{\nu}_\mu N \to \mu^+ X\right) + \varepsilon_R^2\sigma\left(\nu_\mu N \to \mu^- X\right)\,,\end{aligned} \tag{5.16}$$

where

$$\varepsilon_{L(R)}^2 := g_{uL(R)}^2 + g_{dL(R)}^2\,. \tag{5.17}$$

The experimental bounds come from the following ratios:

$$\begin{aligned}R^\nu &:= \frac{\sigma\left(\nu_\mu N \to \nu_\mu X\right)}{\sigma\left(\nu_\mu N \to \mu^- X\right)} = \varepsilon_L^2 + r\,\varepsilon_R^2\\ R^{\bar\nu} &:= \frac{\sigma\left(\overline{\nu}_\mu N \to \overline{\nu}_\mu X\right)}{\sigma\left(\overline{\nu}_\mu N \to \mu^+ X\right)} = \varepsilon_L^2 + \frac{\varepsilon_R^2}{r}\end{aligned} \tag{5.18}$$

JHEP08(2011)106

where $r := \sigma(\bar{\nu}_\mu N \to \mu^+ X)/\sigma(\nu_\mu N \to \mu^- X)$. Most useful is the Paschos-Wolfenstein ratio [155], from which the comparatively uncertain ratio r cancels:

$$R^- := \frac{R^\nu - rR^{\bar{\nu}}}{1-r} = \frac{\sigma(\nu_\mu N \to \nu_\mu X) - \sigma(\bar{\nu}_\mu N \to \bar{\nu}_\mu X)}{\sigma(\nu_\mu N \to \mu^- X) - \sigma(\bar{\nu}_\mu N \to \mu^+ X)} = \varepsilon_L^2 - \varepsilon_R^2 \,. \tag{5.19}$$

Experiments measure the following values [156]

$$\begin{aligned} \varepsilon_L^2 &= 0.30005 \pm 0.00137 \\ \varepsilon_R^2 &= 0.03076 \pm 0.00110 \,. \end{aligned} \tag{5.20}$$

To constrain the X-boson coupling parameters we work in the regime with $\sqrt{-t} \ll M_X$, for which the effects of X-boson mixing and exchange can both be rolled into a set of effective neutral-current couplings. The cross sections for quark-level scattering are then given by integrating eqs. (5.4) using (5.5), leading to expressions identical with eqs. (5.14) but with

$$g_{qI} \to g_{qI}^{\text{eff}} := 2\left[g_{qI} g_{\nu L} + \left(\frac{M_Z^2}{M_X^2}\right)\frac{k_{qI} k_{\nu L}}{e_Z^2}\right] , \tag{5.21}$$

where $q = u, d$ and $I = L, R$. Using these in eq. (5.19) gives constraints on $\varepsilon_I^2 = \left(g_{uI}^{\text{SM}} + \Delta g_{uI}^{\text{eff}}\right)^2 + \left(g_{dI}^{\text{SM}} + \Delta g_{dI}^{\text{eff}}\right)^2$.

Figure 12 plots the constraint found by requiring $\Delta\varepsilon_L^2 \leq 0.00137$, assuming that $X = B - L$. The plots are cut off at low mass where the condition $\left|t/M_X^2\right| \leq 0.01$ breaks down. Notice that for $\eta = 0$ the bound is similar to that found for neutrino-electron scattering, with stronger bounds on α_X at smaller M_X. For nontrivial η the strength of $X - Z$ mixing eventually provides the strongest constraint, leading to strong bounds even for small g_X at sufficiently low M_X.

6 Low-energy constraints

We finally turn to constraints coming from lower-energy processes.

6.1 Anomalous magnetic moments

The accuracy of anomalous magnetic moment (AMM) measurements [149] produce a strong constraint on the parameters of an extra gauge boson. We consider the bound arising from both the electron and muon AMM on the X gauge coupling as a function of the mass M_X, for various values of the kinetic mixing parameter $\text{sh}\,\eta$.

The correction to the AMM of a lepton, ℓ, is given by [16]

$$\delta a_\ell = \frac{m_\ell^2}{4\pi^2 M_X^2}\int_0^1 dz \frac{k_{\ell V}^2 z(1-z)^2 - k_{\ell A}^2\left[z(1-z)(3+z) + 2(1-z)^3 m_\ell^2/M_X^2\right]}{z + (1-z)^2 m_\ell^2/M_X^2} \,, \tag{6.1}$$

where the vector and axial couplings to the X boson are of the form

$$\begin{aligned} k_{\ell V} &:= \frac{k_{\ell L} + k_{\ell R}}{2} = c_\xi\left[\text{ch}\,\eta\, g_X X_{\ell V} - \text{sh}\,\eta\,\frac{e}{c_W}\left(-\frac{1}{4} + 1\right)\right] - s_\xi e_Z\left(-\frac{1}{4} + s_W^2\right) \\ k_{\ell A} &:= \frac{k_{\ell L} - k_{\ell R}}{2} = c_\xi\left[\text{ch}\,\eta\, g_X X_{\ell A} - \text{sh}\,\eta\,\frac{e}{c_W}\left(-\frac{1}{4}\right)\right] - s_\xi e_Z\left(-\frac{1}{4}\right) \,. \end{aligned} \tag{6.2}$$

JHEP08(2011)106

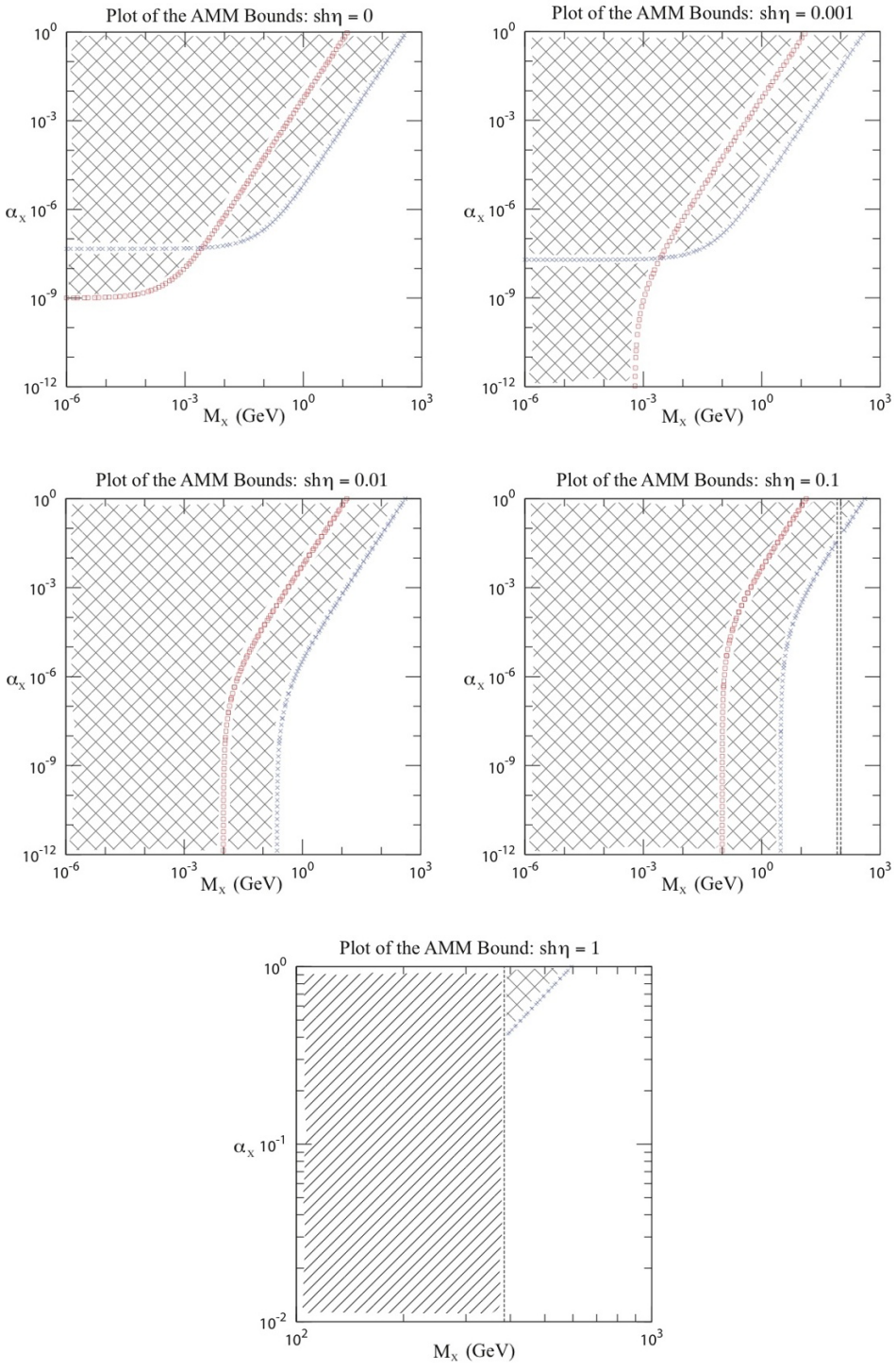

Figure 13. Plots of the constraint on the gauge coupling α_X arising from the electron and muon AMM as a function of M_X, for various values of $\sh\eta$. The electron AMM bound is marked with blue crosses; the muon AMM bound is marked with red squares. The plot assumes a coupling $X_{\ell_L} = X_{\ell_R} = -1$, such as would be true if $X = B - L$. Hatched regions are excluded.

JHEP08(2011)106

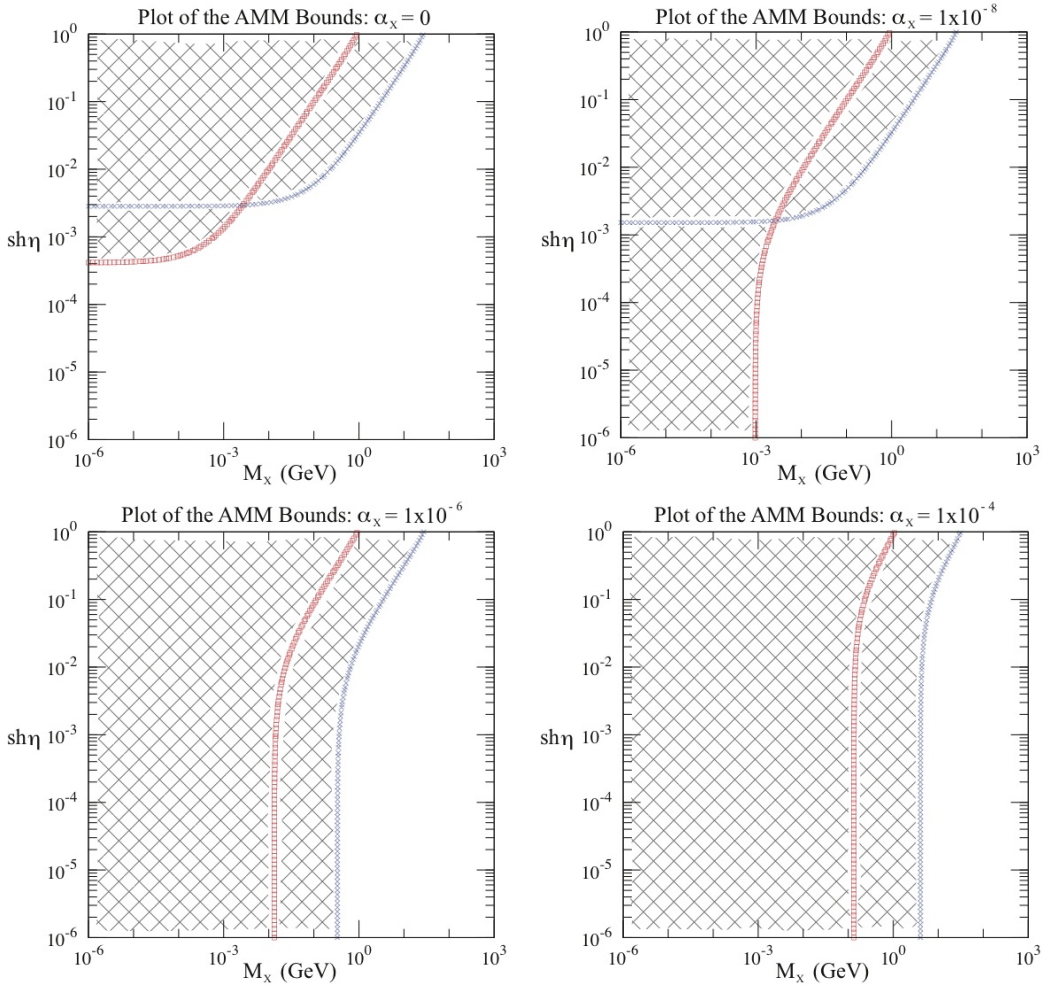

Figure 14. Plots of the constraint on the kinetic mixing, $\sinh\eta$, arising from the electron and muon AMM as a function of M_X, for various values of the gauge coupling α_X. The electron AMM bound is marked with blue crosses; the muon AMM bound is marked with red squares. The plot assumes a coupling $X_{\ell_L} = X_{\ell_R} = -1$, such as would be true if $X = B - L$. Hatched regions are excluded.

There is, however, some subtlety in comparing this shift with experiment [31–33]: since the electron AMM, δa_e, is used to determine the fine-structure constant, α. The best bound on X boson couplings therefore comes from the next most precise experiment that measures α, and not the errors from the $(g-2)$ experiments themselves. Following [31–33] this leads to the constraints $\delta a_e < 1.59\times10^{-10}$ and $\delta a_\mu < 7.4\times10^{-9}$, which when compared with the above expression gives the bounds shown in figure 13. These plots reproduce the results found in [16] when $\sinh\eta = 0$. In particular, the M_X values below which any gauge coupling is excluded are consistent with the bounds shown in [31–33].

Since these bounds are often considered (e.g. in [14, 15, 29–33]) in the context of a constraint on kinetic mixing, we also plot the constraint on $\sinh\eta$ as a function of the X boson mass, for various values of the gauge coupling. This is shown in figure 14.

JHEP08(2011)106

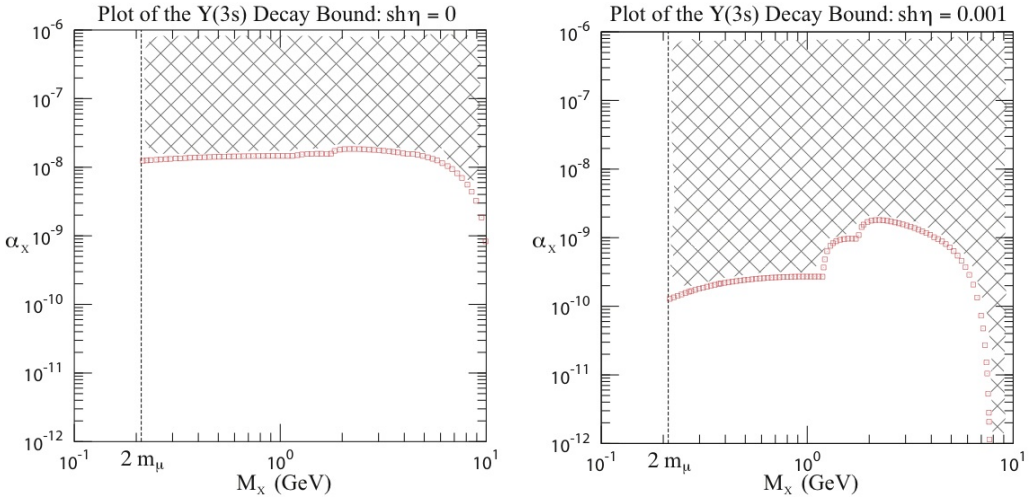

Figure 15. Plots of the constraint on the gauge coupling α_X arising from $\Upsilon(3s)$ decay as a function of M_X, for $\sh\eta = 0, 0.001$. The plot assumes a coupling $X_{\ell_L} = X_{\ell_R} = -1$, such as would be true if $X = B - L$. Hatched regions are excluded.

6.2 Upsilon decay

The bound we present here is an extension of the result found in [14, 15]. By looking at the decay rate of the $\Upsilon(3s)$ $b\bar{b}$ bound state, researchers from the BABAR collaboration were able to place a bound on the occurrence of a particular channel involving a light pseudoscalar A_0 [157]:

$$e^+ + e^- \to \Upsilon(3s) \to \gamma + A_0 \to \gamma + \mu^+ + \mu^- \,. \tag{6.3}$$

Their upper limit on the number of events

$$N = \sigma(e^+ + e^- \to \Upsilon(3s)) \times \mathcal{L} \times \mathrm{Br}(\Upsilon(3s) \to \gamma + A_0) \times \mathrm{Br}(A_0 \to \mu^+ + \mu^-) \,, \tag{6.4}$$

places a bound on the quantity $Q := \mathrm{Br}(\Upsilon(3s) \to \gamma + A_0) \times \mathrm{Br}(A_0 \to \mu^+ + \mu^-)$.

However, the reaction of interest to us is

$$e^+ + e^- \to \gamma + X \to \gamma + \mu^+ + \mu^- \,, \tag{6.5}$$

which would have an identical signature. So the measured bound can also be reinterpreted as applying to the quantity

$$Q_X := \frac{\sigma(e^+ + e^- \to \gamma + X)}{\sigma(e^+ + e^- \to \Upsilon(3s))} \times \mathrm{Br}(X \to \mu^+ + \mu^-) \tag{6.6}$$

The experimental limit [157] $Q_X < 3 \times 10^{-6}$ gives the plots found in figure 15 over the range $2m_\mu < M_X < E_{cm} (= 10.355\,\mathrm{GeV})$. This bound is quite strong, as it eliminates the entire region for $\sh\eta \gtrsim 0.002$ (as is shown in [14, 15]). For smaller $\sh\eta$, the bound is roughly constant when $M_X \ll E_{cm}$.

As in the case of the AMM bounds, we also plot the constraint on $\sh\eta$ as a function of the X boson mass for various values of the gauge coupling — as shown in figure 16.

JHEP08(2011)106

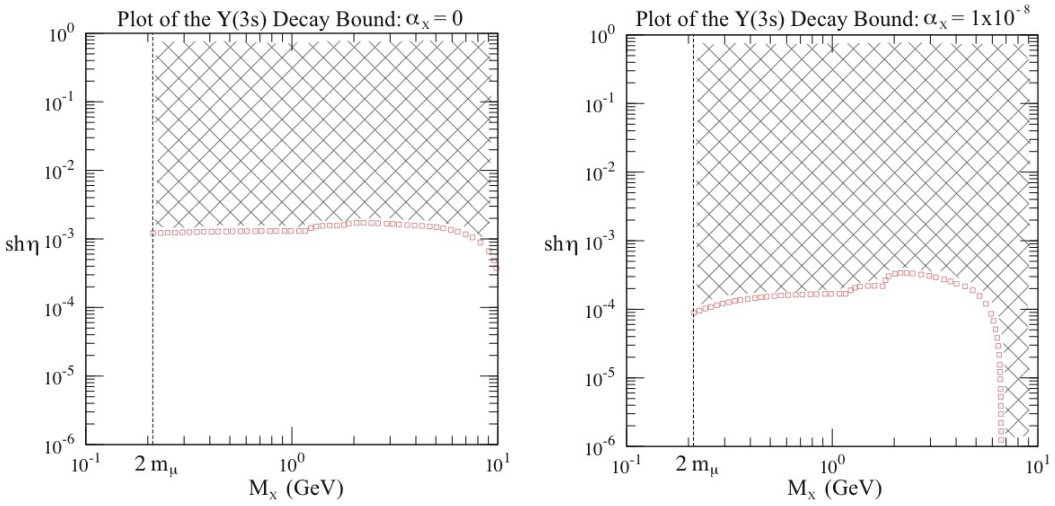

Figure 16. Plots of the constraint on the kinetic mixing, $\sinh\eta$, arising from $\Upsilon(3s)$ decay as a function of M_X, for $\alpha_X = 0, 1 \times 10^{-8}$. The plot assumes a coupling $X_{eL} = X_{eR} = -1$, such as would be true if $X = B - L$. Hatched regions are excluded.

Experiment	Target	N_e	Beam Energy	t	D
E774	W	0.52×10^{10}	275 GeV	30 cm	7.25 m
E141	W	2×10^{15}	9 GeV	12 cm	35 m
E137	Al	1.87×10^{20}	20 GeV	200 m	400 m

Table 1. Parameter values for the E774, E141, and E137 beam dump experiments.

6.3 Beam-dump experiments

In the MeV−GeV mass range, small g_X and η are constrained by several beam dump experiments. These bounds are considered in detail in [14, 15]; we apply a simplified version of their analysis here.

In these experiments, a large number N_e of electrons with initial energy E are collided with a fixed target made of either aluminum or tungsten. Many of the resulting collision products are absorbed either by the target or by some secondary shielding. (Here, we use t to denote the total thickness of both the target and the shielding.) The remaining products continue along an evacuated tube to the detector, located at some distance D away from the target. For a summary of values for these parameters, see table 1.

The bound arises from the non-observation of X decay products. The incoming electron emits an X boson as bremsstrahlung during photon exchange with the nucleon (N): $e^- + N \to e^- + N + X$. The X can then decay into either an e^+e^- or $\mu^+\mu^-$ pair. However, a decay that occurs too soon is absorbed by the shield while a decay that occurs too late occurs past the detector. Therefore, the number of lepton anti-lepton pairs observed at the detector can be computed by multiplying the number of X bosons produced, N_X, by the

JHEP08(2011)106

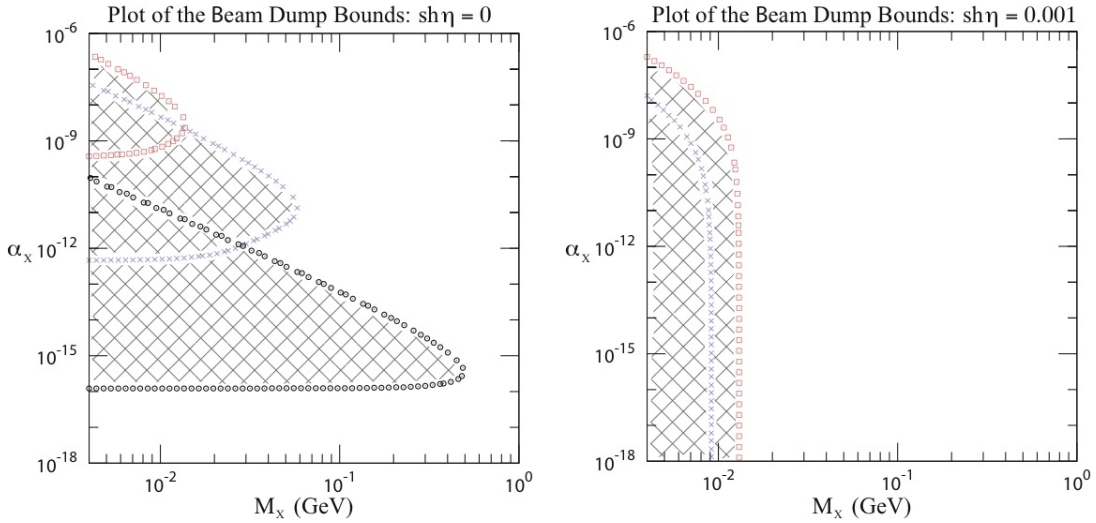

Figure 17. The constraint arising from beam dump experiments on the coupling $\alpha_X = g_X^2/4\pi$ as a function of M_X, for $\sh\eta = 0, 0.001$. The E774 bound is marked with red squares; the E141 bound is marked with blue crosses; the E137 bound is marked with black circles. The plot assumes a coupling $X_{\ell_L} = X_{\ell_R} = -1$, such as would be true if $X = B - L$. Hatched regions are excluded.

probability for the X to decay between $z = t$ to $z = D$:

$$N_{\rm obs} = N_X \int_t^D dz \left(\frac{1}{\ell_0} e^{-z/\ell_0}\right) . \tag{6.7}$$

Here, we write the lab frame decay length as $\ell_0 := \gamma c\tau$, where $\gamma = (1 - v^2)^{-1/2}$ is the relativistic time-dilation factor and τ is the inverse of the X rest-frame decay rate: $\tau := 1/\Gamma_X$.

In estimating the number of X's produced, we use the following result from [14, 15]:

$$N_X \sim N_e \, \mu^2 \frac{\epsilon^2}{M_X^2} , \tag{6.8}$$

where $\epsilon = \chi c_W$ and $\mu^2 \simeq 2.5$ MeV^2 is an overall factor that contains information regarding the details of the nuclear interaction, and is shown in [14, 15] to be roughly constant for M_X between 1 and 100 MeV. There is, however, an obstacle in applying this result directly to our analysis: it was derived without including any coupling to J_X^μ. In order to introduce the $k_{eL(R)}$-dependence in this expression, we note from [14, 15] that the ϵ-dependence above arises from the cross section $\sigma(e^-\gamma \to e^- X)$ under the assumption that the electron is massless. This means that the left- and right-handed helicity $X - e$ interactions contribute equally to the cross section, allowing the substitution

$$\epsilon^2 \to \frac{1}{4\pi\alpha}\left(\frac{k_{eL}^2 + k_{eR}^2}{2}\right) , \tag{6.9}$$

with the normalization chosen so that the above expression reduces to $\chi^2 c_W^2$ in the case where $X_{eL(R)} = 0$, $\sh\eta \ll 1$ and $M_X \ll M_Z$.

JHEP08(2011)106

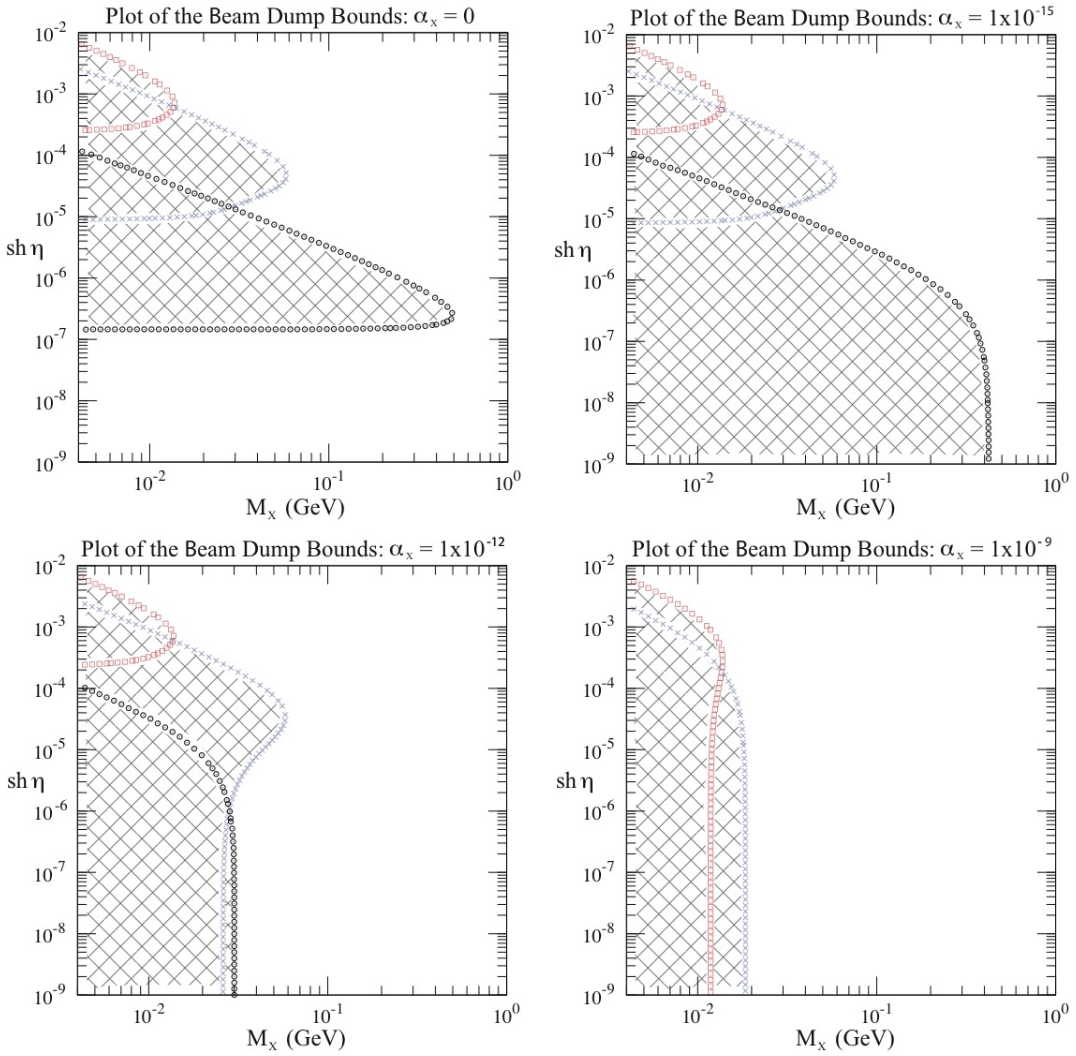

Figure 18. The constraint arising from beam dump experiments on the kinetic mixing $\mathrm{sh}\,\eta$ as a function of M_X, for $\alpha_X = 0$, 1×10^{-15}, 1×10^{-12}, and 1×10^{-9}. The E774 bound is marked with red squares; the E141 bound is marked with blue crosses; the E137 bound is marked with black circles. The plot assumes a coupling $X_{\ell_L} = X_{\ell_R} = -1$, such as would be true if $X = B - L$. Hatched regions are excluded.

All in all, we find that the number of X's we expect to observe is given by

$$N_{\mathrm{obs}} \sim \frac{N_e\,\mu^2}{M_X^2}\left(\frac{k_{eL}^2 + k_{eR}^2}{8\pi\alpha}\right)\left(e^{-t/\ell_0} - e^{-D/\ell_0}\right) . \tag{6.10}$$

Applying the experimental exclusions [14, 15] $N_{\mathrm{obs}} < 17$ events (E774), $N_{\mathrm{obs}} < 1000$ events (E141), and $N_{\mathrm{obs}} < 10$ events (E137) gives the bounds shown in figure 17.

The plot for $\mathrm{sh}\,\eta = 0$ gives good agreement with a similar plot in [16] (in the region over which these results overlap). The lower bounds for each experiment are approximately flat because, in the region where $t \ll D \ll \ell_0$, the fraction of X's that decay is just D/ℓ_0,

JHEP08(2011)106

which gives

$$N_{\rm obs} \sim \frac{N_e\,\mu^2}{M_X^2}\left(\frac{k_{eL}^2+k_{eR}^2}{8\pi\alpha}\right)\frac{D}{\ell_0}\,. \tag{6.11}$$

The leading M_X-dependence then cancels since $\ell_0 \sim 1/M_X^2$. The upper bound results from the situation where the X bosons decay too quickly, and the decay products do not escape the shielding.

We have only included plots for the cases where $\mathrm{sh}\,\eta = 0$ and 0.001 because the bounds become too weak to constrain any region of this parameter space whenever $\mathrm{sh}\,\eta > 0.007$.

An interesting feature of these bounds is that, at any given value of $\mathrm{sh}\,\eta$, the gauge coupling can be increased such that the bounds are evaded. This occurs because a stronger gauge coupling causes the X bosons to decay within the shielding. Therefore, any bound on kinetic mixing which results from these experiments can weaken if the direct coupling of electrons to the X is taken to be non-zero. To demonstrate this, consider the bounds shown in figure 18, which plots the bound on kinetic mixing as a function of the X-boson mass, for various values of α_X. Note that, for $\alpha_X \gtrsim 1\times10^{-6}$, these bounds are satisfied for all values of $\mathrm{sh}\,\eta$ in the relevant mass range.

6.4 Neutron-nucleus scattering

Low-energy neutron-nucleus scattering is important because most of the other low-energy bounds evaporate if the new boson doesn't couple to leptons (such as if $X = B$). For neutron-nucleus scattering a bound is obtained by considering the effects of the new Yukawa-type potential that would arise from a non-zero vector coupling of the X to neutrons. For light X bosons this can be seen over the strong nuclear force because it has a longer range, and can affect the angular dependence of the differential cross section for elastic scattering, $d\sigma(nN \to nN)/d\Omega$. This bound is discussed in the context of a scalar boson in [158] and more generally in [159].

Following these authors we parameterize the differential cross section as

$$\frac{d\sigma}{d\Omega} = \frac{\sigma_0}{4\pi}\left(1+\omega E cos\theta\right)\,, \tag{6.12}$$

where σ_0 and ω are to be taken from experiments. Then an interaction of the form

$$\Delta V_{nN}(r) = \left(\frac{g_n^2}{4\pi}\right)\frac{e^{-M_X r}}{r} \tag{6.13}$$

leads to a correction to the expected value of ω, which is measured experimentally in the energy range $E \sim$ 1-10 keV for neutrons scattering with ^{208}Pb.

Agreement with observations leads to the bound [158, 159]

$$\frac{k_{nV}^2}{4\pi M_X^4} < 3.4\times10^{-11}\,, \tag{6.14}$$

where $k_{nV} = k_{uV} + 2k_{dV}$ with $k_{fV} := \frac{1}{2}(k_{fL}+k_{fR})$, as above. Figure 19 shows a plot of this bound for the nominal case $\mathrm{sh}\,\eta = 0$.

JHEP08(2011)106

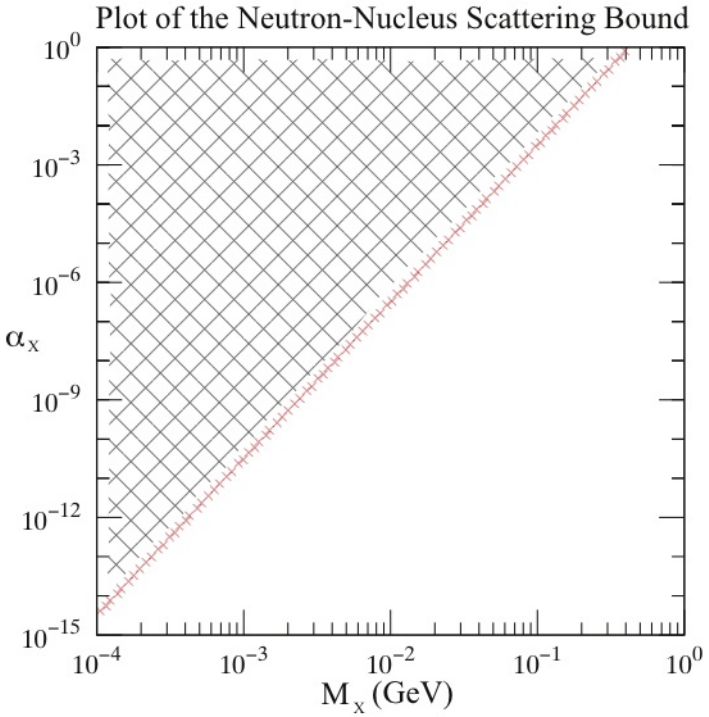

Figure 19. Plot of the constraint on the gauge coupling α_x due to neutron-nucleus scattering as a function of the X-boson mass M_X. The hatched regions are excluded.

For this combination of couplings, an interesting cancellation occurs. For small kinetic mixing, the correction $\Delta k_{f_{L(R)}}$ has the form

$$\begin{aligned}\Delta k_{f_{L(R)}} &= \eta \tfrac{e}{c_W}(Q_f c_W^2 - g^{\mathrm{SM}}_{f_{L(R)}}) + \eta s_W e_Z g^{\mathrm{SM}}_{f_{L(R)}} + \mathcal{O}(\eta^2) \\ &= \eta e c_W Q_f + \mathcal{O}(\eta^2)\,, \end{aligned} \tag{6.15}$$

and so the leading correction in η vanishes for any electrically neutral particle, like a neutron. This makes this bound relatively insensitive to changes in kinetic mixing, not varying appreciably over the range $0 \leq \mathrm{sh}\,\eta \leq 1$. A similar cancellation occurs in the case of nucleosynthesis, considered in section 6.6.

6.5 Atomic parity violation

The Standard Model predicts a low-energy effective coupling between the electron axial current and the vector currents within a given nucleus. The so-called weak charge of a nucleus with Z protons and N neutrons is defined (up to an overall constant) as the coherent sum of the Z-boson vector couplings over the constituents of that nucleus [160]:

$$Q_W(Z,N) := 4\left[Z\left(2g_{uV} + g_{dV}\right) + N\left(g_{uV} + 2g_{dV}\right)\right]. \tag{6.16}$$

where

$$g_{fVf} := \frac{g_{fL} + g_{fR}}{2} \quad \text{and} \quad g_{fA} := \frac{g_{fL} - g_{fR}}{2}\,. \tag{6.17}$$

JHEP08(2011)106

In terms of these the leading parity-violating effective electron-nuclear interaction generated by Z boson exchange is

$$\mathcal{L}_{\text{eff}} = -\sqrt{2} G_F g_{eA} Q_W \left(\bar{e}\gamma_\mu\gamma_5 e\right)\left(\overline{\Psi}\gamma^\mu\Psi\right) . \tag{6.18}$$

where Ψ is the field describing the nucleus. X-boson exchange adds an additional term to this effective lagrangian of the form

$$\mathcal{L}^X_{\text{eff}} = -\frac{k_{eA} Q_X}{M_X^2}\left(\bar{e}\gamma_\mu\gamma_5 e\right)\left(\overline{\Psi}\gamma^\mu\Psi\right) \tag{6.19}$$

where

$$Q_X := Z\left(2k_{uV} + k_{dV}\right) + N\left(k_{uV} + 2k_{dV}\right) . \tag{6.20}$$

Therefore, the total shift in the Q_W due to the X boson is

$$\Delta Q_W = \left[\frac{g_{eA}}{(-1/4)} Q_W - Q_W^{\text{SM}}\right] - \frac{2\sqrt{2}}{G_F}\frac{k_{eA} Q_X}{M_X^2} \tag{6.21}$$

where

$$\begin{aligned} Q_W^{\text{SM}}(Z,N) &= 4\left[Z\left(2g_{uV}^{\text{SM}} + g_{dV}^{\text{SM}}\right) + N\left(g_{uV}^{\text{SM}} + 2g_{dV}^{\text{SM}}\right)\right] \\ &= Z\left(1 - 4s_W^2\right) - N . \end{aligned} \tag{6.22}$$

Notice that the bracketed term in ΔQ_W goes to 0 as $\eta \to 0$, whereas the second term does not as long as k_{Ae} does not vanish in the same limit. The total effective lagrangian for this system can then be written as

$$\mathcal{L}_{\text{eff}} + \mathcal{L}^X_{\text{eff}} = \frac{G_F}{2\sqrt{2}}\left(Q_W^{\text{SM}} + \Delta Q_W\right)\left(\bar{e}\gamma_\mu\gamma_5 e\right)\left(\overline{\Psi}\gamma^\mu\Psi\right) . \tag{6.23}$$

It is expected that the second term in eq. (6.21) will be dominant, so it is useful to consider the form of k_{Ae}/M_X^2 in the limit where $M_X \ll M_Z$ and $\eta \ll 1$:

$$\frac{k_{eA}}{G_F M_X^2} = \frac{g_X X_{eA}\left(1 + \frac{1}{2}c_W^2\eta^2\right)}{G_F M_X^2} - \sqrt{2}\,\frac{s_W}{e_Z}\eta . \tag{6.24}$$

Therefore, if $X_{Le} = X_{Re}$, then the constraint becomes significantly less stringent at low masses since, instead of bounding the ratio g_X^2/M_X^2, it is now the combination $g_X\eta$ that is bounded. In order to emphasize the strength of this bound when $X_{Ae} \neq 0$, we use the charge assignments as shown in table 2.

If the X boson is light enough the above effective interaction eventually becomes inaccurate in describing the electron-nucleus interactions. In this case, rather than pursuing a detailed analysis of the microscopic lagrangian, we follow ref. [160] and introduce a corrective factor $K(M_X)$ to account for the non-locality caused by the small mass of the X boson. This modifies our expression for ΔQ_W as follows:

$$\Delta Q_W = \left[\frac{g_{eA}}{(-1/4)} Q_W - Q_W^{\text{SM}}\right] - \frac{2\sqrt{2}}{G_F}\frac{k_{eA} Q_X}{M_X^2} K(M_X) . \tag{6.25}$$

JHEP08(2011)106

SM Fermion	Charge X
u_L, d_L	0
u_R	$-1/3$
d_R	$+1/3$
ν_L, e_L	0
e_R	$-1/3$

Table 2. Charge assignments for the "right-handed" $U(1)$.

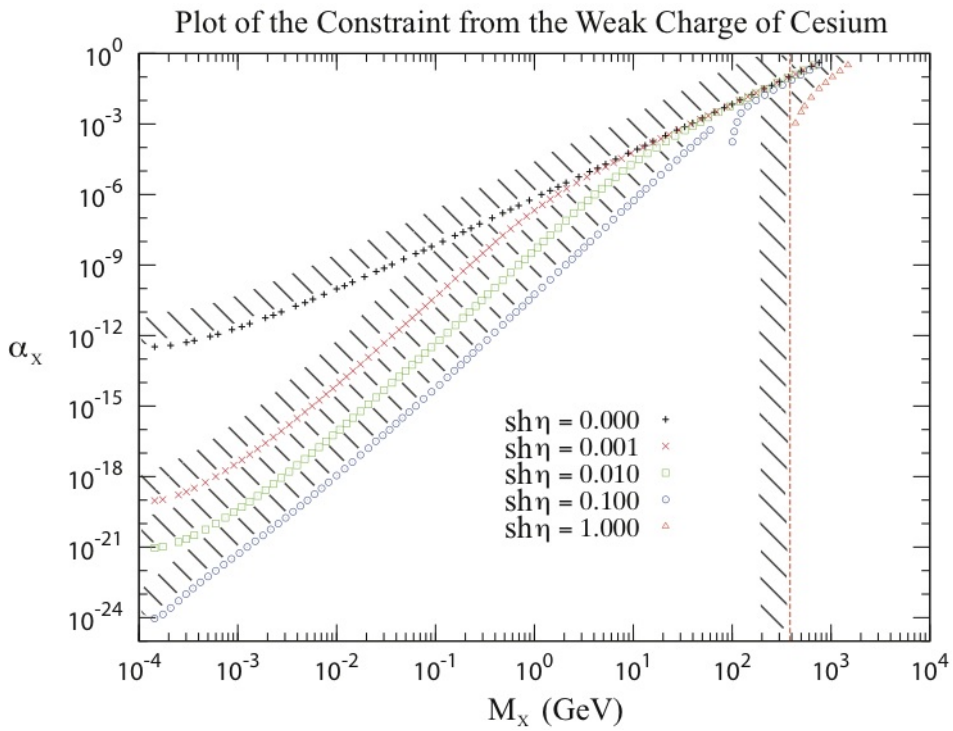

Figure 20. Plot of the constraint on the gauge coupling α_x due to the weak charge of cesium as a function of the X-boson mass M_X, for various values of $\sh\eta$. The hatched regions are excluded.

In [160] a table is given for K for various values of M_X in the range $0.1\,\text{MeV} < M_X < 100\,\text{MeV}$. In order to render the graphs shown here, we have interpolated values of K by doing a least squares fit to the values in [160].

As with the neutrino-electron scattering bounds, the slope of the bound changes for $\eta \neq 0$ due to the production of a new dominant term through cancellation with the modified Z-fermion coupling. Once again, we exclude the region below 385 GeV for the $\sh\eta = 1$ plot in order to avoid conflict with the electroweak oblique fits that require $z \ll 1$.

Since this bound relies crucially on there being an axial vector coupling to the electron, we did not include it when compiling the summary of bounds given in figures in section 1.

JHEP08(2011)106

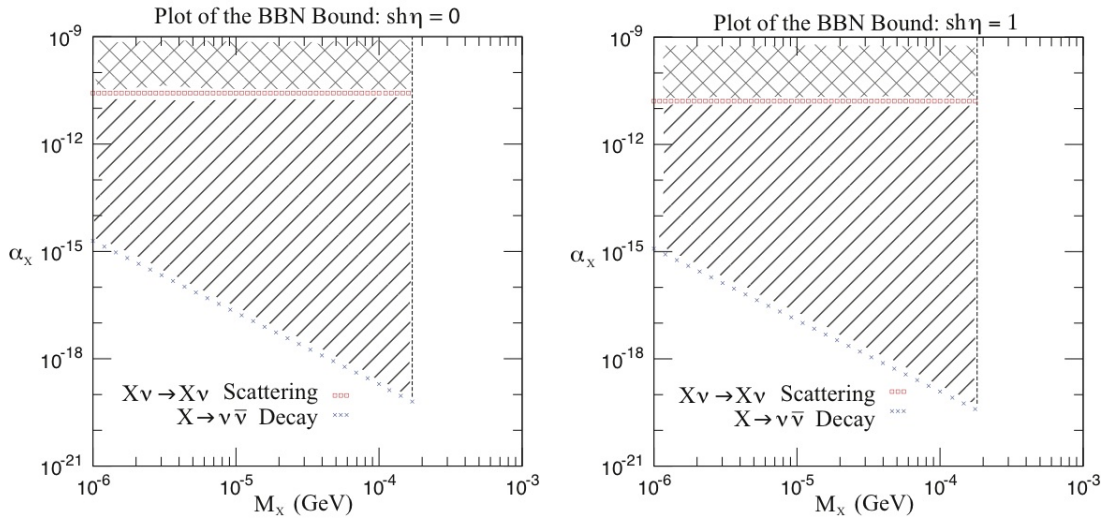

Figure 21. Constraint on the gauge coupling of the X due to its effect on nucleosynthesis, as a function of the X-boson mass. The red squares indicate the bound due to $X\nu \to X\nu$ scattering; the blue crosses indicate the bound due to $X \to \nu\bar{\nu}$ decay.

6.6 Primordial nucleosynthesis

We close with the study of constraints coming from cosmology, which for the mass range of interest in this paper consists dominantly of Big Bang Nucleosynthesis.

Any X bosons light enough to be present in the primordial soup at temperatures below $T \sim 1\,\mathrm{MeV}$ can destroy the success of Big Bang Nucleosynthesis (BBN) if they make up a sufficiently large fraction ($\lesssim 10\%$) of the universal energy density, leading to potentially strong constraints. In particular, such a boson poses a problem if it is in thermal equilibrium at these temperatures.

Quantitatively, measurements of primordial nuclear abundances forbid the existence of the number of additional neutrino species (beyond the usual 3 of the SM) to be [161] $\delta N_\nu \leq 1.44$ (at 95% C.L.). But since each boson in equilibrium counts $\frac{8}{7}$ times more strongly in the equilibrium abundance, and since a massive X boson carries 3 independent spin states, the corresponding bound on the number, N_X, of new species of spin-1 particles in equilibrium at BBN is

$$N_X \leq 0.84\,. \tag{6.26}$$

Even just one additional massive spin-1 boson into relativistic equilibrium is excluded at the 95% confidence level.

In a universe containing only the X boson and ordinary SM particles at energies of order 1 MeV, this leads to two kinds of constraints: either the X boson's couplings are weak enough that it does not ever reach equilibrium; or if the X boson is in equilibrium it must be heavy enough ($\gtrsim 1\,\mathrm{MeV}$) to have a Boltzmann-suppressed abundance. Figure 21 sketches the regions in the coupling-mass plane that are excluded by these conditions. The vertical line corresponds to the situation where abundance is suppressed by Boltzmann factors.

JHEP08(2011)106

The constraints on couplings arise only for sufficiently light particles, and express the condition that the couplings be weak enough to avoid equilibrium, at least up until the freeze-out temperature T_F. There are two curves of this type drawn, which differ by whether it is collision or decay processes that are the dominant equilibration mechanisms. Qualitatively, the requirement that reactions like $X\nu \leftrightarrow X\nu$ not equilibrate the X bosons leads to a constraint on the couplings that is M_X-independent in the limit where $M_X \ll T_F$, because then the size of both the reaction rate and Hubble scale is set by the temperature. The same is not true for decay reactions, $X \leftrightarrow \overline{\nu}\,\nu$, since the rate for this also depends on the X-boson mass.

A few other comments are appropriate for figure 21. First, because they are outside the main scope of this study, the bounds shown are derived assuming that $M_X \ll T$ (rather than being evaluated numerically as a function of M_X) and so are drawn only up to the mass range within 0.5 MeV of the freeze-out temperature. Second, the resulting expressions depend only weakly on η, showing little difference over the range $0 < \mathrm{sh}\,\eta < 1$. As discussed in earlier sections, this is a consequence of the neutrino's electrical neutrality, which ensures that the leading small-η limit of the kinetic mixing first arises at $\mathcal{O}(\eta^2)$ rather than $\mathcal{O}(\eta)$.

Acknowledgments

We would like to thank Brian Batell, Joseph Conlon, Rouven Essig, Sven Krippendorf, David Poland, Maxim Pospelov, Philip Schuster, Natalia Toro and Michael Trott for helpful discussions. AM and FQ thank McMaster University and Perimeter Institute for hospitality. CB and AM thank the Abdus Salam International Centre for Theoretical Physics (ICTP) for its kind hospitality while part of this work was done. The work of AM was supported by the EU through the Seventh Framework Programme and Cambridge University. CB and MW's research was supported in part by funds from the Natural Sciences and Engineering Research Council (NSERC) of Canada. Research at the Perimeter Institute is supported in part by the Government of Canada through Industry Canada, and by the Province of Ontario through the Ministry of Research and Information (MRI).

Note added. Since posting, we have learned of a beam dump analysis [162] that has enlarged[5] the exclusion regions discussed in section 6.3.

A Diagonalizing the gauge action

This appendix provides the details of the diagonalization of the gauge boson kinetic and mass mixings. The starting point is eq. (3.11),

$$\mathcal{L} = -\frac{1}{4}\hat{\mathbf{V}}^T_{\mu\nu}\hat{K}\hat{\mathbf{V}}^{\mu\nu} - \frac{1}{2}\hat{\mathbf{V}}^T_{\mu}\hat{M}\hat{\mathbf{V}}^{\mu} + \hat{\mathbf{J}}^T_{\mu}\hat{\mathbf{V}}^{\mu}\,, \tag{A.1}$$

with $\hat{K}$ and $\hat{M}$ given in eqs. (3.12).

[5] We thank Johannes Blümlein for bringing this to our attention

JHEP08(2011)106

Diagonalization. We begin by performing the usual weak-mixing rotation to diagonalize the mass term:

$$\hat{\mathbf{V}} = R_1 \check{\mathbf{V}} := \begin{bmatrix} \hat{c}_W & \hat{s}_W & 0 \\ -\hat{s}_W & \hat{c}_W & 0 \\ 0 & 0 & 1 \end{bmatrix} \begin{bmatrix} \check{Z} \\ \check{A} \\ \check{X} \end{bmatrix} \tag{A.2}$$

where

$$\hat{c}_W := \cos\hat{\theta}_W := \frac{g_2}{\sqrt{g_1^2+g_2^2}} \quad \text{and} \quad \hat{s}_W := \sin\hat{\theta}_W := \frac{g_1}{\sqrt{g_1^2+g_2^2}}\,. \tag{A.3}$$

The lagrangian then becomes

$$\mathcal{L} = -\frac{1}{4}\check{\mathbf{V}}^T_{\mu\nu}\check{K}\check{\mathbf{V}}^{\mu\nu} - \frac{1}{2}\check{\mathbf{V}}^T_{\mu}\check{M}\check{\mathbf{V}}^{\mu} + \check{\mathbf{J}}^T_{\mu}\check{\mathbf{V}}^{\mu}\,, \tag{A.4}$$

with new matrices

$$\check{K} = R_1^T\hat{K}R_1 = \begin{bmatrix} 1 & 0 & \chi\hat{s}_W \\ 0 & 1 & -\chi\hat{c}_W \\ \chi\hat{s}_W & -\chi\hat{c}_W & 1 \end{bmatrix} \quad \text{and} \quad \check{M} = R_1^T\hat{M}R_1 = \begin{bmatrix} m_Z^2 & 0 & 0 \\ 0 & 0 & 0 \\ 0 & 0 & m_X^2 \end{bmatrix} \tag{A.5}$$

where $m_Z^2 := \frac{1}{4}\left(g_1^2+g_2^2\right)v^2$. Under the same transformation the currents become

$$\begin{aligned} \check{\mathbf{J}}_\mu = R_1^T\hat{\mathbf{J}}_\mu &= \begin{bmatrix} \hat{J}^3_\mu\,\hat{c}_W - \hat{J}^Y_\mu\,\hat{s}_W \\ \hat{J}^3_\mu\,\hat{s}_W + \hat{J}^Y_\mu\,\hat{c}_W \\ \hat{J}^X_\mu \end{bmatrix} \\ &= \sum_f \begin{bmatrix} \hat{i}e_Z\overline{f}\gamma_\mu\left[T_{3f}\gamma_L - Q_f\hat{s}_W^2\right]f \\ ie\,\overline{f}\gamma_\mu Q_f f \\ ig_X\overline{f}\gamma_\mu\left[X_{fL}\gamma_L + X_{fR}\gamma_R\right]f \end{bmatrix} := \begin{bmatrix} \check{J}^Z_\mu \\ \check{J}^A_\mu \\ \check{J}^X_\mu \end{bmatrix}\,, \end{aligned} \tag{A.6}$$

which defines $\hat{e}_Z := e/(\hat{s}_W\hat{c}_W)$ and uses the standard SM relations $g_2\hat{s}_W = g_1\hat{c}_W := e$ and $Q_f = T_{3f} + Y_{fL} = Y_{fR}$.

The kinetic term is diagonalized by letting

$$\check{\mathbf{V}} := L\tilde{\mathbf{V}} := \begin{bmatrix} 1 & 0 & -\hat{s}_W\,\mathrm{sh}\,\eta \\ 0 & 1 & \hat{c}_W\,\mathrm{sh}\,\eta \\ 0 & 0 & \mathrm{ch}\,\eta \end{bmatrix} \begin{bmatrix} \tilde{Z} \\ \tilde{A} \\ \tilde{X} \end{bmatrix} \tag{A.7}$$

with

$$\mathrm{sh}\,\eta := \sinh\eta := \frac{\chi}{\sqrt{1-\chi^2}} \quad \text{and} \quad \mathrm{ch}\,\eta := \cosh\eta := \frac{1}{\sqrt{1-\chi^2}}\,. \tag{A.8}$$

This gives, by construction

$$\tilde{K} = L^T\check{K}L = \begin{bmatrix} 1 & 0 & 0 \\ 0 & 1 & 0 \\ 0 & 0 & 1 \end{bmatrix} \tag{A.9}$$

and

$$\tilde{M} = L^T\check{M}L = \begin{bmatrix} m_Z^2 & 0 & -m_Z^2\hat{s}_W\mathrm{sh}\,\eta \\ 0 & 0 & 0 \\ -m_Z^2\hat{s}_W\mathrm{sh}\,\eta & 0 & m_X^2\mathrm{ch}^2\,\eta + m_Z^2\hat{s}_W^2\mathrm{sh}^2\,\eta \end{bmatrix}\,, \tag{A.10}$$

JHEP08(2011)106

while the currents become

$$\tilde{\mathbf{J}}_\mu := L^T \check{\mathbf{J}}_\mu = \begin{bmatrix} \check{J}^Z_\mu \\ \check{J}^A_\mu \\ -\check{J}^Z_\mu \hat{s}_W \mathrm{sh}\,\eta + \check{J}^A_\mu \hat{c}_W \mathrm{sh}\,\eta + \check{J}^X_\mu \mathrm{ch}\,\eta \end{bmatrix} . \tag{A.11}$$

(Notice that L and R_1 satisfy $LR_1 = R_1 L$, so it is immaterial whether we first diagonalize the SM mass or the kinetic terms.)

Finally, the mass matrix is diagonalized by letting

$$\tilde{\mathbf{V}} = R_2 \mathbf{V} := \begin{bmatrix} c_\xi & 0 & -s_\xi \\ 0 & 1 & 0 \\ s_\xi & 0 & c_\xi \end{bmatrix} \begin{bmatrix} Z \\ A \\ X \end{bmatrix} \tag{A.12}$$

where $c_\xi := \cos\xi$ and $s_\xi := \sin\xi$ with the angle ξ given by

$$\tan 2\xi = \frac{-2\hat{s}_W \mathrm{sh}\eta}{1 - \hat{s}_W^2 \mathrm{sh}^2\eta - r_X^2 \mathrm{ch}^2\eta} , \tag{A.13}$$

where we define for convenience

$$r_X := \frac{m_X}{m_Z} . \tag{A.14}$$

The diagonalized lagrangian then is

$$\mathcal{L} = -\frac{1}{4} \mathbf{V}^T_{\mu\nu} \mathbf{V}^{\mu\nu} - \frac{M_Z^2}{2} Z_\mu Z^\mu - \frac{M_X^2}{2} X_\mu X^\mu + \mathbf{J}^T_\mu \mathbf{V}^\mu , \tag{A.15}$$

where the physical masses are

$$M_X^2 = \frac{m_Z^2}{2} \left(1 + \hat{s}_W^2 \mathrm{sh}^2\eta + r_X^2 \mathrm{ch}^2\eta + \vartheta_X \sqrt{\left(1 + \hat{s}_W^2 \mathrm{sh}^2\eta + r_X^2 \mathrm{ch}^2\eta\right)^2 - 4 r_X^2 \mathrm{ch}^2\eta} \right) \tag{A.16}$$

$$M_Z^2 = \frac{m_Z^2}{2} \left(1 + \hat{s}_W^2 \mathrm{sh}^2\eta + r_X^2 \mathrm{ch}^2\eta - \vartheta_X \sqrt{\left(1 + \hat{s}_W^2 \mathrm{sh}^2\eta + r_X^2 \mathrm{ch}^2\eta\right)^2 - 4 r_X^2 \mathrm{ch}^2\eta} \right) \tag{A.17}$$

with ϑ_X defined such that $M_Z \to m_Z$ and $M_X \to m_X$ as $\eta \to 0$:

$$\vartheta_X := \begin{cases} +1 & \text{if} \quad r_X > 1 \\ -1 & \text{if} \quad r_X < 1 \end{cases} . \tag{A.18}$$

The currents in the physical basis are similarly read off as

$$\mathbf{J}_\mu = \begin{bmatrix} \check{J}^Z_\mu c_\xi + \left(-\check{J}^Z_\mu \hat{s}_W \mathrm{sh}\,\eta + \check{J}^A_\mu \hat{c}_W \mathrm{sh}\,\eta + \check{J}^X_\mu \mathrm{ch}\,\eta \right) s_\xi \\ \check{J}^A_\mu \\ -\check{J}^Z_\mu s_\xi + \left(-\check{J}^Z_\mu \hat{s}_W \mathrm{sh}\,\eta + \check{J}^A_\mu \hat{c}_W \mathrm{sh}\,\eta + \check{J}^X_\mu \mathrm{ch}\,\eta \right) c_\xi \end{bmatrix} := \begin{bmatrix} J^Z_\mu \\ J^A_\mu \\ J^X_\mu \end{bmatrix} . \tag{A.19}$$

Since we are eventually interested in obtaining bounds in terms of the physical masses M_Z and M_X, it is useful to invert these mass equations to find the input parameters m_Z^2 and m_X^2 as a function of the physical masses and η. This gives

$$m_X^2 = \frac{M_Z^2}{2\mathrm{ch}^2\eta} \left(1 + R_X^2 + \vartheta_X \sqrt{\left(1 + R_X^2\right)^2 - 4\left(1 + \hat{s}_W^2 \mathrm{sh}^2\eta\right) R_X^2} \right) \tag{A.20}$$

$$m_Z^2 = \frac{M_Z^2}{2\left(1 + \hat{s}_W^2 \mathrm{sh}^2\eta\right)} \left(1 + R_X^2 - \vartheta_X \sqrt{\left(1 + R_X^2\right)^2 - 4\left(1 + \hat{s}_W^2 \mathrm{sh}^2\eta\right) R_X^2} \right) \tag{A.21}$$

JHEP08(2011)106

where R_X is used to denote the ratio of the physical masses:

$$R_X := \frac{M_X}{M_Z}\,. \tag{A.22}$$

Also, the sign ϑ_X is now $+1$ for $R_X > 1$ and -1 for $R_X < 1$.

Given this inversion, the angle ξ can now be written as a function of R_X and η only:

$$\tan 2\xi(R_X,\eta) = -\left(\frac{2\hat{s}_W \mathrm{sh}\eta}{1-\hat{s}_W^2\mathrm{sh}^2\eta - r_X^2(R_X,\eta)\mathrm{ch}^2\eta}\right)\,, \tag{A.23}$$

where

$$r_X^2(R_X,\eta) = \frac{\left(1+\hat{s}_W^2\mathrm{sh}^2\eta\right)\left(1+R_X^2+\vartheta_X\sqrt{\left(1+R_X^2\right)^2-4\left(1+\hat{s}_W^2\mathrm{sh}^2\eta\right)R_X^2}\right)}{\mathrm{ch}^2\eta\left(1+R_X^2-\vartheta_X\sqrt{\left(1+R_X^2\right)^2-4\left(1+\hat{s}_W^2\mathrm{sh}^2\eta\right)R_X^2}\right)}\,. \tag{A.24}$$

A.1 Physical couplings

We are now in a position to read off the physical implications of the X boson. That is, we may write

$$\mathcal{L} = \mathcal{L}_{\mathrm{SM}} + \delta\mathcal{L}_{\mathrm{SM}} + \mathcal{L}_X\,, \tag{A.25}$$

where the modification to the SM self-couplings are given by

$$\delta\mathcal{L}_{\mathrm{SM}} = -\frac{z}{2}\,m_Z^2 Z_\mu Z^\mu + i\hat{e}_Z\sum_f\left[\overline{f}\gamma^\mu\left(\delta g_{fL}\gamma_L + \delta g_{fR}\gamma_R\right)f\right]Z_\mu\,, \tag{A.26}$$

with [142]

$$z(R_X,\eta) := \frac{M_Z^2-m_Z^2}{m_Z^2} = \frac{\hat{s}_W^2\mathrm{sh}^2\eta - \Delta_X + \vartheta_X\sqrt{\Delta_X^2 - R_X^2\hat{s}_W^2\mathrm{sh}^2\eta}}{1+\Delta_X-\vartheta_X\sqrt{\Delta_X^2-R_X^2\hat{s}_W^2\mathrm{sh}^2\eta}}\,, \tag{A.27}$$

where

$$\Delta_X := \frac{1}{2}(R_X^2-1)\,. \tag{A.28}$$

(Note that the $\eta \to 0$ limit of z is easily verified by implementing the identity $\Delta_X = \vartheta_X\sqrt{\Delta_X^2}$.)

Given the form of z, one might worry that, for some choice of the parameters M_X and $\mathrm{sh}\,\eta$, z would yield a complex value. However, any such choice does not correspond to a choice of real values for the original parameters of the lagrangian, m_X, m_Z, and χ. This happens because sufficiently large kinetic mixing tends to preclude the existence of mass eigenvalues, M_X and M_Z, that are too close to one another. This is why this region of parameter space is excluded from the plots of section 4.

The fermion couplings are similarly

$$\delta g_{fL(R)} = (c_\xi - 1)\,\hat{g}_{fL(R)} + s_\xi\left(\mathrm{sh}\,\eta\,\hat{s}_W(Q_f\hat{c}_W^2 - \hat{g}_{fL(R)}) + \mathrm{ch}\eta\,\frac{g_X}{\hat{e}_Z}X_{fL(R)}\right)\,. \tag{A.29}$$

JHEP08(2011)106

The terms explicitly involving the X boson are

$$\begin{aligned}\mathcal{L}_X &= -\frac{1}{4}X_{\mu\nu}X^{\mu\nu} - \frac{M_X^2}{2}X_\mu X^\mu \\ &\quad + i\sum_f \overline{f}\gamma_\mu\left(k_{fL}\gamma_L + k_{fR}\gamma_R\right) f X^\mu\,,\end{aligned} \tag{A.30}$$

with

$$k_{fL(R)} = c_\xi\left(\mathrm{ch}\,\eta\, g_X X_{fL(R)} + \mathrm{sh}\,\eta\,\frac{e}{\hat{c}_W}(Q_f\hat{c}_W^2 - \hat{g}_{fL(R)})\right) - s_\xi\hat{e}_Z\hat{g}_{fL(R)}\,. \tag{A.31}$$

Notice that in this basis X_μ does not couple directly to the electroweak gauge bosons at tree-level, but has acquired modified fermion couplings due to the mixing.

Oblique parameters. The only remaining step is to eliminate parameters like $\hat{s}_W$ and m_Z in the lagrangian in favour of a physically defined weak mixing angle, s_W, and mass M_Z. This process reveals the physical combination of new-physics parameters that is relevant to observables, and thereby provides a derivation [142] of the X-boson contributions to the oblique electroweak parameters [143–146].

We have already seen how to do this for the Z mass, for which

$$m_Z \simeq M_Z\left(1 - \frac{z}{2}\right)\,. \tag{A.32}$$

For the weak mixing angle it is convenient to define s_W so that the Fermi constant, G_F, measured in muon decay is given by the SM formula,

$$\frac{G_F}{\sqrt{2}} := \frac{e^2}{8s_W^2c_W^2M_Z^2}\,. \tag{A.33}$$

But this can be compared with the tree-level calculation of the Fermi constant obtained in our model from W-exchange,

$$\frac{G_F}{\sqrt{2}} = \frac{g_2^2}{8m_W^2} = \frac{e^2}{8\hat{s}_W^2\hat{c}_W^2m_Z^2}\,, \tag{A.34}$$

to infer

$$\hat{s}_W^2\hat{c}_W^2 = s_W^2c_W^2\,(1+z)\,, \tag{A.35}$$

which, to linear order in z, implies that

$$\hat{s}_W^2 = s_W^2\left[1 + \frac{z\,c_W^2}{c_W^2 - s_W^2}\right]\,. \tag{A.36}$$

Eliminating $\hat{s}_W$ in favour of s_W in the fermionic weak interactions introduces a further shift in these couplings, leading to our final form for the neutral-current lagrangian:

$$\begin{aligned}\mathcal{L}_{\rm NC} &= \frac{ie}{\hat{s}_W\hat{c}_W}\sum_f\left[\overline{f}\gamma^\mu\left(T_{3f}\gamma_L - Q_f\hat{s}_W^2\right)f\right. \\ &\qquad \left. + \overline{f}\gamma^\mu\left(\delta g_{fL}\gamma_L + \delta g_{fR}\gamma_R\right)f\right]Z_\mu \\ &\simeq \frac{ie}{s_Wc_W}\left(1-\frac{z}{2}\right)\sum_f\left\{\overline{f}\gamma^\mu\left[T_{3f}\gamma_L - Q_fs_W^2\left(1 + \frac{z\,c_W^2}{c_W^2 - s_W}\right)\right]f\right. \\ &\qquad \left. + \ \overline{f}\gamma^\mu\left(\delta g_{fL}\gamma_L + \delta g_{fR}\gamma_R\right)f\right\}Z_\mu \\ &:= ie_Z\sum_f\overline{f}\gamma^\mu\left[\left(g_{fL}^{\rm SM} + \Delta g_{fL}\right)\gamma_L + \left(g_{fR}^{\rm SM} + \Delta g_{fR}\right)\gamma_R\right]f\,Z_\mu\,,\end{aligned} \tag{A.37}$$

JHEP08(2011)106

where $e_Z := e/s_W c_W$ and

$$\Delta g_{f_{L(R)}} = -\frac{z}{2} g^{\rm SM}_{f_{L(R)}} - z\left(\frac{s_W^2 c_W^2}{c_W^2 - s_W^2}\right) Q_f + \delta g_{f_{L(R)}}\,, \tag{A.38}$$

where (as usual) $g^{\rm SM}_{f_L} := T_{3f} - Q_f s_W^2$ and $g^{\rm SM}_{f_R} := -Q_f s_W^2$. It is assumed throughout that the corrections z, $\delta g_{f_{L(R)}}$, and

$$\Delta k_{f_{L(R)}} := k_{f_{L(R)}} - g_X X_{f_{L(R)}} \tag{A.39}$$

are small, so that any expression can be linearized in these variables. In particular, this means that one can replace hatted electroweak parameters (i.e. $\hat{s}_W$, etc.) with unhatted ones in our previous expressions to give:

$$z(R_X,\eta) = \frac{s_W^2 {\rm sh}^2\eta - \Delta_X + \vartheta_X\sqrt{\Delta_X^2 - R_X^2 s_W^2 {\rm sh}^2\eta}}{1 + \Delta_X - \vartheta_X\sqrt{\Delta_X^2 - R_X^2 s_W^2 {\rm sh}^2\eta}} \tag{A.40}$$

$$\delta g_{f_{L(R)}} = (c_\xi - 1)\, g^{\rm SM}_{f_{L(R)}} + s_\xi\left({\rm sh}\,\eta\, s_W (Q_f c_W^2 - g^{\rm SM}_{f_{L(R)}}) + {\rm ch}\eta\,\frac{g_X}{e_Z} X_{f_{L(R)}}\right) \tag{A.41}$$

$$\Delta k_{f_{L(R)}} = (c_\xi {\rm ch}\,\eta - 1)\, g_X X_{f_{L(R)}} + c_\xi {\rm sh}\,\eta\,\frac{e}{c_W}(Q_f c_W^2 - g^{\rm SM}_{f_{L(R)}}) - s_\xi e_Z g^{\rm SM}_{f_{L(R)}}\,. \tag{A.42}$$

Alternatively, one can use the relationship between z and η to determine the contribution to the oblique parameters [143–146] $S = U = 0$ and $\alpha T = -z$, where (as usual) $\alpha := e^2/4\pi$. In this case, $\Delta g_{f_{L(R)}}$ can be written as in [142]

$$\Delta g_{f_{L(R)}} = \frac{\alpha T}{2}\, g^{\rm SM}_{f_{L(R)}} + \alpha T\left(\frac{s_W^2 c_W^2}{c_W^2 - s_W^2}\right) Q_f + \delta g_{f_{L(R)}}\,. \tag{A.43}$$

References

[1] D. Feldman, B. Körs and P. Nath, *Extra-weakly interacting dark matter*, *Phys. Rev.* **D 75** (2007) 023503 [hep-ph/0610133] [SPIRES].

[2] D. Feldman, Z. Liu and P. Nath, *The Stückelberg Z' extension with kinetic mixing and milli-charged dark matter from the hidden sector*, *Phys. Rev.* **D 75** (2007) 115001 [hep-ph/0702123] [SPIRES].

[3] M. Pospelov, A. Ritz and M.B. Voloshin, *Secluded WIMP dark matter*, *Phys. Lett.* **B 662** (2008) 53 [arXiv:0711.4866] [SPIRES].

[4] N. Arkani-Hamed, D.P. Finkbeiner, T.R. Slatyer and N. Weiner, *A theory of dark matter*, *Phys. Rev.* **D 79** (2009) 015014 [arXiv:0810.0713] [SPIRES].

[5] M. Pospelov and A. Ritz, *Astrophysical signatures of secluded dark matter*, *Phys. Lett.* **B 671** (2009) 391 [arXiv:0810.1502] [SPIRES].

[6] D. Feldman, Z. Liu and P. Nath, *PAMELA positron excess as a signal from the hidden sector*, *Phys. Rev.* **D 79** (2009) 063509 [arXiv:0810.5762] [SPIRES].

[7] P.J. Fox and E. Poppitz, *Leptophilic dark matter*, *Phys. Rev.* **D 79** (2009) 083528 [arXiv:0811.0399] [SPIRES].

JHEP08(2011)106

[8] E.J. Chun and J.-C. Park, *Dark matter and sub-GeV hidden* U(1) *in GMSB models*, *JCAP* **02** (2009) 026 [arXiv:0812.0308] [SPIRES].

[9] R. Allahverdi, B. Dutta, K. Richardson-McDaniel and Y. Santoso, *A supersymmetric B-L dark matter model and the observed anomalies in the cosmic rays*, *Phys. Rev.* **D 79** (2009) 075005 [arXiv:0812.2196] [SPIRES].

[10] C. Cheung, J.T. Ruderman, L.-T. Wang and I. Yavin, *Kinetic mixing as the origin of light dark scales*, *Phys. Rev.* **D 80** (2009) 035008 [arXiv:0902.3246] [SPIRES].

[11] D.E. Morrissey, D. Poland and K.M. Zurek, *Abelian hidden sectors at a GeV*, *JHEP* **07** (2009) 050 [arXiv:0904.2567] [SPIRES].

[12] J.L. Feng, M. Kaplinghat, H. Tu and H.-B. Yu, *Hidden charged dark matter*, *JCAP* **07** (2009) 004 [arXiv:0905.3039] [SPIRES].

[13] D. Feldman, Z. Liu, P. Nath and G. Peim, *Multicomponent dark matter in supersymmetric hidden sector extensions*, *Phys. Rev.* **D 81** (2010) 095017 [arXiv:1004.0649] [SPIRES].

[14] J.D. Bjorken, R. Essig, P. Schuster and N. Toro, *New fixed-target experiments to search for dark gauge forces*, *Phys. Rev.* **D 80** (2009) 075018 [arXiv:0906.0580] [SPIRES].

[15] R. Essig, P. Schuster and N. Toro, *Probing dark forces and light hidden sectors at low-energy e^+e^- colliders*, *Phys. Rev.* **D 80** (2009) 015003 [arXiv:0903.3941] [SPIRES].

[16] M. Freytsis, G. Ovanesyan and J. Thaler, *Dark force detection in low energy e-p collisions*, *JHEP* **01** (2010) 111 [arXiv:0909.2862] [SPIRES].

[17] B. Holdom, *Two* U(1)*'s and epsilon charge shifts*, *Phys. Lett.* **B 166** (1986) 196 [SPIRES].

[18] E.D. Carlson, *Limits on a new* U(1) *coupling*, *Nucl. Phys.* **B 286** (1987) 378 [SPIRES].

[19] R. Foot, G.C. Joshi and H. Lew, *Gauged baryon and lepton numbers*, *Phys. Rev.* **D 40** (1989) 2487 [SPIRES].

[20] D.C. Bailey and S. Davidson, *Is there a vector boson coupling to baryon number?*, *Phys. Lett.* **B 348** (1995) 185 [hep-ph/9411355] [SPIRES].

[21] S. Davidson and M.E. Peskin, *Astrophysical bounds on millicharged particles in models with a paraphoton*, *Phys. Rev.* **D 49** (1994) 2114 [hep-ph/9310288] [SPIRES].

[22] H. Gies, J. Jaeckel and A. Ringwald, *Polarized light propagating in a magnetic field as a probe of millicharged fermions*, *Phys. Rev. Lett.* **97** (2006) 140402 [hep-ph/0607118] [SPIRES].

[23] H. Gies, J. Jaeckel and A. Ringwald, *Accelerator cavities as a probe of millicharged particles*, *Europhys. Lett.* **76** (2006) 794 [hep-ph/0608238] [SPIRES].

[24] S.N. Gninenko, N.V. Krasnikov and A. Rubbia, *Search for millicharged particles in reactor neutrino experiments: a probe of the PVLAS anomaly*, *Phys. Rev.* **D 75** (2007) 075014 [hep-ph/0612203] [SPIRES].

[25] J. Redondo and A. Ringwald, *Light shining through walls*, arXiv:1011.3741 [SPIRES].

[26] J. Jaeckel and A. Ringwald, *The low-energy frontier of particle physics*, *Ann. Rev. Nucl. Part. Sci.* **60** (2010) 405 [arXiv:1002.0329] [SPIRES].

[27] M. Cicoli, M. Goodsell, J. Jaeckel and A. Ringwald, *Testing string vacua in the lab: from a hidden CMB to dark forces in flux compactifications*, *JHEP* **07** (2011) 114 [arXiv:1103.3705] [SPIRES].

JHEP08(2011)106

[28] W.-F. Chang, J.N. Ng and J.M.S. Wu, *A very narrow shadow extra Z-boson at colliders*, *Phys. Rev.* **D 74** (2006) 095005 [hep-ph/0608068] [SPIRES].

[29] J. Kumar and J.D. Wells, *LHC and ILC probes of hidden-sector gauge bosons*, *Phys. Rev.* **D 74** (2006) 115017 [hep-ph/0606183] [SPIRES].

[30] L. Ackerman, M.R. Buckley, S.M. Carroll and M. Kamionkowski, *Dark matter and dark radiation*, *Phys. Rev.* **D 79** (2009) 023519 [arXiv:0810.5126] [SPIRES].

[31] M. Pospelov, *Secluded* U(1) *below the weak scale*, *Phys. Rev.* **D 80** (2009) 095002 [arXiv:0811.1030] [SPIRES].

[32] B. Batell, M. Pospelov and A. Ritz, *Probing a secluded* U(1) *at B-factories*, *Phys. Rev.* **D 79** (2009) 115008 [arXiv:0903.0363] [SPIRES].

[33] B. Batell, M. Pospelov and A. Ritz, *Exploring portals to a hidden sector through fixed targets*, *Phys. Rev.* **D 80** (2009) 095024 [arXiv:0906.5614] [SPIRES].

[34] A. Mirizzi, J. Redondo and G. Sigl, *Microwave background constraints on mixing of photons with hidden photons*, *JCAP* **03** (2009) 026 [arXiv:0901.0014] [SPIRES].

[35] P. Hořava and E. Witten, *Eleven-dimensional supergravity on a manifold with boundary*, *Nucl. Phys.* **B 475** (1996) 94 [hep-th/9603142] [SPIRES].

[36] P. Hořava and E. Witten, *Heterotic and type-I string dynamics from eleven dimensions*, *Nucl. Phys.* **B 460** (1996) 506 [hep-th/9510209] [SPIRES].

[37] E. Witten, *Strong coupling expansion of Calabi-Yau compactification*, *Nucl. Phys.* **B 471** (1996) 135 [hep-th/9602070] [SPIRES].

[38] J.D. Lykken, *Weak scale superstrings*, *Phys. Rev.* **D 54** (1996) 3693 [hep-th/9603133] [SPIRES].

[39] I. Antoniadis, N. Arkani-Hamed, S. Dimopoulos and G.R. Dvali, *New dimensions at a millimeter to a Fermi and superstrings at a TeV*, *Phys. Lett.* **B 436** (1998) 257 [hep-ph/9804398] [SPIRES].

[40] K. Benakli, *Phenomenology of low quantum gravity scale models*, *Phys. Rev.* **D 60** (1999) 104002 [hep-ph/9809582] [SPIRES].

[41] C.P. Burgess, L.E. Ibáñez and F. Quevedo, *Strings at the intermediate scale or is the Fermi scale dual to the Planck scale?*, *Phys. Lett.* **B 447** (1999) 257 [hep-ph/9810535] [SPIRES].

[42] I. Antoniadis and K. Benakli, *Large dimensions and string physics in future colliders*, *Int. J. Mod. Phys.* **A 15** (2000) 4237 [hep-ph/0007226] [SPIRES].

[43] N. Arkani-Hamed, S. Dimopoulos and G.R. Dvali, *The hierarchy problem and new dimensions at a millimeter*, *Phys. Lett.* **B 429** (1998) 263 [hep-ph/9803315] [SPIRES].

[44] N. Arkani-Hamed, S. Dimopoulos and G.R. Dvali, *Phenomenology, astrophysics and cosmology of theories with sub-millimeter dimensions and TeV scale quantum gravity*, *Phys. Rev.* **D 59** (1999) 086004 [hep-ph/9807344] [SPIRES].

[45] L. Randall and R. Sundrum, *A large mass hierarchy from a small extra dimension*, *Phys. Rev. Lett.* **83** (1999) 3370 [hep-ph/9905221] [SPIRES].

[46] L. Randall and R. Sundrum, *An alternative to compactification*, *Phys. Rev. Lett.* **83** (1999) 4690 [hep-th/9906064] [SPIRES].

JHEP08(2011)106

[47] Y. Aghababaie, C.P. Burgess, S.L. Parameswaran and F. Quevedo, *SUSY breaking and moduli stabilization from fluxes in gauged 6D supergravity*, *JHEP* **03** (2003) 032 [hep-th/0212091] [SPIRES].

[48] Y. Aghababaie, C.P. Burgess, S.L. Parameswaran and F. Quevedo, *Towards a naturally small cosmological constant from branes in 6D supergravity*, *Nucl. Phys.* **B 680** (2004) 389 [hep-th/0304256] [SPIRES].

[49] L.E. Ibáñez and F. Quevedo, *Anomalous* U(1)*'s and proton stability in brane models*, *JHEP* **10** (1999) 001 [hep-ph/9908305] [SPIRES].

[50] R. Kallosh, A.D. Linde, D.A. Linde and L. Susskind, *Gravity and global symmetries*, *Phys. Rev.* **D 52** (1995) 912 [hep-th/9502069] [SPIRES].

[51] T. Banks and L.J. Dixon, *Constraints on string vacua with space-time supersymmetry*, *Nucl. Phys.* **B 307** (1988) 93 [SPIRES].

[52] C.P. Burgess et al., *Continuous global symmetries and hyperweak interactions in string compactifications*, *JHEP* **07** (2008) 073 [arXiv:0805.4037] [SPIRES].

[53] V. Balasubramanian, P. Berglund, J.P. Conlon and F. Quevedo, *Systematics of moduli stabilisation in Calabi-Yau flux compactifications*, *JHEP* **03** (2005) 007 [hep-th/0502058] [SPIRES].

[54] J.P. Conlon, F. Quevedo and K. Suruliz, *Large-volume flux compactifications: moduli spectrum and D3/D7 soft supersymmetry breaking*, *JHEP* **08** (2005) 007 [hep-th/0505076] [SPIRES].

[55] C.P. Burgess and L. van Nierop, *Bulk axions, brane back-reaction and fluxes*, *JHEP* **02** (2011) 094 [arXiv:1012.2638] [SPIRES].

[56] C.P. Burgess and L. van Nierop, *Large dimensions and small curvatures from supersymmetric brane back-reaction*, *JHEP* **04** (2011) 078 [arXiv:1101.0152] [SPIRES].

[57] S. Weinberg, *Feynman rules for any spin*, *Phys. Rev.* **133** (1964) 1318.

[58] S. Weinberg, *Feynman rules for any spin: II massless particles*, *Phys. Rev.* **134** (1964) 882.

[59] S. Weinberg, *Feynman rules for any spin. III*, *Phys. Rev.* **181** (1969) 1893 [SPIRES].

[60] S. Weinberg, *Photons and gravitons in S-matrix theory: derivation of charge conservation and equality of gravitational and inertial mass*, *Phys. Rev.* **135** (1964) 1049.

[61] S. Weinberg, *Photons and gravitons in perturbation theory: derivation of Maxwell's and Einstein's equations*, *Phys. Rev.* **138** (1965) 988.

[62] S. Deser, *Self-interaction and gauge invariance*, *Gen. Rel. Grav.* **1** (1970) 9 [gr-qc/0411023] [SPIRES].

[63] S. Weinberg and E. Witten, *Limits on massless particles*, *Phys. Lett.* **B 96** (1980) 59 [SPIRES].

[64] J.M. Cornwall, D.N. Levin and G. Tiktopoulos, *Uniqueness of spontaneously broken gauge theories*, *Phys. Rev. Lett.* **30** (1973) 1268 [SPIRES].

[65] J.M. Cornwall, D.N. Levin and G. Tiktopoulos, *Derivation of gauge invariance from high-energy unitarity bounds on the s matrix*, *Phys. Rev.* **D 10** (1974) 1145 [SPIRES].

[66] J. Preskill, *Gauge anomalies in an effective field theory*, *Ann. Phys.* **210** (1991) 323 [SPIRES].

JHEP08(2011)106

[67] C.P. Burgess and D. London, *On anomalous gauge boson couplings and loop calculations*, *Phys. Rev. Lett.* **69** (1992) 3428 [SPIRES].

[68] C.P. Burgess and D. London, *Uses and abuses of effective Lagrangians*, *Phys. Rev.* **D 48** (1993) 4337 [hep-ph/9203216] [SPIRES].

[69] S. Weinberg, *Quantum theory of fields, vol. I*, Cambridge University Press, Cambridge U.K. (1996).

[70] C.P. Burgess, *Quantum gravity in everyday life: General relativity as an effective field theory*, *Living Rev. Rel.* **7** (2004) 5 [gr-qc/0311082] [SPIRES].

[71] C.P. Burgess, *Introduction to effective field theory*, *Ann. Rev. Nucl. Part. Sci.* **57** (2007) 329 [hep-th/0701053] [SPIRES].

[72] C.P. Burgess and G. Moore, *The standard model: a primer*, Cambridge University Press, Cambridge U.K. (2007).

[73] M.C. Gonzalez-Garcia and Y. Nir, *Developments in neutrino physics*, *Rev. Mod. Phys.* **75** (2003) 345 [hep-ph/0202058] [SPIRES].

[74] M. Maltoni, T. Schwetz, M.A. Tortola and J.W.F. Valle, *Status of global fits to neutrino oscillations*, *New J. Phys.* **6** (2004) 122 [hep-ph/0405172] [SPIRES].

[75] M.C. Gonzalez-Garcia and M. Maltoni, *Phenomenology with massive neutrinos*, *Phys. Rept.* **460** (2008) 1 [arXiv:0704.1800] [SPIRES].

[76] C.M. Will, *The confrontation between general relativity and experiment*, *Living Rev. Rel.* **4** (2001) 4 [gr-qc/0103036] [SPIRES].

[77] C.M. Will, *The confrontation between general relativity and experiment*, *Living Rev. Rel.* **9** (2005) 3 [gr-qc/0510072] [SPIRES].

[78] E.G. Adelberger, B.R. Heckel and A.E. Nelson, *Tests of the gravitational inverse-square law*, *Ann. Rev. Nucl. Part. Sci.* **53** (2003) 77 [hep-ph/0307284] [SPIRES].

[79] C.D. Hoyle et al., *Sub-millimeter tests of the gravitational inverse-square law*, *Phys. Rev.* **D 70** (2004) 042004 [hep-ph/0405262] [SPIRES].

[80] J.A. Harvey and S.G. Naculich, *Cosmic strings from pseudoanomalous* U(1)*'s*, *Phys. Lett.* **B 217** (1989) 231 [SPIRES].

[81] M.B. Green and J.H. Schwarz, *Anomaly cancellation in supersymmetric* $D = 10$ *gauge theory and superstring theory*, *Phys. Lett.* **B 149** (1984) 117 [SPIRES].

[82] J. Wess and B. Zumino, *Consequences of anomalous Ward identities*, *Phys. Lett.* **B 37** (1971) 95 [SPIRES].

[83] M. Dine, N. Seiberg and E. Witten, *Fayet-Iliopoulos terms in string theory*, *Nucl. Phys.* **B 289** (1987) 589 [SPIRES].

[84] C.P. Burgess, A. Maharana and F. Quevedo, *Uber-naturalness: unexpectedly light scalars from supersymmetric extra dimensions*, *JHEP* **05** (2011) 010 [arXiv:1005.1199] [SPIRES].

[85] S. Weinberg, *Baryon and lepton nonconserving processes*, *Phys. Rev. Lett.* **43** (1979) 1566 [SPIRES].

[86] F. Wilczek and A. Zee, *Operator analysis of nucleon decay*, *Phys. Rev. Lett.* **43** (1979) 1571 [SPIRES].

JHEP08(2011)106

[87] H. Georgi and S.L. Glashow, *Unity of all elementary particle forces*, *Phys. Rev. Lett.* **32** (1974) 438 [SPIRES].

[88] H. Fritzsch and P. Minkowski, *Unified interactions of leptons and hadrons*, *Ann. Phys.* **93** (1975) 193 [SPIRES].

[89] F. Gursey, P. Ramond and P. Sikivie, *A universal gauge theory model based on E_6*, *Phys. Lett.* **B 60** (1976) 177 [SPIRES].

[90] P. Langacker, *Grand unified theories and proton decay*, *Phys. Rept.* **72** (1981) 185 [SPIRES].

[91] G.G. Ross, *Grand unified theories*, Benjamin/Cummings, Reading U.S.A. (1984).

[92] H. Nishino and E. Sezgin, *Matter and gauge couplings of $N = 2$ supergravity in six-dimensions*, *Phys. Lett.* **B 144** (1984) 187 [SPIRES].

[93] H. Nishino and E. Sezgin, *The complete $N = 2$, $D = 6$ supergravity with matter and Yang-Mills couplings*, *Nucl. Phys.* **B 278** (1986) 353 [SPIRES].

[94] S. Randjbar-Daemi, A. Salam, E. Sezgin and J.A. Strathdee, *An anomaly free model in six-dimensions*, *Phys. Lett.* **B 151** (1985) 351 [SPIRES].

[95] M.B. Green, J.H. Schwarz and P.C. West, *Anomaly free chiral theories in six-dimensions*, *Nucl. Phys.* **B 254** (1985) 327 [SPIRES].

[96] J. Erler, *Anomaly cancellation in six-dimensions*, *J. Math. Phys.* **35** (1994) 1819 [hep-th/9304104] [SPIRES].

[97] A. Salam and E. Sezgin, *Chiral compactification on Minkowski $\times S^2$ of $N = 2$ Einstein-Maxwell supergravity in six-dimensions*, *Phys. Lett.* **B 147** (1984) 47 [SPIRES].

[98] C.P. Burgess, D. Hoover and G. Tasinato, *UV caps and modulus stabilization for 6D gauged chiral supergravity*, *JHEP* **09** (2007) 124 [arXiv:0705.3212] [SPIRES].

[99] C.P. Burgess, D. Hoover, C. de Rham and G. Tasinato, *Effective field theories and matching for codimension-2 branes*, *JHEP* **03** (2009) 124 [arXiv:0812.3820] [SPIRES].

[100] L.E. Ibáñez, R. Rabadán and A.M. Uranga, *Anomalous U(1)'s in type-I and type IIB $D = 4$, $N = 1$ string vacua*, *Nucl. Phys.* **B 542** (1999) 112 [hep-th/9808139] [SPIRES].

[101] T. Weigand, *Lectures on F-theory compactifications and model building*, *Class. Quant. Grav.* **27** (2010) 214004 [arXiv:1009.3497] [SPIRES].

[102] D.M. Ghilencea, L.E. Ibáñez, N. Irges and F. Quevedo, *TeV-Scale Z' bosons from D-branes*, *JHEP* **08** (2002) 016 [hep-ph/0205083] [SPIRES].

[103] D.M. Ghilencea, U(1) *masses in intersecting D-brane SM-like models*, *Nucl. Phys.* **B 648** (2003) 215 [hep-ph/0208205] [SPIRES].

[104] J.P. Conlon, A. Maharana and F. Quevedo, *Towards realistic string vacua*, *JHEP* **05** (2009) 109 [arXiv:0810.5660] [SPIRES].

[105] M. Buican, D. Malyshev, D.R. Morrison, H. Verlinde and M. Wijnholt, *D-branes at singularities, compactification and hypercharge*, *JHEP* **01** (2007) 107 [hep-th/0610007] [SPIRES].

[106] D. Berenstein and S. Pinansky, *The minimal quiver standard model*, *Phys. Rev.* **D 75** (2007) 095009 [hep-th/0610104] [SPIRES].

JHEP08(2011)106

[107] D. Berenstein, R. Martinez, F. Ochoa and S. Pinansky, *Z-prime boson detection in the minimal quiver standard model*, *Phys. Rev.* **D 79** (2009) 095005 [arXiv:0807.1126] [SPIRES].

[108] E. Salvioni, G. Villadoro and F. Zwirner, *Minimal Z' models: present bounds and early LHC reach*, *JHEP* **11** (2009) 068 [arXiv:0909.1320] [SPIRES].

[109] E. Salvioni, A. Strumia, G. Villadoro and F. Zwirner, *Non-universal minimal Z' models: present bounds and early LHC reach*, *JHEP* **03** (2010) 010 [arXiv:0911.1450] [SPIRES].

[110] C. Corianò', N. Irges and E. Kiritsis, *On the effective theory of low scale orientifold string vacua*, *Nucl. Phys.* **B 746** (2006) 77 [hep-ph/0510332] [SPIRES].

[111] M. Goodsell, J. Jaeckel, J. Redondo and A. Ringwald, *Naturally light hidden photons in LARGE volume string compactifications*, *JHEP* **11** (2009) 027 [arXiv:0909.0515] [SPIRES].

[112] D. Chang, R.N. Mohapatra and M.K. Parida, *Decoupling parity and $\mathrm{SU}(2)_R$ breaking scales: a new approach to left-right symmetric models*, *Phys. Rev. Lett.* **52** (1984) 1072 [SPIRES].

[113] D. Chang, R.N. Mohapatra, J. Gipson, R.E. Marshak and M.K. Parida, *Experimental tests of new* SO(10) *grand unification*, *Phys. Rev.* **D 31** (1985) 1718 [SPIRES].

[114] R.W. Robinett and J.L. Rosner, *Prospects for a second neutral vector boson at low mass in* SO(10), *Phys. Rev.* **D 25** (1982) 3036 [Erratum ibid. **27** (1983) 679] [SPIRES].

[115] P. Langacker, R.W. Robinett and J.L. Rosner, *New heavy gauge bosons in pp and $p\bar{p}$ collisions*, *Phys. Rev.* **D 30** (1984) 1470 [SPIRES].

[116] Q. Shafi, *E_6 as a unifying gauge symmetry*, *Phys. Lett.* **B 79** (1978) 301 [SPIRES].

[117] R. Barbieri and D.V. Nanopoulos, *An exceptional model for grand unification*, *Phys. Lett.* **B 91** (1980) 369 [SPIRES].

[118] F. Gursey and M. Serdaroglu, *E_6 gauge field theory model revisited*, *Nuovo Cim.* **A 65** (1981) 337 [SPIRES].

[119] V.D. Barger, N.G. Deshpande and K. Whisnant, *Phenomenological mass limits on extra Z of E_6 superstrings*, *Phys. Rev. Lett.* **56** (1986) 30 [SPIRES].

[120] D. London and J.L. Rosner, *Extra gauge bosons in E_6*, *Phys. Rev.* **D 34** (1986) 1530 [SPIRES].

[121] F. del Aguila, M. Quirós and F. Zwirner, *Detecting E_6 neutral gauge bosons through lepton pairs at hadron colliders*, *Nucl. Phys.* **B 287** (1987) 419 [SPIRES].

[122] A. Font, L.E. Ibáñez and F. Quevedo, *Does proton stability imply the existence of an extra Z_0?*, *Phys. Lett.* **B 228** (1989) 79 [SPIRES].

[123] J.L. Hewett and T.G. Rizzo, *Low-energy phenomenology of superstring inspired E_6 models*, *Phys. Rept.* **183** (1989) 193 [SPIRES].

[124] K.R. Dienes, *String theory and the path to unification: a review of recent developments*, *Phys. Rept.* **287** (1997) 447 [hep-th/9602045] [SPIRES].

[125] G. Senjanović and R.N. Mohapatra, *Exact left-right symmetry and spontaneous violation of parity*, *Phys. Rev.* **D 12** (1975) 1502 [SPIRES].

[126] X. Li and R.E. Marshak, *Low-energy phenomenology and neutral weak boson masses in the $\mathrm{SU}(2)_L \times \mathrm{SU}(2)_R \times \mathrm{U}(1)_{B-L}$ electroweak model*, *Phys. Rev.* **D 25** (1982) 1886 [SPIRES].

JHEP08(2011)106

[127] M.S. Carena, A. Daleo, B.A. Dobrescu and T.M.P. Tait, *Z-prime gauge bosons at the Tevatron*, *Phys. Rev.* **D 70** (2004) 093009 [hep-ph/0408098] [SPIRES].

[128] B. Holdom, *Oblique electroweak corrections and an extra gauge boson*, *Phys. Lett.* **B 259** (1991) 329 [SPIRES].

[129] K.S. Babu, C.F. Kolda and J. March-Russell, *Implications of generalized Z Z' mixing*, *Phys. Rev.* **D 57** (1998) 6788 [hep-ph/9710441] [SPIRES].

[130] A. Leike, *The phenomenology of extra neutral gauge bosons*, *Phys. Rept.* **317** (1999) 143 [hep-ph/9805494] [SPIRES].

[131] A. Hook, E. Izaguirre and J.G. Wacker, *Model independent bounds on kinetic mixing*, arXiv:1006.0973 [SPIRES].

[132] J. Erler, P. Langacker, S. Munir and E.R. Pena, *Improved constraints on Z' bosons from electroweak precision data*, *JHEP* **08** (2009) 017 [arXiv:0906.2435] [SPIRES].

[133] J.D. Wells, *How to find a hidden world at the Large Hadron Collider*, arXiv:0803.1243 [SPIRES].

[134] D0 collaboration, S. Abachi et al., *Search for additional neutral gauge bosons*, *Phys. Lett.* **B 385** (1996) 471 [SPIRES].

[135] C.D. Carone and H. Murayama, *Realistic models with a light* U(1) *gauge boson coupled to baryon number*, *Phys. Rev.* **D 52** (1995) 484 [hep-ph/9501220] [SPIRES].

[136] K.T. Mahanthappa and P.K. Mohapatra, *Limits on mixing angle and mass of Z-prime using Delta rho and atomic parity violation*, *Phys. Rev.* **D 43** (1991) 3093 [SPIRES].

[137] A.E. Faraggi and D.V. Nanopoulos, *A superstring Z-prime at $O(1\ TeV)$?*, *Mod. Phys. Lett.* **A 6** (1991) 61 [SPIRES].

[138] J.L. Lopez and D.V. Nanopoulos, *New bounds on primordial nucleosynthesis in the presence of a cornered Z-prime*, *Phys. Lett.* **B 241** (1990) 392 [SPIRES].

[139] S. Cassel, D.M. Ghilencea and G.G. Ross, *Electroweak and dark matter constraints on a Z' in models with a hidden valley*, *Nucl. Phys.* **B 827** (2010) 256 [arXiv:0903.1118] [SPIRES].

[140] C.P. Burgess, S. Godfrey, H. Konig, D. London and I. Maksymyk, *Bounding anomalous gauge boson couplings*, *Phys. Rev.* **D 50** (1994) 7011 [hep-ph/9307223] [SPIRES].

[141] P. Bamert, C.P. Burgess, J.M. Cline, D. London and E. Nardi, *$R(b)$ and new physics: a comprehensive analysis*, *Phys. Rev.* **D 54** (1996) 4275 [hep-ph/9602438] [SPIRES].

[142] C.P. Burgess, S. Godfrey, H. Konig, D. London and I. Maksymyk, *Model independent global constraints on new physics*, *Phys. Rev.* **D 49** (1994) 6115 [hep-ph/9312291] [SPIRES].

[143] G. Altarelli and R. Barbieri, *Vacuum polarization effects of new physics on electroweak processes*, *Phys. Lett.* **B 253** (1991) 161 [SPIRES].

[144] M.E. Peskin and T. Takeuchi, *Estimation of oblique electroweak corrections*, *Phys. Rev.* **D 46** (1992) 381 [SPIRES].

[145] I. Maksymyk, C.P. Burgess and D. London, *Beyond S, T and U*, *Phys. Rev.* **D 50** (1994) 529 [hep-ph/9306267] [SPIRES].

[146] C.P. Burgess, S. Godfrey, H. Konig, D. London and I. Maksymyk, *A global fit to extended oblique parameters*, *Phys. Lett.* **B 326** (1994) 276 [hep-ph/9307337] [SPIRES].

JHEP08(2011)106

[147] ALEPH collaboration, *Precision electroweak measurements on the Z resonance*, *Phys. Rept.* **427** (2006) 257 [hep-ex/0509008] [SPIRES].

[148] E.J. Chun, J.-C. Park and S. Scopel, *Dark matter and a new gauge boson through kinetic mixing*, *JHEP* **02** (2011) 100 [arXiv:1011.3300] [SPIRES].

[149] Particle Data Group collaboration, C. Amsler et al., *Review of particle physics*, *Phys. Lett.* **B 667** (2008) 1 [SPIRES].

[150] CHARM-II collaboration, P. Vilain et al., *Precision measurement of electroweak parameters from the scattering of muon-neutrinos on electrons*, *Phys. Lett.* **B 335** (1994) 246 [SPIRES].

[151] L.A. Ahrens et al., *Determination of electroweak parameters from the elastic scattering of muon-neutrinos and anti-neutrinos on electrons*, *Phys. Rev.* **D 41** (1990) 3297 [SPIRES].

[152] G. Radel and R. Beyer, *Neutrino electron scattering*, *Mod. Phys. Lett.* **A 8** (1993) 1067 [SPIRES].

[153] A. de Gouvêa and J. Jenkins, *What can we learn from neutrino electron scattering?*, *Phys. Rev.* **D 74** (2006) 033004 [hep-ph/0603036] [SPIRES].

[154] CDF collaboration, T. Aaltonen et al., *Search for new physics in high mass electron-positron events in $p\bar{p}$ collisions at $\sqrt{s} = 1.96$ TeV*, *Phys. Rev. Lett.* **99** (2007) 171802 [arXiv:0707.2524] [SPIRES].

[155] E.A. Paschos and L. Wolfenstein, *Tests for neutral currents in neutrino reactions*, *Phys. Rev.* **D 7** (1973) 91 [SPIRES].

[156] NuTeV collaboration, G.P. Zeller et al., *A precise determination of electroweak parameters in neutrino nucleon scattering*, *Phys. Rev. Lett.* **88** (2002) 091802 [hep-ex/0110059] [SPIRES].

[157] BABAR collaboration, B. Aubert et al., *Search for dimuon decays of a light scalar boson in radiative transitions $\Upsilon \to \gamma A_0$*, *Phys. Rev. Lett.* **103** (2009) 081803 [arXiv:0905.4539] [SPIRES].

[158] R. Barbieri and T.E.O. Ericson, *Evidence against the existence of a low mass scalar boson from neutron-nucleus scattering*, *Phys. Lett.* **B 57** (1975) 270 [SPIRES].

[159] V. Barger, C.-W. Chiang, W.-Y. Keung and D. Marfatia, *Proton size anomaly*, *Phys. Rev. Lett.* **106** (2011) 153001 [arXiv:1011.3519] [SPIRES].

[160] C. Bouchiat and P. Fayet, *Constraints on the parity-violating couplings of a new gauge boson*, *Phys. Lett.* **B 608** (2005) 87 [hep-ph/0410260] [SPIRES].

[161] R.H. Cyburt, B.D. Fields, K.A. Olive and E. Skillman, *New BBN limits on physics beyond the standard model from ^{4}He*, *Astropart. Phys.* **23** (2005) 313 [astro-ph/0408033] [SPIRES].

[162] J. Blumlein and J. Brunner, *New exclusion limits for dark gauge forces from beam-dump data*, *Phys. Lett.* **B 701** (2011) 155 [arXiv:1104.2747] [SPIRES].

JHEP08(2011)106